Finite Element Stress Analysis of Artificial Femur Head on Hip Joint Prosthesis

Yigezu Bantirga G/Michael

A Thesis submitted to

The Department of Mechanical Engineering

Presented in Partial Fulfillment of the Requirements for the Degree of Master of Science

Addis Ababa University

Institute of Technology

Addis Ababa, Ethiopia

January, 2013

Addis Ababa Institute of Technology

Addis Ababa University

School of Graduate Studies

This is to certify that the thesis prepared by Yigezu Bantirga, entitled: Finite Element Stress Analysis of Artificial Femur Head on Hip Joint Prosthesis and submitted in partial fulfillment of the requirements for the degree of Degree of Master of Science complies with regulations of the University and meets the accepted standards with respect to originality and quality.

Signed by the Examining Committee:

Examiner Dr.Ing Tamrat Tesfaye Signature _____ Date _____

Examiner Dr.Ing. Zewdu Abadi Signature _____ Date _____

Adviser Dr.Daniel Tilahun Signature _____ Date _____

Adviser Dr.Daniel Tilahun Signature _____ Date _____

ABSTRACT

Finite Element Stress Analysis on Artificial Femur Head of Hip Joint Prosthesis

Yigezu Bantirga

Addis Ababa Institute of Technology, 2013

Cobalt-chromium-molybdenum ball heads for total hip replacement are highly loaded in finite element load step on the basis of ISO 5832-12 rupture test to meet the stress requirements concerning strength and safety. High stresses inside the ball head originate from the press fit between the conical stem neck (made of titanium alloy) and the borehole of the ball. The aim of this study was the development of an optimized contour at the fillet inside the ball head and the borehole contact length depth by means of numerical methods, in order to reduce local stress concentrations. The finite element optimization method was applied on the customary engineering fillet radius to reduce local stress peaks. Since the static load from experimental realistic hip implant test is governed by the maximum von-mises, shear, normal and principal stresses in the contact area of the taper. The optimal reduced local stress of the examined ball head design was obtained in the medium neck contact length at o.8mm fillet for the relevant realistic load case of stumbling.

Keywords: Femoral head, Stem neck, Optimum geometry, Stress concentration, FEA

ACKNOWLEDGEMENTS

I am most grateful to my loving grandfather, Aba G/Michael next to God. His overwhelming confidence in me continues to be a driving force in both my personal and professional life. Words cannot express the joy you have added to my life and foster me one step ahead to my existence next to God. I thank you for all your love, support and patience with your age tiredness and sickness.

I would especially like to thank my advisor Dr. Daniel Tilahun. This thesis has been improved greatly due to his support and guidance. Moreover special thanks to him for giving me numerous opportunities to investigate the window in finding a solution and expand my horizons to meet my aim. I have a great deal of respect for him and consider it a blessing to have worked with him as well.

I owe a debt of gratitude from bottom of my heart to Shiferaw Gadissa. He went beyond the call of duty to help me with this thesis, in finding me of all the reference materials and software. His thoughtfulness and kindness will be remembered fondly.

Once again it is my pleasure to thank all my friends around me that contributed to my work with material and wishing the best of all to me to finish my work. On this regard I would not dare to forget Shewaye Temesgen and Chalachew Setegn for their valuable help. Finally I would also like to thank the Addis Ababa Institute of Technology Graduate School for the financial support they have given me.

TABLE OF CONTENTS

LIST OF FIGURES

LIST OF TABLES

ABBREVIATIONS

CATIA Computer Aided Three Dimensional Interactive Application

CoC Ceramic femoral head on Ceramic acetabular cup hip prosthesis

CoCrMo Cobalt Chromium Molybdenum alloy

CoM Ceramic femoral head on Metal coupling acetabular cup hip prosthesis

CoP Ceramic femoral head on Polymer coupling acetabular cup hip prosthesis

FDA Food and Drug Administration

FEA Finite Element Analysis

FEM Finite Element Method

HRS Hip Resurfacing System

ISO International Organization for Standardization

LN Long Neck

MoM Metal femoral head on Metal coupling acetabular cup hip prosthesis

MoMHR MoM Hip Resurfacing

MoP Metal femoral head on Polymer coupling acetabular cup hip prosthesis

MN Medium Neck

PMMA PolyMethylMethAcrylate

PTFE Poly Tetra Fluoro

Ethylene

SN Short Neck

THA Total Hip Arthroplasty

THR Total Hip Replacement

TKA Total Knee Arthroplasty

UHMWPE Ultra High Molecular Weight PolyEthylene

CHAPTER ONE

INTRODUCTION

1.1 Introduction

The increase of knowledge in all areas of research forms the premises for an increase in the life expectancy of the population as well as the quality of life, this increase of life expectancy are achieved through efficient medical care to meet the main objectives of improving and ensuring an adequate mobility for performing daily tasks [1]. For this maximum mobility the hip joint is a major structure within the human body, it supports most of the upper body weight. The hip joints are connecting the torso to the legs and, the weight of the upper body and decrease the impulsion loading from lower body to the upper body. Experimental studies have found that the resultant force acting through the hip joint during normal walking is around 300% body weight. Having known the load, the hip joint could be destroyed under complex working conditions and needs to be replaced. [2] The replacement of the natural hip with artificial replacement is the most effective way of restoring mobility for patients that suffer from chronic diseases such as

osteoarthritis, chronic arthritis and severe trauma. Attempts at replacing the diseased hip joint can be traced back as far as 1890 when Gluck described the use of ivory to replace the femoral head. Early attempts were largely unsuccessful and more recent developments in hip prostheses owe much to the work of Charnley in the 1960s and 1970s. [3] Since the 1950's, a very common solution to the debilitating pain associated with this condition has been a procedure termed Total Hip Arthroplasty, or Total Hip Replacement (THR). The first "highly successful" device was designed by Charnley in the mid-1950 and to the present, the fundamental design has remained virtually unchanged, though many incremental improvements have occurred, particularly as a result of materials advances. A total hip replacement device consists of two primary components: the femoral head/ and stem, and the acetabular component. [4] The story of replacement hip joint engineering and surgeryrepresents but one aspect of progress in bio-tribology. Everyone seems to know of someone who has benefited from hip joint replacement. The field has been dominated for some forty years by implants based articulation. [5] But the performance of the prosthesis is not reliable since the average service life of a hip prosthesis is considered to be between 15 and 20 years. This number is influences by a series of factors such as: body mass index, age and level of activity of the patient as well as the type of prosthesis and post-surgery complications. Statistical data show that out of the total number of hip replacement procedures about 10% will have to be revised before their expected service life [1], due to complications caused by stress concentration on femur ball head and ball head is mounted on a metallic stem by frictional fitting, and the system is then pivoted on the accetabule cups. Although femoral ball heads have proved their exceptional mechanical reliability, recent clinical studies do show their fracture failure due to a number of causes. Among the possible causes to failure, improper assembly and contamination of the contact surfaces between the stem and the taper-borehole of a femoral ball

head during surgery are reportedly significant. While these causes are, to some extent, unavoidable, the mechanical reliability of the ball heads has to be continuously raised by increasing the strength of component itself. One way to improve this is to optimize the design of the femoral heads. This paper aims to study the stress distributions in the femoral heads, by analyzing both the existing taper-borehole shapes and some new designs of the authors to understand the effect of borehole shapes on the variation of stresses and hence to provide some useful guidelines for improving the mechanical reliability of the femoral heads. In the current study, the finite element (FE) method was used to evaluate the stress distributions in the proximal region of a femur head in a static hip condition.

1.2 Background

1.2.1 Artificial Hip Joint Prosthesis

Hip joint fractures among the elderly population. Some associated factors leading to a patient sustaining an intertrochanteric fracture are advancing age, increasing number of comorbidities, increased dependency in activities of daily living and a history of other oseoporosis related fractures [6]. Intertrochantric fractures in younger individuals are associated to high-energy injury. Some examples of high-energy injuries are motor vehicle accident and fall from a height. In elderly patients, 90 percent of intertrochanteric fractures occur from simple falls.

An individual must land on or near the hip for the energy to be transmitted to the proximal femur. In elderly individuals are more likely for this type of fracture due to their deteriorating strength and reaction times being too slow

In 1923, one of the first artificial hip socket components was installed on a patient by Marius Nygaard Smith-Peterson. The cup was composed of glass and failed as time passed, but paved the way to construction of hip cups in similar fashion, only using different materials such as plastic and metal [8]. In 1925 [9], a surgeon in Boston, Massachusetts, M.N. Smith-Petersen, M.D., molded a piece of glass into the shape of a hollow hemisphere which could fit over the ball of the hip joint and provide a new smooth surface for movement. As early as 1938, Dr. Jean Judet and his brother, Dr. Robert Judet, of Paris, attempted to use an acrylic material to replace arthritic hip surfaces. This acrylic provided a smooth surface, but unfortunately tended to come loose.

The next rather noticeable advance in hip surgery came from Sir John Charnley, an English surgeon, who reduced the head size of the standard femoral component. By 1961, he was performing the surgery regularly with good results. He further improved the techniques and component designs. In 1962, working out of a small hospital in the countryside of England, Sir Charnley replaced an arthritic hip socket with a plastic cup and replaced the femoral head with a metal prosthesis.This total hip replacement procedure was the first of its kind. Survivorship on Sir John Charnley's patients between 20-25 years was astounding, rounding off at around 85%. Thousands of people were successfully relieved of their hip pain and the long term results became very predictable. The Queen of England knighted him for his immense contributions. He is now known as Sir John Charnley [8-11].

Since the successful operation performed by Sir John Charnley over forty years ago, total hip replacement surgery has come a long way. Today there are a multitude of different components, allowing for a variety of options based on a patient's specific needs.

1.2.2 Hip Joint

The hip joint consists of a ball and socket joint. The top of the thighbone (femur) is a largest bone of human body, called femur joins with the horizontal pelvic coxal bone and lower end of that is fixed at the knee. The ball (femoral head) at the top of the thighbone fits into a portion of the pelvic bone forms the cup (acetabulum) or socket as shown in figure1. Between joining surfaces of the acetabulum and femoral lies a smooth glassy substance called cartilage. It provides frictionless cushion for constrained motion to femoral head within acetabular socket as shown in figure below.

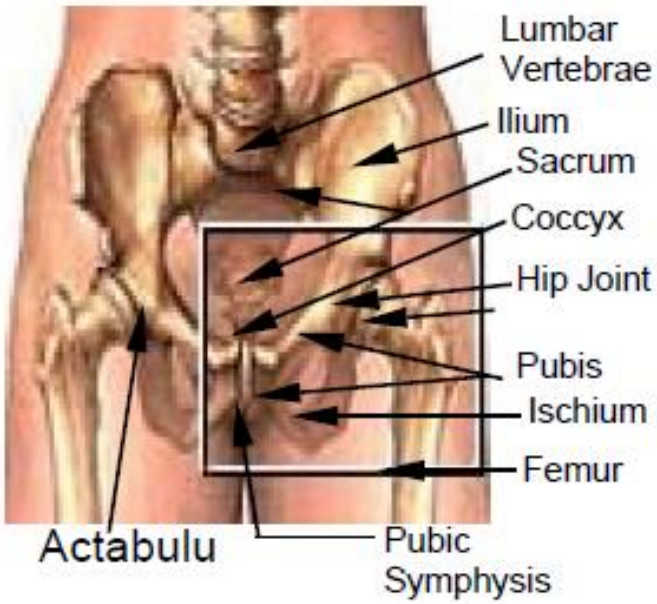

Fig1: Front view of pelvic bone [12]

There are several basic components of the hip that are dealt with in hip surgery. The anatomy section of figure 2 will give you some diagrams dealing with the different components accompanied by a brief synopsis of those parts. The different diseases that can be attributed to the need for total hip surgery affect both the socket and the femoral head. As there are a variety of different procedures that can take place depending on injury or disease, be sure to also look at the treatment section as it spells out some of the more common ones with different diagrams as well [7]. There are several basic components to the hip joint that are commonplace in total hip surgery. The numbers below coincide with the figure directly.

1. Femoral Head
2. Acetabulum Lining
3. Greater Trochanter
4. Lesser Trochanter
5. Femur Bone
6. Iliac Crest

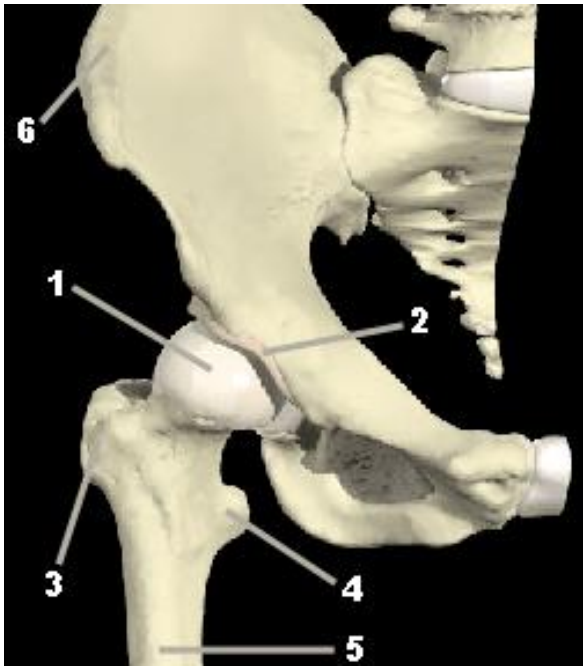

Fig1.2: Femur Thigh Bone [7]

1.2.3 Total Hip Replacement (THR)

Over the years hip replacement surgery (also known as Total Hip Arthroplasty) has made major advances. Patients who used to experience hip disease or injury in the past were forced to live with the pain and discomfort. Total hip replacement surgeries, as well as many other surgical and non- surgical alternatives, are able to restore function and mobility to hip joints, enhancing the quality of life for patients. As a patient, it is important to understand you have many options when it comes to total hip replacement. In this section, you will be able to learn about the many options for total hip replacement, including the different products and techniques used to restore quality of life in total hip patients.

The need for total hip replacement surgery is prompted either by severe injury to the hip joint, or more commonly, a disease in the hip joint. Disease in the hip joint can degenerate the bone and cartilage in the joint, leading to pain and restricted motion. Due to the fact that bone repair in children is more rapid than that of a grown adult, blood flow re-establishment often leads to the regeneration of healthy bone to the affected area. This in turn brings about a better long term outcome for children with Perthes as opposed to adults with a similar problem affecting their femoral head.

In general hip replacement is a procedure in which the hip joint is repaired or replaced. Hip Joints can become diseased or sustain injury that requires them to be replaced. In a "total hip arthroplasty", the ball of the femur is cut off a "prosthetic stem" is inserted into the femur, the hip socket is cleaned out of diseased bone, and an artificial socket is inserted. A prosthetic "head" is installed, and the reconstruction of the hip joint is complete. Hip prosthesis is performed with

the goal of improving range of motion, reducing pain, and improving the overall quality of life for patients.

1.2.4 Femur Prosthesis

Femoral prosthesis is the replacing of the old femoral stems and head with a new one. Femoral prosthesis can be needed if the old stem is loose, infected, or chronically dislocates. The stem can loosen due to poor cement techniques, bad fall, bone degeneration, or infection. The femur is reamed; removing old diseased bone and a new femoral component is fitted and installed, utilizing the existing acetabular component (cup). Repeated dislocations can be eliminated by correctly matching the size of the stem, the stem's offset, and the head size to the patient's anatomy.

1.3 Statement of the problem

The hip joint replacement was predicted to have a useful life of over 15 years which would have exceeded the life expectancy of many of the recipients; however some of these devices have failed after just a few years with most expected to fail within 10 years. When a primary hip replacement surgery fails, the decision for a joint revision surgery is needed based on many factors. Although joint replacement is successful in many patients, certain signs and symptoms would indicate that the implant has failed in others.

Joint revision surgery is necessary when pain, swelling, limp, stiffness, or instability of a failed prosthesis become too great. Hence, most recipients of the faulty device now face the prospect of further surgery, with pain and discomfort, in order to replace the artificial hip joint with an alternative, in addition to potential financial losses. It is obvious that any surgical attempt

may have potential complications. The complexity of revision joint surgery increases the chance of complications, including a likely defective hip device, bleeding, infection, and trauma to nerves or blood vessels are possible. The risk of these complications is higher than primary procedures during the revision surgery [13-16].

According to clinical results, there are lots of reasons that cause artificial hip joints failure. These include infection, dislocation, wear, stem fracture, loosening,etc.Other factors such as bone quality, weight, and activity level also affect the long-term success rate of artificial joints.

The challenge of aseptic loosening of prosthesis remains,the major post-surgeryconcern from the amongest failures [17, 18].Four principal causes of aseptic loosening are; mechanical failure of the implant, introduction of wears debris into the interface region, relative motion across the interface, and stress development in the femur thigh. Each of these phenomena can initiate an eventual loosening of the implant [18].

In the natural state, the stress is distributed over the entire cross section of the femur as shown in the figure 3. Bending and axial compression are the major modes of loading. The post-surgerystress state is significantly different mainly due to the manner in which the load is transferred to the femur. In this case, the load is partially transferred through shear across the prostheses interfaces [19, 20]. This altered load transfer leads to increased stresses at the interface and unloading of the bone away from the prosthesis. The reduced bending unloads the outer fibers of femur leading to a state of stress shielding. The change in the load distribution increases stresses in some regions and reduces them in others. If these changes are large enough, they can lead to a loosening effect. The other factors mentioned earlier might also play a role in the mechanical loosening but stress on prosthesis femur head is often implicated.Because the

failure rate is in the order of 1 in 10,000 for the ball head [21–24], and it is higher by an order of magnitude for thecomplete system (failure due to loosening of the stem, rupture of the stem and wear).

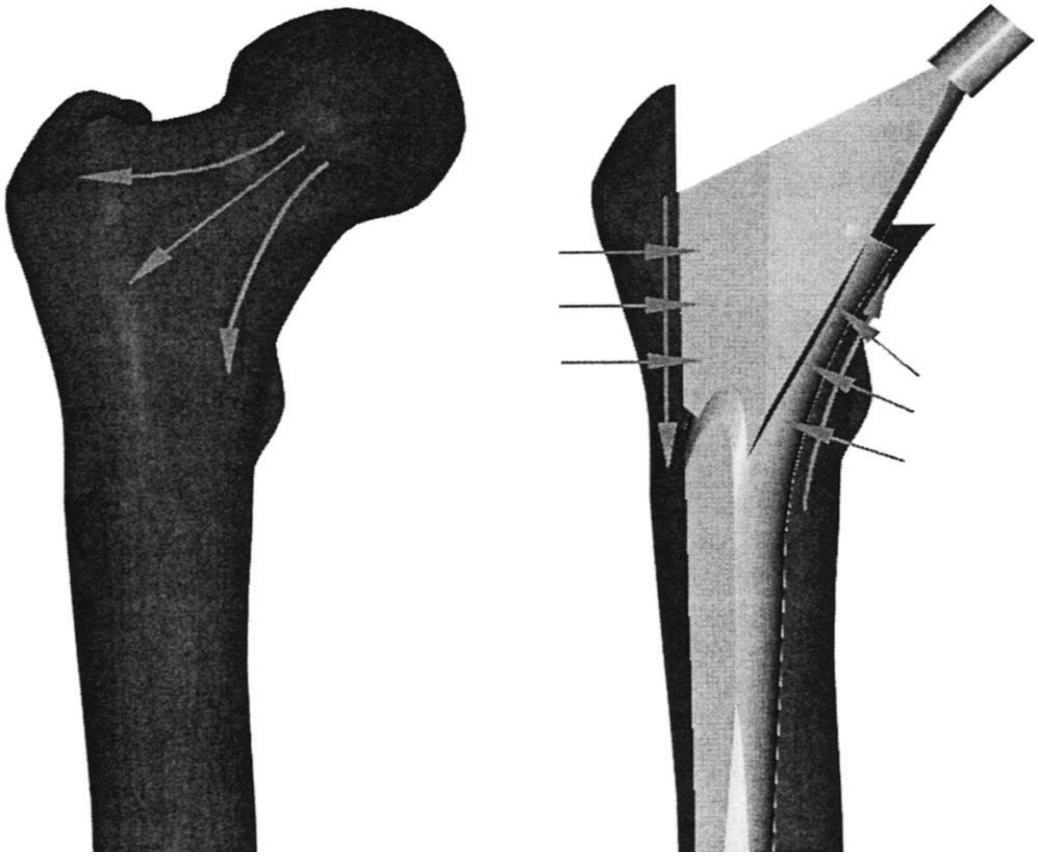

A B

Fig 1.3: Schematic Representation of the load Transfer in the Femur before (A) and after (B) hipreplacement [18]

Looking more closely at ball fractures, a minor fraction thereof has to be associated with flaws or insufficient material strength.

A higher portion originates from contamination of the contact surface between the stem and the conical borehole of the ball during surgery [25].

Hence, the reliability and the safety margin of each component have to be continuously increased to maximize the patient's benefit. Safety can be raised by reducing the load or by increasing the strength of the components. As the external load on femoral heads cannot be influenced, the focus has to be on the component's strength. Besides theuse of quality controls, the load capacity of femoral heads can be increased further by increasing the strength of the component, via material or design optimization [26, 27]. All stress components can be influenced by the design. These stresses in the contact area between stem and ball head are mainly defined by the taper angle, and affected by the fillet shape and the wall thickness of the bottom. Reducing the stress concentrations in the femoral head may also improve its durability; it therefore contributes to a greater reliability of the entire system.

The motivating hypothesis for the current study isthat an alternate femoral head borehole shape design will reducethe level of stress around femur head connection. We reiterate that other issues will generally be of concern, but for the purposes of this paper, prosthetic femur head stress is the primary design criterion.Hence, the present study attempts to improve the long term performance of the total hip joint replacement by reduction of stresses on the artificial femur head through introducing appropriate geometric shape and selection of prosthetic material for the femur head and neck. A 3D finite element modeling has been used to investigate the changes in the stress values to predict the safe zone from the introduced geometries.

1.4 Objective of the Thesis

- **General Objective**

Minimization of stress concentration developed oncontact surface between the stem neckand the conical borehole of the artificial femur head in hip joint prosthesis. This can be achieved by varying the borehole shapes design and selecting the proper prosthetic material.

- **Specific objectives**

- ❖ General evaluation of mechanical reliability for femur head in terms of stress concentration.
- ❖ Determining the effect of taper bore conical contact length using FEM.
- ❖ Analyzing the stress concentration on femur head considering design of borehole geometry.
- ❖ Minimizing the stress till having the safe zone with minimum value.
- ❖ Recommending the feasible borehole geometry and the material we should be using in future implant surgery.

1.5 Organization of the Thesis

The focus of this thesis is the stress minimization on artificial femur head prosthesis. Computational methods were used for this thesis to answer research questions that could not be addressed. The first Chapter well describes the general introduction, back ground, statement of the problem and main objective of the thesis. In Chapter 2 sufficient literature review is

provided so the reader can understand the structures that are being studied as well as the methods that are being used for the research. Geometric design and finite element analysis is the concern of Chapter 3. The geometries, which are introduced, are the most relevant alternatives for finding of best geometry that provide safe zone. Computational approach was used to display the failure stress values using finite element method. In Chapter 4 the methods utilized in Chapter 3 are extended to give results. Results are described in this chapter. The fifth chapter discusses the findings of the previous four chapters. The final chapter concluded all the work that has been done and the limitation of the study as well as further work which supposed to be done in future are highlighted.

CHAPTER TWO

LITERATURE REVIEW

2.1 Femur Bone

The femur is the longest and strongest bone in the body of the skeleton, with the thickened shaft preferentially preserving in archaeological deposits.Long bones are characterized by a shaft, the diaphysis that is much longer than it is wide. The femur bone is the most proximal bone of the leg in vertebrates capable of walking or jumping. In human anatomy, the femur is the longest and largest bone but strongest under compression only.The femur at its bottom portion meshes with the tibia bone to create the knee joint. At its top end, the femur meshes with the acetabulum to create the hip joint. The femur is responsible for bearing the largest percentage of body weight during normal weight bearing activities. [28]

The shaft of the femur is fairly cylindrical and bowed with a forward convexity. On its proximal end a rounded articular head projects medially on a short neck and articulate with the acetabulum of the innominate. Distally the shaft expands into a broad, double condyle which articulates with the tibia. The femur has five ossification centers, one each in the shaft, head, greater and lesser trochanter and distal end. Epiphyseal union is normally completed by 17-18.5 years, with the distal epiphyses closing last of all.

Femora are able to provide information for purposes of stature estimation, sex determination and the identification of regional, or "racial", origin. Because in the erect posture it is not vertical, being separated above from its fellow by a considerable interval, which corresponds to the breadth of the pelvis, but inclining gradually downward and medialward, so as to approach its fellow toward its lower part, for the purpose of bringing the knee-joint near the line of gravity of the body. So, the degree of this inclination varies in different people, and is greater in the female than in the male, due to the greater breadth of the pelvis. [29]

The femur, like other long bones, is divisible into a body and two extremities.The upper extremity, the more important in this work, presents for examination a head, a neck, a greater and a lesser trochanter. The head, which is globular and forms rather more than a hemisphere, is directed upward, medialward, and a little forward, the greater part of its convexity being above and in front. Its surface is smooth, coated with cartilage in the fresh state, except over an ovoid depression, the fovea capitisfemoris, which is situated a little below and behind the center of the head, and gives attachment to the ligamentumteres. The femur is ossified from *five* centers: one for the body, one for the head, one for each trochanter, and one for the lower extremity.

In every part of the femur there is a remarkable adaptation of the inner structure of the bone to the

mechanical requirements due to the load on the femur-head. The various parts of the femur taken together form a single mechanical structure wonderfully well-adapted for the efficient, economical transmission of the loads from the acetabulum to the tibia. The bony material is arranged in the paths of the maximum internal stresses, which are thereby resisted with the greatest efficiency, and hence with maximum economy of material [30].

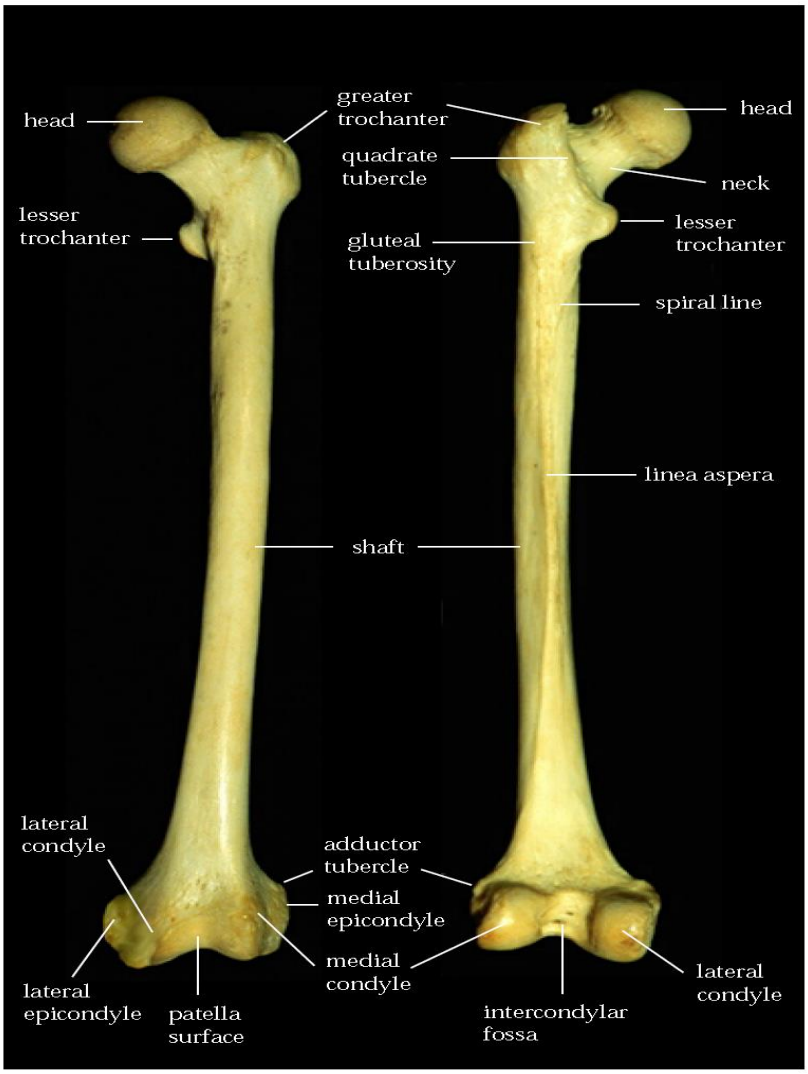

Fig 2.1: Femur Bone Structure[28]

The inner structure and external form of human bone are closely adapted to the mechanical conditions existing at every point in the bone. The inner architecture of normal bone is determined by definite and exact requirements of mathematical and mechanical laws to produce a maximum of strength with a minimum of material. The spongy bone of the upper femur (to the lower limit of the lesser trochanter) is composed of two distinct systems of trabeculae arranged in curved paths: one, which has its origin in the medial (inner) side of the shaft and curving upward in a fan-like radiation to the opposite side of the bone; the other, having origin in the lateral (outer) portion of the shaft and arching upward and medially to end in the upper surface of the greater trochanter, neck and head. These two systems intersect each other at right angles.In the shaft, the inner architecture is configured in order to be economic for resisting shearing stresses, bending moment and axial stress. Its structure is such as to secure great strength with a relatively small amount of material.

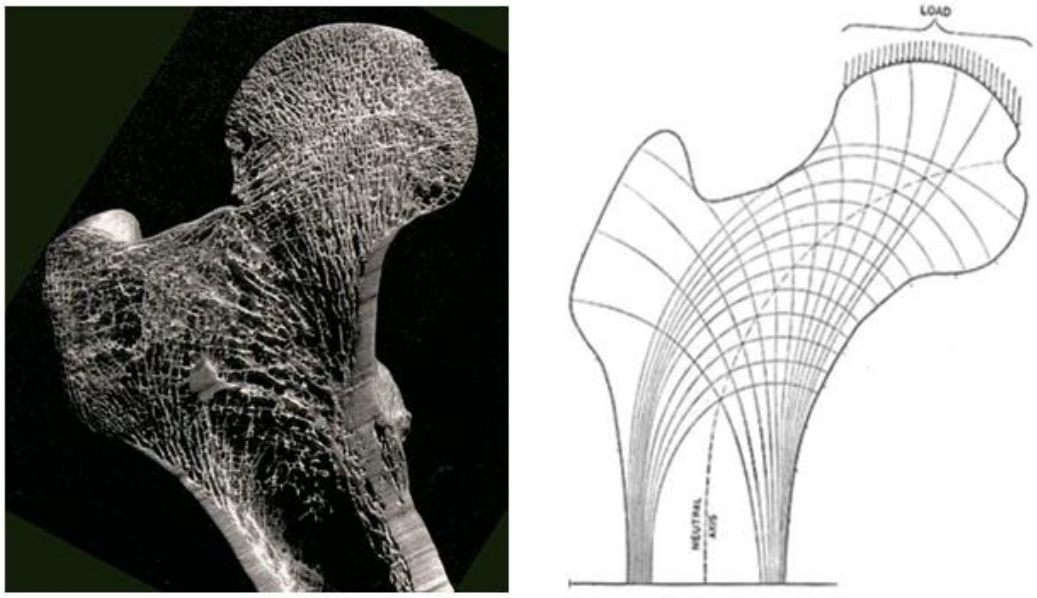

Fig 2.2: Photograph of the Upper Femur in Coronal Section (left), and Diagram of Lines of Stress (right), based upon the mathematical analysis of the right femur [18].

The human femoral head shape is not a perfect sphere; butthe artificial femoral head is made spherical due to simple manufacturing. The shape may significantly affect the mechanical characteristics of artificial hip joint.

2.2 Femur Borehole Shape

The structure, geometrical shape and material are the three main parts of the femur of hip joint prostheses. The geometrical shape of human natural femoral head is similar to the ellipse, but, the artificial femoral head is rotundity shape. There is difference between ellipse and rotundity femoral head. Two models are developed and analyzed by Finite element analysis method. Based on the calculation results, it is shown that the ellipse shape femoral head have the similar characteristics to the natural joint than rotundity model. But the ellipse has the more lowness stress distribution area and more smalldistortion magnitude than rotundity shape artificial femoral head. It should have themore kind effect replace rotundity femoral head with ellipse shape artificial formal head [31].

AO Andrisano, E Dragoni and A Strozzi, [32] an alternative head design, characterized by a cylindrical engagement with the stem, is analyzed with the same techniques and its merits are explored. The selection of aparticular head is made during implantation according to the specific anatomical needs. The three balls are now referred to as short neck, medium neck, and long neck heads. Due to the presence of frictional forces and to the small size of the cone angle, the press-fit connection proves to be self-locking, thus requiring no additional fasteners**.**Unfortunately, the simplicity and stability features of this engagement are coupled with a serious drawback. As a

result of the wedge effect, the compression load transferred by the joint promotes high tensile hoop stresses within the head. This state of affairs is particularly detrimental for ceramic materials, which can exhibit a tensile to compressive strength ratio as low as 0.1. Consequently, thejoint ruptures generally concern the ceramic head, rightly regarded as the weakest part of the implant. In the case of the above shape medium neck and long neck balls, the load capacity decreases as the angular error increases, this is consistent with the outcome of the contact pressure peak in a region of reduced radial thickness. Conversely, for short neck balls the rupture load remains appreciably constant within the limits of a higher scatter of the results.

C. Affolter et al [33] In order to hold a ceramic head firmly, a metallic stem is fitted into the taper-borehole of the ceramic ball head. Depending on the preference of manufacturers and the ease of manufacturing, at that time there were two types of taper borehole shapes are used in THR. One is the flat bottom shape with a filet at the corner of a ceramic taper-borehole, where a stress concentration occurs at the filet corner.

J. Middleton et al [34] have introduced the other shape which is known by the keyhole shape which has an undercut at the corner of the taper-borehole. The surface with such an undercut shape is difficult to machine, which often leaves a low surface finish and causes further stress concentration sites. As ceramic is brittle and prone to fracture under a critical tensile stress, these currently used borehole shapes can actually reduce the mechanical reliability of ceramic femoral heads in THR.

In order to minimize the stress concentrations, M. Sharif Uddin and L.C. Zhang [35] introduced the following new shapes of borehole designs for stress evaluation: dome arc, and dome ellipse on the bottom of the ceramic taper bore. In the case of the dome arc, a spherical dome is formed at the bottom of taper-bore, while for the dome ellipse; the taper-bore's bottom

surface is a half of an ellipsoid. The radii of the dome arc and dome ellipse can be chosen such that the transition between the taper-bore and the bottom dome is smooth (tangent to each other) to avoid the local stress concentration.

Since the geometric shapes of these new designs are simple, they are easy to fabricate in the pre sintering stage of the ceramic heads to achieve a surface finish.

According to S.Shan and S. Ge [36] they had been studyingthe shape effect of femoral head onmechanical behaviors of artificial hip joint. Three hip joint models with different femoral head shapes (spherical, ellipsoidal and rotational conchoids) were established in the finite element analysis software, and the differences among the proposed models in terms of deformation, stress were studied in both static and dynamic conditions.Later on the results indicated that, the ellipsoidal femoral head is the best of all. The natural femoral head is most likely a rotational ellipsoid shape, which will lead to redesign of artificial femoral head, and improve the service life of artificial hip joint. Even though, in other study by Menschik's reports, the human femoral head was verified to be a rotational conchoids [37].

The human hip joint is a typical ball and socket joint, and primarily consisted of the femoral head and the acetabulum. According to Hammond et al.'s study, the human femoral head is spherical [38]. Due to its convenience in manufacturing and good effect in clinic, thespherical femoral head is adopted in every artificial hip joint todate. However, more and more scientists query the shape of natural hip joint in recent years.

2.3 Implant Material Review

A material used as an artificial body is known by biomaterial which is a material that interacts with human tissue and body fluids to treat, improve, or replace anatomical element(s) of the human body. Biomaterial devices used in orthopaedics are commonly called *implants*; these are manufactured for a great number of orthopaedic applications. Among those materials used in artificial hip joints is one of the biomaterial that should have to meet high demands. The optimal material should be biocompatible, corrosion resistant, sufficiently strong to sustain the cyclic loading endured by the joint, and should be high wear resistance to minimize debris generation.

It is important for orthopaedic surgeons to understand the nature of biomaterials, their structural configurations, and their properties, as well as the effects of their interaction with soft and hard tissues, blood, and intra- and extracellular fluids of the human body. The orthopaedics field has benefited from the great efforts of many orthopaedicurgeons, experimental surgery laboratories, and research centers and from research work at universities, academies, societies, scientific organizations, and many interdisciplinary groups. However, many challenges remain to be conquered in the development of new biomaterials that will improve the long-term performance of clinical results in orthopaedic surgery. The main biomaterials used in orthopaedic surgery are reviewed possibly in their chronological order.

Wood: Carnochan (1840) was the first surgeon, who thought that hip joint could also be replaced artificially. A wooden block was installed between the damaged ends of a hip joint in New York by Carnochan. Later on, several other biological and foreign materials were used. These included as skin, fascia, muscle, pig bladder, and gold foil. Unfortunately, all these

surgeries led to unpredictable, painful results and failures. Wooden prosthesis produces very large wear particles in the body fluid.

Gluck introduced femoral stem in 1890, which was experimented with the ivory joint and found that human body could not tolerate large foreign objects [39].

In 1919, Delbet used a rubber femoral head to treat femoral neck fractures. Groves placed an ivory nail to replace the articular surface of the femoral head, in 1926. Later on, this technique became a model for short stemmed femoral prosthesis.

A surgeon in Boston, Massachusetts, Dr Marius N Smith-Petersen, MD [39], introduced the mouldarthroplasty (1925). He used a reactive synovial like membrane that he found around a piece of glass in a workman's backyard. The original design was ball-shaped hollow hemisphere of glass as shown in Figure 2, which could fit over the ball of the hip joint. The objective was to stimulate cartilage regeneration on both sides of the moulded glass joint. Smith-Peterson intended to remove the glass after the cartilage had been restored. Glass provide new smooth surface for movement. While proving biocompatible, the glass could not withstand the stresses of walking and quickly failed. This led to use of other materials, such as Viscaloid (a celluloid derivative, 1925), Pyrex (1933), Bakelite (1939), and later that year, an alloy of Cobalt-Chromium is called Vitallium (1936). Vitallium turned out to be inert and durable material for this type of surgery. This was a significant of 1936. This Vitallium material was very strong and resistant to corrosion, and continued to be employed in various prostheses since that time. However, surface quality of this alloy was less than adequate, hence, pain relief was not as predictable as expected and hip movement remained limited for several patients.

Fig 2.3: Bell Shape of the MouldArthroplasty[12]

Plastic: Plastics have superior surface finish and very low co-efficient of friction. But it has low strength, and produces very fine wear debris, which are absorbed by bone and blood, leading to adverse effects in brain. Wear debris generation is one of the main problems with modern hip replacements. The particles of polyethylene from the cup liner are attacked by body's immune system, destroying the bone in and around the implant, eventually leading to loosening of the implant. Wear debris induced osteolysis is caused by adverse cellular reactions with wear particles in the body [39]. Dr. Jean Judet and his brother, Dr. Robert Judet (1938) of Paris, attempted to use an acrylic plastic material to replace arthritic hip surfaces. This acrylic provided a smooth surface, but unfortunately became loose after implantation. The Judet brothers developed the first short stemmed prosthesis in 1946. Designed on the basis of Groves nail, it was made out of poly-methyl-methacrylate (PMMA) with a head that was 3/2 of a sphere attached to a short stem [39].

Metal-on-Metal: Metallic prosthesis has high strength and toughness. However, it causes problem in human body due to corrosion, wear and adverse reaction with host tissues. The metallic ions produce soluble metallic salts that enter the body fluids like blood and urine.

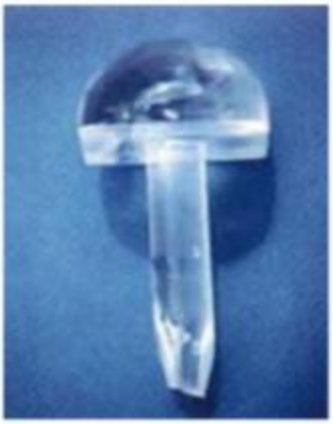

Fig 2.4: First Judet Stem Installed in 1946, Failed due to wear debris of the Acrylic [12]

A cobalt chromium hip prosthesis was first used in 1938 for cup arthroplasty by Dr. Marion Smith- Peterson [40]. The original alloy (Vitallium) came from the dental industry, where it was used for bridges, dentures, and orthodontia. Dr. Smith-Peterson's dentist, Dr. J.W. Cook, called his attention to the work of Drs. Charles Venable and Walter Stuck in 1938 [40,41]. H.R. Bohlman first used a Vitallium femoral head and neck replacement in 1939 by attaching a Vitallium ball to a tri-flanged nail.Bohlman and Austin Moore performed the first successful femoral head prosthesis implantation in 1940 [42]. Vitallium was attractive because of its corrosion resistance and electrolytic inertness. Bohlmanburied different metallic prostheses on his farm and implanted them in animals before determining they were suitably inert [42, 43].All implants will ionize after implantation but cobalt chromium remains the most corrosion resistant [41, 42, 44]. In 1951, George McKee began using stainless steel for total hip replacement but all prostheses failed. He began using cobalt-chromium Thompson prosthesis in 1956 and refined his McKee-Farrar Prosthesis in 1966 (Fig. 1) [45, 46, 47] Dr. Charles O. Townley originally used stainless steel for femoral head resurfacing in 1951 but also quickly moved to cobalt chromium [48]. The Peter Ring prosthesis, starting in 1964, also utilized cobalt chromium [49].

Marshall Urist, Earl McBride, and Maurice Mueller all used cobalt-chromium but Sir John Charnleyused stainless steel, articulating it with polyethyleneafter a failed attempt using Teflon [50, 51, 52, 53]. McKee in 1971 first reported metallosis following metal-on-metal total hip replacement. He described two patients who developed pain 3½ and 4½ years following total hip replacement. Both had sterile necrotic material at exploration [46]. Seven additional patients were described by Jones, et al in 1975. Their patients developed symptoms between 9 months and 4 years following McKee-Farrar total hip replacement [54].Affected patients developed progressive pain and a feeling of instability. Bone loss with soft tissue necrosis was found in all cases. Two patients had spontaneous dislocations. The tissues were stained green or grey and a paste was found around a thickened capsule. Highly elevated levels of cobalt were found in the serum and joint fluid. Large joint effusions with either rust, green, cloudy yellow or grey-colored fluid were found in all cases [46, 54].

McKee-Farrar prostheses were manufactured as a matched set with the acetabular component made, matched, and tested to accompany the femoral prosthesis [45]. This manufacturing technique would be desirable today but no manufacturer offers their implants prepared and tested together. McKee-Farrar hip replacement was abandoned in the early 1970s as other prostheses proved more successful. Metal-on-metal hip resurfacing was performed initially by Dr. Edward Haboush in 1951 and occasionally until the mid1970's [52, 55, 56 & 57]. There was no mention of metallosis in the early reports. With superior metallurgy, metal-on-metal resurfacing began again in 1988. It increased in popularity and in 2006 a full FDA approval for metal-on-metal resurfacing was obtained [58, 59]. All implant manufacturers indicated their metallurgy had improved and the critical nature of component positioning were not emphasized. In fact, the large diameter of metal prostheses was felt to protect against dislocation even in instances of

component malposition. Starting in 2008 reports of "pseudotumours" with metal on- metal resurfacing began appearing in the literature [60].Such cases are now regularly reported.

Ceramic-on-Ceramic: The advantages of COC over MOM implants are that COC implants show less wear than MOM implants. The most common ceramics Al2O3 and ZrO2 exhibit high mechanical strength and good biocompatibility. COC components demonstrate significantly lower wear compared to conventional metal on- plastic prostheses [61]. Therefore, these improved wear characteristics extend life of the implant. However, ceramics implants have very low fracture toughness values compared to metals or polymers, which turn is undesirable for an implant.

Bio- ceramic: More recently, in last two decades, there has been considerable interest in bio-ceramic materials like hydroxyapatite (HA). Development of this material has stabilized the Femoral Stem Technique [62]. Development of medical grade hydroxyapatite and various other apatite materials are under research for hip joint prosthesis development.

2.4Force and Stress on Femur Head prosthesis

Knowledge of the forces acting on the human femur is of significant importance to health care professionals. Determination of these forces during walking and other daily living activities allows the subsequent calculation of the stresses induced in the femur and therefore the localization of the areas of frequent appearance of femur fractures. Furthermore, these forces are of great interest in the cases of total hip prostheses as well as in femoral neck and head fractures. In all these cases mechanical failures have been observed and therefore, a more sophisticated

design of the surgical procedures and implants used to repair such cases necessitates knowledge of the forces responsible for the failures.

The first attempt to determine such forces was made by Braune and Fischer [63]. They tried to calculate the forces acting in various parts of the body during walking. However, the lack of a suitable instrument for measuring the ground reaction on the foot limited their experimentations. Other early investigations on this subject have been performed by Fick [64].

Later, Bernstein et al. [65] improved the techniques of Braune and Fischer but their results suffer in the mathematical analysis. Elftman [66-68], using an instrument for measuring ground force on the foot, advanced the analysis of joint and muscle forces was made. Pauwels' performed an analysis of forces acting at the hip joint during walking based on the experimental work of Braune and Fischer.

Inman [69] made an analysis of the forces exerted by the abductor muscles of the hip for the one-legged standing. Other two-dimensional analyses of the forces in one-legged standing were performed by Blount [70] and Strange [71]. A three dimensional analysis for this case was made by Williams [72]. Bresler and Frankel [73] analyzed the forces and moments in the leg during level walking and determined the resultant force transmitted by the leg to the trunk. However, they did not calculate muscle and joint forces.

Rydell [74, 75] was the first to perform direct measurements of the loads transmitted by the hip joint during invivo experiments. He used instrumented prostheses implanted in two patients who had suffered femoral neck fractures. By fitting strain gauges to the prostheses he obtained the hip contact force during gait. However, the values of the forces thus obtained are not, generally, equal to the forces existing in the normal joint. Sorbie and Zalter [76] used a correlation of the

torque at the hip joint and the electrical activity of the muscle for the determination of the tensile forces generated in the individual muscles of the hip joint. It was found that such correlation can only be precisely computed when activity is restricted to a single muscle of a given opposing pair, a condition which is obtained only for a limited period of a full cycle. More recently, Ghista et al. [77] proposed a semi- direct experimental method for the determination of muscle forces. This method used electromyography and was based on the assumption that the force exerted by a muscle depends exponentially on the time-derivative of the rectified integrated EMG signal. However, due to the fact that this assumption has not yet completely been verified and the EMG data obtained were not satisfactorily accurate, the proposed method has not yet been established. Due to the difficulties inherent in the direct or semi - direct methods of measuring the forces acting on the femur, other indirect methods have been introduced. According to these methods the resulting forces and moments at the human body joints are determined by modeling the body as a system of rigid links and applying the laws of statics and dynamics to the corresponding system. Experimental measurements of the pertinent kinetic quantities are used. Then the resulting forces are distributed to the various load-carrying parts of the joint according to the joint anatomy. At this point some simplifying representations of the load-carrying parts must be made.

For the distribution of the resulting forces to the load-carrying parts of the joint, two main methods have been developed. The first method reduces the initially indeterminate problem to a determinate one and was developed by Paul [78-81] and Morrison [82]. These investigators measured photographically the three-dimensional configuration of the leg segments during a walking cycle and used a dynamometer to measure the corresponding ground-to-foot forces. From these measurements they calculated the resulting forces and moments acting at the various

leg segments by using the procedure introduced by Bresler and Frankel [73]. For the determination of the forces acting at the joints the whole anatomical system of muscles was analyzed. The twenty-two muscles acting at the hip and the fourteen muscles and the six ligaments acting at the knee are simplified to groups; and the forces at each group were determined from equilibrium equations. Then from these forces the joint forces were obtained. For the knee, explicit solutions for these forces were produced, while for the hip only limit curves between which the actual joint forces lie were determined. The above presented method was also used by Chao et al. [83] to distribute the resulting forces in the finger joint.

The second method for the distribution of the resulting forces to the load-carrying parts of the joint is called the 'optimization' method and was introduced by Seireg and Arvikar [84] and Penrodet al. [85] This method was based on the assumption that the distribution of forces occurs in such a way as to fulfill the requirement of optimization of some kinetic property called the objective function. Because it is not known in advance, the proper objective function, the suitability of the elective function must be established from the results obtained. This method was first applied to gait by Seireg and Arvikar [84]. Crowninshieldet al. [86] used the optimization method to distribute the resulting forces to the load-carrying structures in the neighborhood of the hip and to the two joint muscles that flex and extend the knee and ankle. Kinematic data were obtained by attaching triads of flashing, light-emitting diodes to the pelvis, thigh, shank and foot and photographing them by a bi planar technique, while for obtaining kinetic data a piezoelectric force platform was used. Results concerning the kinematic and kinetic quantities about the hip during level walking, stair climbing and descending, and rising from a chair were presented and discussed.

Finally, Debrunner [87] developed a new model for the determination of the forces acting on the head of the femur as well as the maximum pressure of the femoral head. The model was based on the determination of a fixed point, the attachment of the resultant muscle force at the pelvis and the insertion of the muscle force at the trochanter. After determination of the above point in a single standard radiography of the pelvis and hips, the model calculates the resultant force at the hip joint.

Hence, the determination of the internal stress field induced in the human femur under the action of forces is of significant importance both for the localization of the more severely loaded areas from which fractures would initiate and for the efficient design of implants and joint replacements.

Knowledge of the forces to which the femur is subjected, its internal architecture and the mechanical behavior of its materials, as they were analyzed in the previous sections, constitute the prerequisites for the application of the methods of mechanics for achieving such goals. Due to the complex structure of the femur and the complicated mechanical behaviour of its materials, application of the stress analysis methods to the case of the femur requires the adoption of a number of simplifying assumptions. In the following we will briefly review from the existing literature the mathematical and experimental methods which have been used for the analysis of the mechanical behavior of the femur. From the mathematical methods we will present those using beam theory and finite elements, while from the experimental methods those using brittle coatings, strain gauges and photo elasticity. All these methods can be classified into direct and indirect with respect to whether they use in their analysis the actual femur itself or a model of the femur. Finally, at the end of this section we will present methods dealing with the strength characteristics of the artificial prosthesis from the stress analysis approach

2.5The Stress Analysis Methods

The mathematical methods for the determination of the stress distribution inside the femur necessitate the construction of a model from the actual femur; therefore they are indirect methods. Recourse to a model simulating the real femur is needed for the application of the principles of these methods to the solution of the existing problems. The model should take into account the essential properties of the femur and it should adequately describe the reality. The success of the model can be assessed by comparing the results obtained with the corresponding results of other direct methods. The mathematical methods used for the stress analysis of the femur can be classified into those based on the beam theory and the finite element method.

Beam theory:The first basic work concerning the stress analysis of the human femur is due to Koch' who published the results of his investigations about half a century ago. Although this work presents many inaccuracies it still remains the most thorough and meticulous investigation on the femur. Koch applied the general principles of strength of materials to the case of the femur which he simulated as an isotropic, homogeneous, elastic body. His study concerned the femur of a man of normal health, two-hundred pounds weight who was killed accidentally. He made a complete analysis of the structural properties of the femur sections (determination of Centre of gravity, area, moments of inertia) and determined the axial, shearing force and bending moment diagrams along the femur. He simulated the femur as a two-dimensional beam and assumed that it was loaded to a concentrated in-plane force acting at the femoral head.

Therefore, in his analysis the effects of the torsion moment, bending moment and shearing force along two axes were not incorporated. By using the simple bending theory of straight beams he calculated the normal and shear stresses and from them the values and the directions of the

principal stresses. On the basis of these results he constructed the principal stress trajectories and gave the values of the principal stresses at the points of their intersections for the upper part of the femur as well as the maximum stresses in the femoral shaft. Furthermore, Koch gave a complete description of the inner structure of the femur and based on Wolff's theory of bone architecture [88] he came to the conclusion of the functional form of the femur. He showed that the external form and the internal structure of the femur are such as to resist the stresses produced by the predominant body-weight force in the most economical manner. Thus, the spongy bone of the upper femur resists efficiently the shear stresses which take their maximum values in the head and neck.

In the shaft the shear stresses are minimum and the normal stresses due to bending take their maximum values. Therefore, the hollow construction of the shaft with the cortical bone concentrated at great distance from the neutral plane provides the most economical manner for resisting the bending moments. Finally, the lower end of the femur is formulated by the transition of compact to spongy bone to a large area to render the hinge-action of the knee joint stable against lateral bending.

Many years later Toridis [89] in an interesting work made a further step to improve the mathematical model of the human femur. Handling the problem within the framework of the simple beam theory, he simulated the femur as a three-dimensional space curve. This implied that torsion moments in excess to the axial and shearing forces and bending moments entering in the two-dimensional analysis should be taken into consideration. Furthermore, for the three-dimensional case the shearing forces and bending moments act along two mutually perpendicular axes. Using the principles of the strength of materials he gave the appropriate formulas for the calculation of the resulting normal and shear stresses due to axial and shear forces and bending

and torsion moments. He took into account in his analysis muscle forces in addition to the body-weight which, following Koch, he simulated as concentrated force acting on the head of the femur. However, while in his study Toridis described the method of analysis of the femur and gave the appropriate formulas for the computation of the stress field, he did not make any numerical calculations to show the influence of the three-dimensional analysis on the values of stresses. Therefore, from this work no assessment can be made on the significance of the additional normal and shear stresses produced by the torsion moment as well as by the second component of the shear force and bending moment. Furthermore, the femur was considered as an isotropic material and the different mechanical properties of the cortical and cancellous bones were not incorporated in the analysis.

Rybickiet al. [90]calculated the stresses in the human femur using both the simple beam theory, as in the previous two works, and a continuum theory in the form of a finite element computer program. In the analysis they included both joint and muscle forces. From a comparative study of the results of the two methods they came to the conclusion that the beam theory is appropriate for the calculation of stresses in the shaft of the femur, but it is inadequate for the determination of stress distribution in the upper and lower regions of the femur. This should be expected due to the complexity of the geometrical shape of the femur in such regions, which does not allow its simulation as a beam. For these regions the continuum model should be used.

Piotrowski and Wilcox [91] developed a computer program for the determination of bending and torsional stresses in long bones. The objective of this program was to bypass the difficulties inherent in the calculations due to the complicated geometrical configuration of the bone which is impossible to describe it mathematically in closed form. The description of the geometry of the cross section could be made by any desired number of points. For the case of the torsional

stresses the program allows the numerical solution of the Laplace equation satisfied by the stress function. For this reason the finite difference equivalent of this equation is formulated. Bending stresses were computed by using the basic formulas of the beam theory.

Nowinski and Davis [92] in theoretical investigation simulated the bone as a two-phase poroelastic material with the osseous tissue considered as a perfectly elastic solid and the fluid substances filling the cavities as a viscous compressible fluid. Furthermore, the bone was considered as transversely isotropic material. Using the fundamental equations of the theory of elasticity they obtained seven constitutive equations connecting seven stress components with seven deformation components through eight material constants. These equations were applied to the case of a beam subjected to torsional or bending moments and terminal forces. For the first case the stress and strain fields do not depend on the coordinate along the beam axis, while for the second case a linear relationship was assumed. Examples dealing with cylindrical bending by end couples, pure bending of beams of arbitrary cross section having one axis of symmetry and pure torsion of beams with arbitrary cross section were given. Other works dealing with the investigation of the human femur with the beam theory are those of references [93-95].

Finite elements: From the first days of its appearance, the finite element method has become very popular in the engineering world. This method provides a powerful tool for the mechanical analysis of complex structures, such as dams, aircrafts, and nuclear reactors. The method consists of dividing the structure under investigation into small elements and applying the relevant equations to them instead of the complex structure. The appropriate connection of the elements allows the determination of the values of the mechanical quantities at the nodal points. The finite element method has been widely used in biomechanics for calculating the stress distribution within the body. The first application of the method to the case of the human femur was made by

Brekelmanset al [96]. They simulated the femur as a two-dimensional member consisting of a homogeneous, isotropic elastic material with the same geometrical configuration as that described by Koch. The loading consisted either of one concentrated load, as it was used by Koch, or of two concentrated loads, as it was used by Rydell [75], with the second load representing muscle forces. From the finite element analysis they obtained the displacements at the nodal points of a triangular network inserted into the femur and they calculated the principal stresses and the stress trajectories. They obtained results justified Koch's findings for the functional form of the femur.

In the above work many simplifications regarding the structure of the femur were made and the potentiality of the finite element method was not completely used. The problem was more adequately treated by Valliappanet al [97],some years later, who made a three-dimensional finite element analysis of the proximal end of the femur. Linear isoparametric (with eight nodes) elements were used for four different subdivisions. The femur was modelled as a biomaterial structure with different elastic constants for the cortical and cancellous bones. No anisotropic properties of the cortical bone were taken into account. It was found that the general form of the strain distribution agreed very well with experimental strain analysis, although the absolute magnitudes showed some discrepancy. This was attributed to a possible difference in the material properties assumed in the analysis and those of the laboratory bone and to the approximations entering in the mathematical modeling (with respect to the distribution of the cortical and cancellous bones and the geometrical description of the femur with the above-mentioned elements) of the femur.

Finite element analyses were also used for the investigation of the stress distribution in the femur with implanted prostheses. Svenssonet al [98],made an analysis of the human femur fitted with a

Charnley total hip prosthesis. Due to computer limitations they used a two-dimensional approximation of a three-dimensional problem. The stress field was determined for the cortical bone as well as the acrylic and metal prosthesis stem. The effect of prosthesis location and stem thickening were also investigated. A satisfactory agreement was found with experimental strain measurements. Hampton et al. [99]performed a three-dimensional finite element analysis of the stress distribution in an implanted femoral stem. The ball of the stem was subjected to three orthogonal loads directed inferiorly, laterally and posteriorly. From the resulting stress distribution it was found that the inferiorly directed load is responsible for more clinically observed fractures. However the stresses resulting from the lateral and posterior loads were high enough to endanger the survival of these devices. Other finite element analyses of this problem can be found in references [100-103]. In these analyses the problem is considered as a two-dimensional one.

Finally, in the mathematical methods dealing with the study of stress distribution in the human femur the work by Saha [104] could be incorporated. In this work it is suggested that solutions of two-dimensional problems of the theory of elasticity of anisotropic bodies can be applied to the case of bone which was simulated as an anisotropic body. Treating the bone as an anisotropic material is an improvement over the analysis of bone as an isotropic material.

Experimental methods also used while all the mathematical methods for the determination of the stress and strain distribution in the human femur are indirect methods, some of the experimental methods are direct and some indirect. From the direct methods we will present those using brittle coatings, photo elastic coatings and strain gauges and from the indirect methods those using the photoelastic technique.

Brittle coatings: The brittle coating method was first applied to the case of the femur by Kiintscher [106-107] who used a melted colophonium as coating. The first, however, thorough application of the method to the femur was made by Evans and Lissner [108]. Their experiments comprised sixteen tests on ten adult human cadaver femurs loaded progressively in a testing machine. They observed that deformation patterns formed by cracks on the coating occurred on the superior surface of the neck and on the lateral surface of the shaft of the femur. The first cracks appeared in the neck just distal to the head, while by increasing the load more cracks appeared along the neck and the convex side of the shaft.The positions of appearance of cracks indicated the places where the fracture started, as was verified by fracturing a femur. From the obtained results it was established that the bones fractured under tension stress. Finally, they compared the results of their investigation with those obtained by other methods of study.

Further works on the stress analysis of the femur by the method of brittle coatings are listed in references [109, 110].

Photoelastic coatings: This method is used for a full-field determination of surface strains in two- or three-dimensional bodies. This method was applied to the case of the human femur by Rabischong and Avril [111], Leduc [112] and Blaimont and Wagner [113].

Strain gauges: The strain gauge technique provides a point by- point method for the determination of surface strains of two- and three-dimensional bodies.

Strain gauges have been used in biomechanics shortly following their introduction in engineering applications. Gurdjian and Lissner [114] applied strain gauges to exposed canine crania to analyze the mechanism of concussion. Evans [105] recorded tibia1 strain during gait in living dogs by bonding gauges to a chronically exposed area of the bone. However, due to

technological problems strain gauges were inadequate to monitor strains for long periods in living bones. Most of these earlier works are described and reviewed in references [114-118].

Photo-elasticity: The method of two- and three dimensional photoelasticity consists of the construction of a model of the body under consideration and therefore it is an indirect method.The first photoelastic investigation of the human femur was made by Milch [119] in 1940. He used a two-dimensional model of the femur and obtained the isochromatic fringe patterns when the model was subjected to body-weight and muscle forces. From the form of isochromatics he established a close resemblance between the lines of stress and the known trabecular arrangement of the bone. However, Milch did not make any attempt to further elaborate the obtained isochromatic patterns and his results are only of qualitative character. Haboush [120] made a two-dimensional photoelastic analysis of a femur with a neck fracture fixed with nails or nailplates. He studied the cases when the nail or nailplate were placed to the so-called bull's eye intramedullary position or in the low position resting on the calcar. By making qualitative observations of the obtained isochromatic patterns he came to the conclusion that the nail plate is the ideal appliance and should be inserted in the low position so that it rests on the calcarfemoris distal to the site of fracture. Other two-dimensional photoelastic studies of the human femur were performed by Pauwels [121] and Fessler [122].

Williams and Svensson [123] made a three dimensional photoelastic analysis of the stress field in the head of the human femur and took into consideration body-weight and muscle forces. Their loads correspond to the case of a man supported on one leg, a position which imposes maximum static load on the femur. A homogeneous photoelastic model was constructed and the stresses were locked in by using the frozen stress procedure. The results obtained from the photoelastic model were corrected so as to apply to the case of the femur consisting of two main

regions, the hard cortical shell and the softer cancellous core. They found that the bending and axial stress components show a distribution which can be predicted by an engineering analysis but the shear stress distribution is not so satisfactory. Furthermore, from the determination of the principal stress trajectories it was established that they are close to the trabecular arrangement in the upper end of the femur.

Chand et al [124]used three-dimensional photoelasticity to determine the contact stresses on the condyles of the femur and tibia under normal loading. This problem was also treated by Maquet [115] who made a two-dimensional photoelastic analysis.While the methods of analysis described above deal with the stress and strain distribution in the human femur subjected to a given system of applied loads. This analysis has been progressively advanced during the last twenty years and has been used extensively for the prediction of critical loads and the life of engineering structures.

CHAPTER THREE

GEOMETRIC DESIGN AND FINITE ELEMENT ANALYSIS

This chapter provides details software aided optimization of stress, modeling the geometry, applied materials, meshing strategies, and loading conditions that were used to analyze the models. During this research fifteen 3-D models were required for the stress analysis in order to determine the safe zone from the introduced geometries. The ability to obtain a 3-D model of a femur head with the Neck was generated in CATIA V5R16 software as IGES and STP format. IGES is mostly used format unfortunately was not successful for this paper, as a result STP format is used in exchange. Therefore, the models generated from scratch in CATIA were exported to ANSYS workbench version 12.0 (Fig 3.1)for further "Finite element analysis". The modeling process occurred in four distinct phases: These phases enhance the ANSYS software enabled a smooth transition between each step analysis.

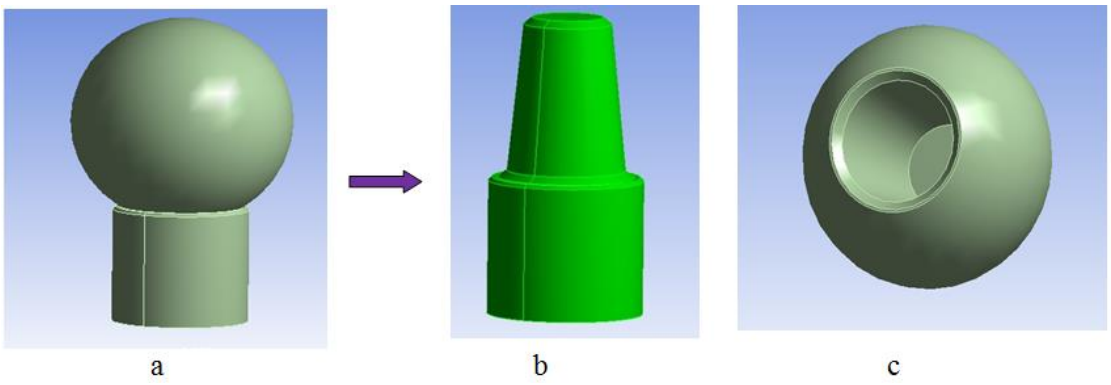

Fig 3.1 Artificial Femur Prosthetic Model in ANSYS; a) Assembled
b) Stem Neck and c) Femur Head

3.1Geometric Design Optimization Method

The basis for the stress optimization was the rupture test according to ISO 5832-12; it was used as a reference load case. The arrangement of this test is shown in (Fig. 3.2). The femur ball head is axially loaded over a replacement stem and pushed into a cone with an aperture angle of 100^0. This configuration strains the ball in all axisymmetric cross-sections in a similar way to the critical cross-section under in-vivo loading conditions.

The computer-aided optimization was applied to achieve an optimized surface shape. The method is well suited to optimize two dimensional and three-dimensional 3Dstructures and allows for the optimization with different failure criteria (the von Misses stress, maximum principal stress, maximum shear stress and Normal stress). The actual model was built in CATIA. CAO provided the superordinate program loop for the optimization using finite element software.

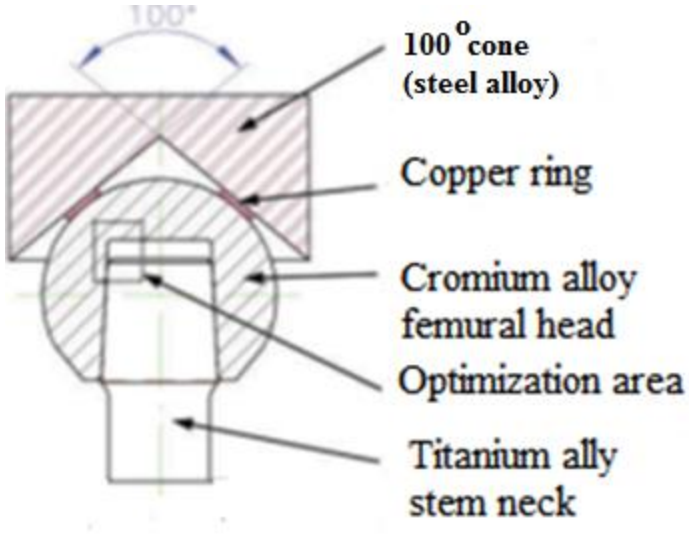

Fig 3.2: Set-up of the ISO 5832-12 Rupture Test with the Major Components Considered for the Optimization

Themethod is an iterative optimization algorithm, which has used a common finite element solver. The static analysesstress was performed with the solver ANSYS v 12.0. The implementation of this optimization routine together with the FEM is explained later in this chapter. Calculations iteratively, the structure grows on its surface in areas of initially high stresses. In the implementation with the FEM, shrinkage of surface elements with stresses below a defined threshold value can also be realized. Applying the described method, the flat bottom cornered shape is changed to a filleted smoothed shape, where the stress concentration has disappeared.

3.2Material Properties For the Femur Head and Stem Neck

Two different materials are used in the present finite element simulation: Cobalt Chromium (Co Cr Mo) alloys fall under two main categories: cast alloys (ISO 5832- 4) and wrought alloys (ISO 5832-12) [126]. Cast Co-Cr-Mo exhibits elevated mechanical properties and optimal corrosion resistance under friction condition. Its main drawbacks are related to their poor fatigue resistance and their high cost. Wrought Co-Cr-Mo is even more expensive than cast material, but the higher cost can be justified by the enhanced corrosion and fatigue resistance [127, 128, and 129]. In the presence study wrought alloy is used to simulate a prosthetic metallic head material due to their high strength and sufficient biocompatibility in clinical conditions. But, in contrast to cast Co-Cr-Mo, the tribological properties of wrought Co-Cr-Mo are poor for bearing surfaces [129]. Taking into account all these studies scholars shall continue the research to in hence the tribological properties of this alloy by Nano structured coating. These could improve topographic characterization of nanostructured coatings the surface. Taking into account that Nano structured coatings offer the opportunity to improve system's properties, and some other materials will be used and characterized to protect against hip prosthesis breakdown [130].

The second prosthetic material is Titanium alloy (Ti6Al4V) is considered one of the most biocompatible metals, which has determined the success of pure Ti (ISO 5832-2) in dentistry. However, the poor mechanical properties of pure Ti, such as smallYoung's elastic modulus and low fracture stress [130, 131], have limited its application in joint replacement. However, titanium alloyed with aluminum (Al), vanadium(V) and niobium (Nb), mainly Ti6Al4V (ISO 5832-3) [132] and Ti6Al7Nb (ISO-5832-11), are best suited for the production of uncemented femoral stems.The numbers in the formulas present the weight percentage of the alloying

elements. The improved mechanical properties of Ti alloys are at the expense of a reduced biocompatibility due to the presence of potentially toxic elements, such as aluminum andvanadium. Another limitation of Ti and Ti alloys is the drastic reduction of its outstanding corrosion resistance under friction conditions [131]. Though, titanium and its alloys are unique in that they are resistant to ductile deformation.This characteristic is related to the process in which the titanium under goes its phasetransformation in the production process. Titanium utilized goes through an alpha-betaphase transformation that improves the strength and ability to resist ductile deformation [133]. The coated Ti alloy is used as neck prosthetic for its high deformation resistance as well as its strength to resist the stress created from the load bearing of head.

Generally, the materials of the hip joint components are assumed to be homogenous, isotropic and linearly elastic. The values of elastic modulus and Poisson's ratio of the hip joint materials are summarized in the following table.

Table 3.1: Material Property of Co-Cr-Mo and Ti6Al4V

Material Properties	***Cobalt-Chromium-Molybdenum Alloy (Co-Cr-Mo)***	***Titanium Alloy (Ti6Al4V)***
Young's Modulus (Gpa)	230	114
Tensile Strength (Mpa)	530	850
Ultimate Tensile Strength (Mpa)	890	960
Density (Kg/m^3)	8300	4420
Expansion ($m/m.c^o$)	$13.6x10^{-6}$	$9x10^{-6}$
Poisson ratio	0.3	0.35

3.3Model Development

This section illustrates the development of baseline 3-D femur head implant model in CATIA. Fifteen different prosthetic models were created with different geometrical parameters. This section enlists the parameters used to design component. A final step to these procedures includes preparation of the developed models to import them into ANSYS 12.0.

3.3.1 Designing of a Baseline Artificial Femur Head Model

The first phase of the Modeling is the geometric design. During this phase of the modeling many factors were taken into account. The first of these were deciding the modeling software. CATIA V5R16 is widely used to create complex mechanical models. Selection of this software basically depended on the ease of manipulating three dimensional models and even to acquire them for future improvements.

First, two major solid components of a hip implant were created: Femoral Stem Neck and Femoral Head (see Figure 3.3). A femur implant was used to generate dimensions during the designing of this baseline femur model. Approximate stem neck dimensions in basic femur model included 20 mm height excluding the neck length.

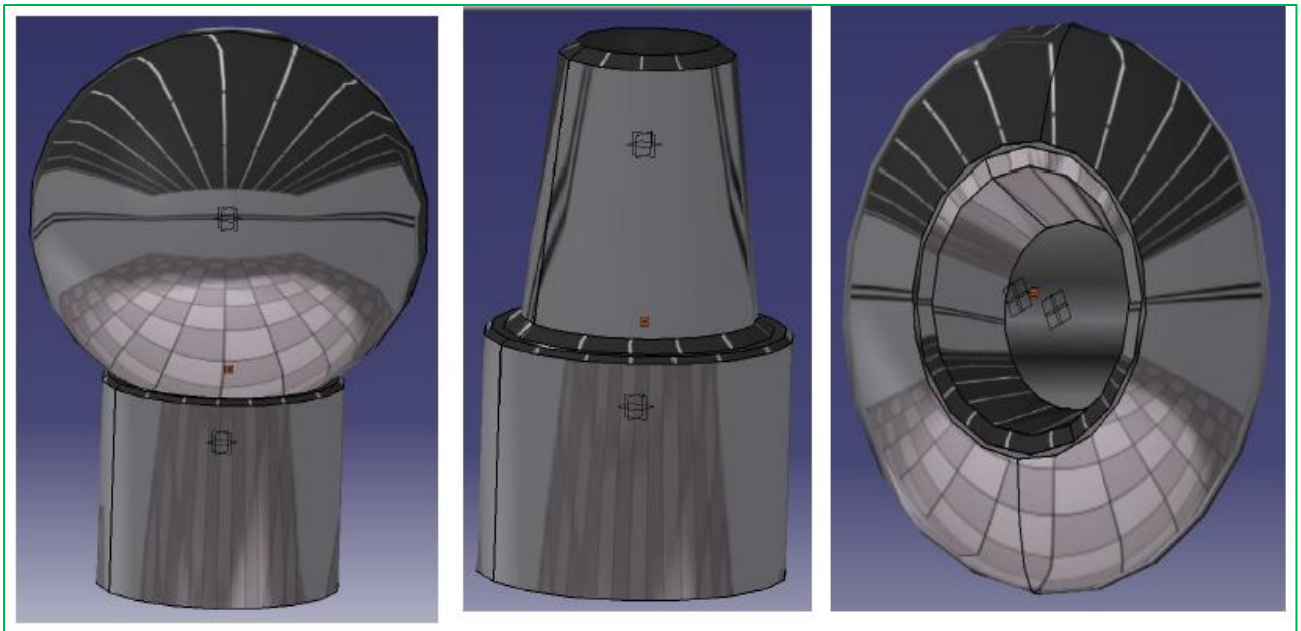

Fig: 3.3 Artificial Femur Model in CATIA

Neck length is varying with changes of desired borehole length during further analysis. Neck diameter is 17mm and neck taper angle is 5.7^0 this factors is vital in the developed femoral stem neck design. Femoral head was designed as a basic model with diameter of 36 mm and a cylindrical cut with radius of 8.5 mm was created to allow stem neck insertion. For femoral head, the changeable parameters were head diameters and the diameter of cylindrical pathway for neck insertion. But for this paper is permanently determined in the above value except the borehole length and fillet radius of the bottom flat. All the two components were used to design a femur implant assembly. Femoral head was fitted on the top of the neck. Neck diameter was adjusted for proper fixation of the femoral head. This assembly completed a design of a femoral component.

3.3.2 Geometrical Parameters and Classification of Femur Models

The head engages with one extremity of the stem neck via a conical press-fit connection this press-fit connection provides self-locking mechanism, thus requiring no additional fasteners. The spherical pair thus obtained behaves kinematic ally as the replaced natural joint. While the geometry of the stem's conical end is fixed, the head cavity is available, according to a modular concept, in two geometries, which essentially not differ in the diameter of the cavity mouth hence the press-fit comes from the taper angle of 12/14 which is globally recommended by manufactures hip implant.

Basically in this paper 15 different femur models was created according to the selected design parameters of interest. The design parameters in this study were the conical borehole depth and the fillet radius at the bottom of borehole ball head. Consistently, three distinct stem penetrations into the head bore and, consequently, three stem projections are obtained, with a borehole depth of 23mm called 36/M, where M refers to a medium neck length with 36 mm diameter of ball head (Fig.3.4 b). The resulting stress distribution for this load case was used as a reference for the optimized designs. As a further prerequisite, the optimized shape also had to be applicable for the two head types: 36/L where, L indicates a long neck length), i.e. the deepest borehole (Fig 3.4 c) and 36/Swhere, S indicates short neck length for the shortest borehole. The selection of a particular head is made during implantation according to the specific anatomical needs. The stress concentration at the actual engineering radius between taper and flat bottom of the borehole has its own effect, hence it was taken as second parameter having the range from minimum to maximum of 0.5 – 0.9 accordingly.Table 3.2 shows all 15 femur models with their design specifications for each model.Importance of the selected geometrical parameters will be discussed later in the next chapter. In this study, these two parameters were adjusted while

designing the femur model assembly to simulate the implant stability and stress state.Conical borehole depths used in this study were 25 mm, 23 mm, and 18 mm long. The fillet radius was combined with the above three specification to develop all 15 different models.

Table 3.2: Summary of all Fifteen Models Parameters

Models .no	Head Diameter(mm)	Fillet Radius (mm)	Contact Length
1	36	0.5	LN
2	36	0.6	LN
3	36	0.7	LN
4	36	0.8	LN
5	36	0.9	LN
6	36	0.5	MN
7	36	0.6	MN
8	36	0.7	MN
9	36	0.8	MN
10	36	0.9	MN
11	36	0.5	SN
12	36	0.6	SN
13	36	0.7	SN
14	36	0.8	SN
15	36	0.9	SN

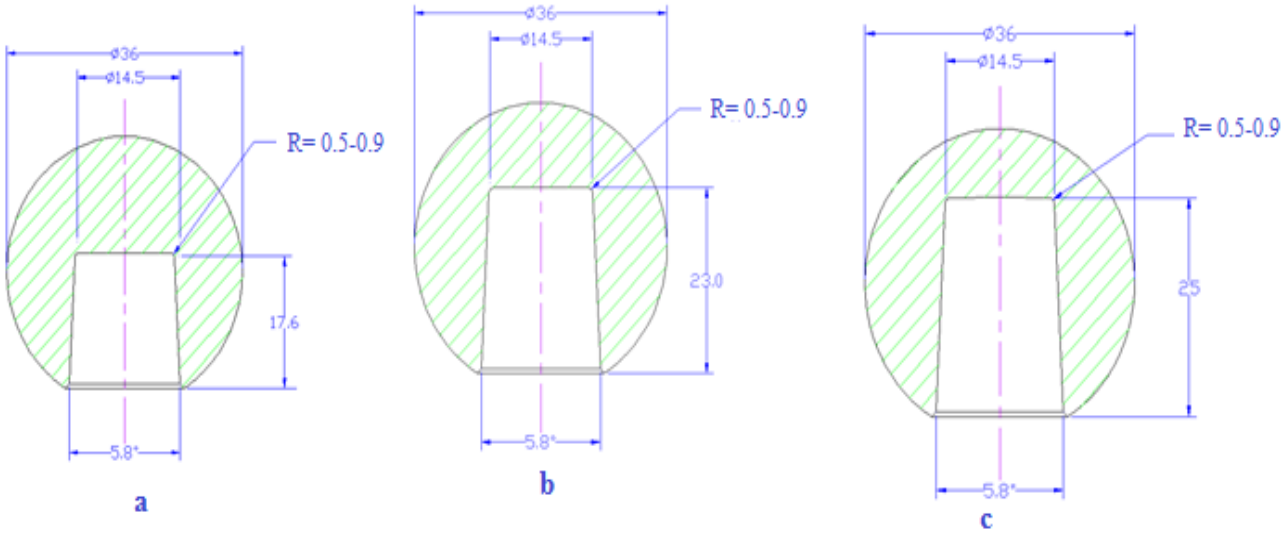

Fig: 3.4 Femur Head Geometric Shape; a) Short Neck (SN) b) Medium Neck (MN) c) Long Neck

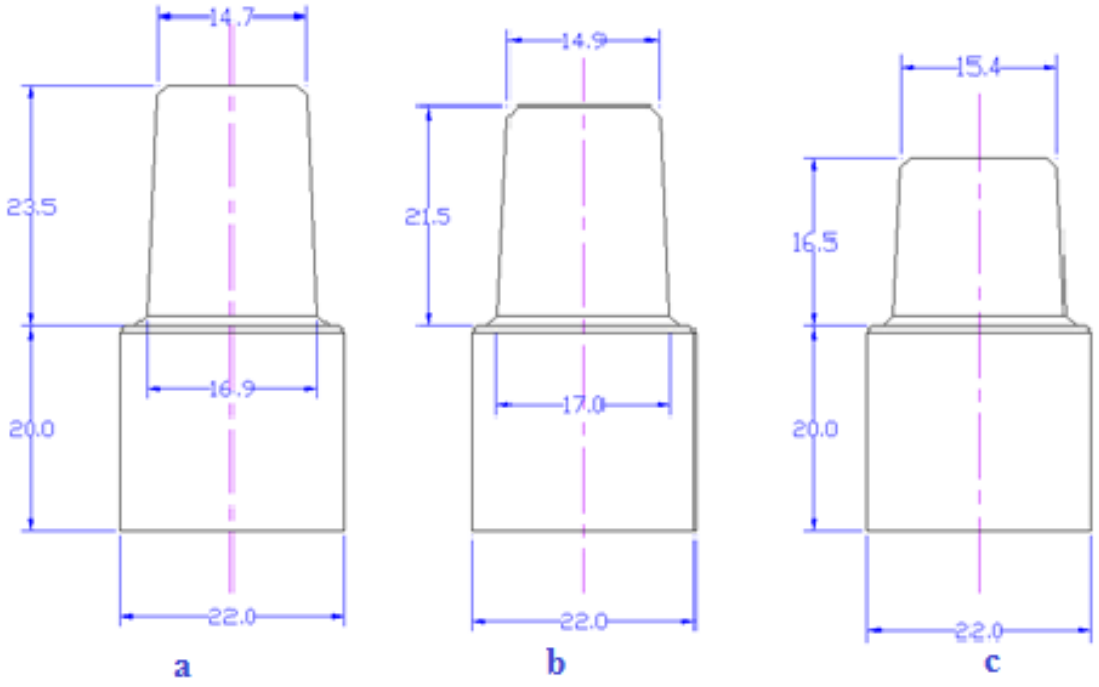

Fig 3.5 Stem Neck Geometry a) Long Neck b) Medium Neck c) Short Neck

3.4DEVELOPMENT OF FINITE ELEMENT MODEL AND FEA

Finite Element Analysis (FEA) or Finite Element Method (FEM) is a relatively new method for solving complex engineering and mathematical problems. Since the 1940s, this method has evolved into the method of choice for computational analysis. In the early years, the finite element method was limited to the manpower available to solve large matrices. However, as technology has evolved FEM has evolved into a computational jug naught. This process is now only limited by the capabilities of the available hardware to solve matrices that can go out to machine epsilon. FEM is a part of many engineering applications such as structural mechanics, heat transfer, fluid flow, electromagnetic, blade design in orthopedic design for implants and prosthetics. It has become a key part of the design and refinement processes in engineering.

3.4.1 Basic Steps in the Finite Element Method

The first step in utilizing the finite element method is to discretize a continuum problem in to a finite problem. This means to break down an infinite number of unknowns into a know number. Through this process a given area, a finite number of nodes and elements represents region or volume of an object. By placing these nodes and elements, an accurate representation of the area, region or volume is able to be studied. Then interpolations or approximation functions are used for the interpolation of the element. Most FEM solvers use polynomial interpolation limiting the polynomial is to the number of nodes in each element. These functions are known as shape functions. Figure 3.6 is an example of full step how a femur head structure is discretized and solved.In using a FEA/ FEM solver, not only are the number of nodes and elements important in the accuracy of the results, but also the type of interpolation chosen. In many solvers, the type of element utilized determines the method used to solve the problem. Continuity of the mesh used

to discretize the geometry is important criteria in receiving accurate results are finite element analysis.

Finite element analysis has several methods for solving given problems. These methods are weighted residual method, variation method, and direct approach. The direct approach is only able to solve elementary problems, which is based on the stiffness matrix for structural analysis. This method, even though effective for elementary problems, can be utilized to solve more complex one. This is accomplished by breaking down the complex geometry into elementary problems, with emphasis being placed on nodes that intersect. By utilizing this concept the designer/ engineer is able to determine a stiffness matrix for the give part of that structure. Then by combining the matrices of the parts, the stiffness of the entire structure can be determined. This method has become known as the direct stiffness method and was the first method utilized for solving finite analysis [134]. The variational approach is represented by calculus variations. Method utilizes both derivation and integral operators. By looking at equations one thru five, the finite element analysis can be related to natural boundary conditions known as the Neumann boundary, seen in equation two. This method is utilized with total potential energy functions [134, 135]. Unlike the direct method, this method can be applied to complex shapes that are governed by the variational function [134, 135].

The most versatile and commonly used method for solving finite element analysis is the weighted residual method. In cases like heat transfer and fluid mechanics,where functions cannot be defined the weight residual method can be used by the incorporation of a trail function. By utilizing this method, there are limitless applications because there is not set defining function like in the direct and variational methods [134, 135]. However, no matter which method is used, the basic steps for formulating the finite element analysis are the same. The first step is to

develop a model of the problem to solve. In conducting this step all parameters must be defined; boundary conditions, initial conditions, geometric image, material properties, the domain and the loads placed on the object. Users must minimize the analysis as much as possible. The main driving factor for these simplifications is the computational power at the user's disposal. If the computational power is unlimited, the model should be maximized. However, in a research situation where computation power is limited, the model should be minimized as much as possible. Once these initial parameters are defined, the model needs to be discretized or meshed. While meshing the model, the factors to take into account are the size of the mesh, shape, number of nodes and the number of elements in the model. While meshing, great care should be taken to ensure uniformity.

The final stages of conducting a finite element analysis consist of choosing an analysis type and verifying the results for accuracy. By choosing the type of analysis to be accomplished, it dictates the method to be used to achieve the results; i.e. direct, variational or weighted residual method; of the finite element model. Once this process is successfully completed, results must be checked for accuracy. The ways to conduct such checks are to refine the elements and/or to conduct a parametric comparison. In addition, conduct a parametric comparison by utilizing graphical representation. After the refinement process, graph the results and check for convergence to verify accuracy.

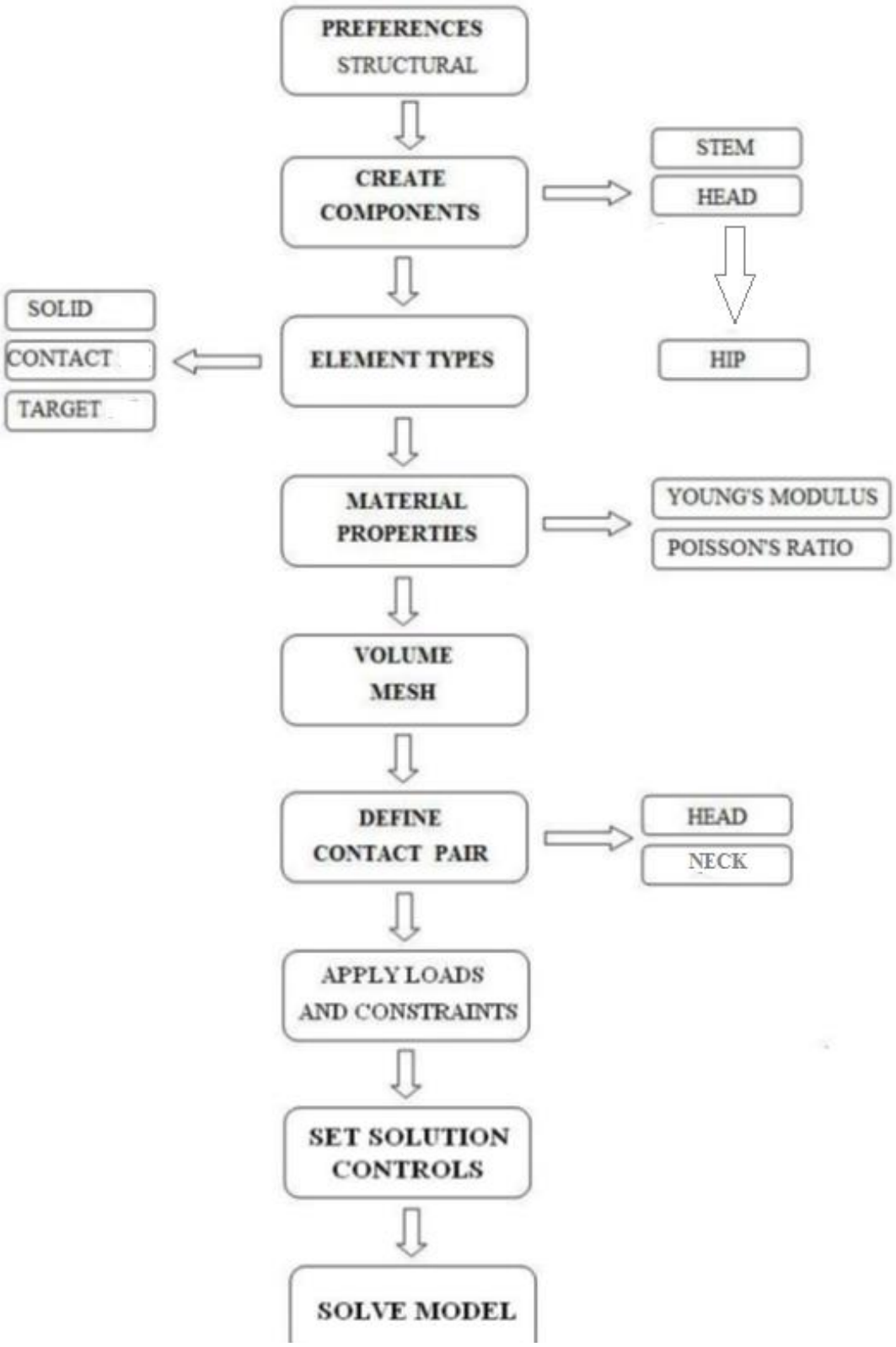

Fig: 3.6 Flowchart describing systematic procedures for static analysis in ANSYS

3.4.2 Preparation for Further Processing into ANSYS 12.0

ANSYS 12.0 is a powerful finite element analysis tool/software widely used for linear/nonlinear structural, thermal or acoustic simulations. It is reliable software extensively used in the industrial, biomedical, automotive and aerospace fields. Finite element analysis can be used to develop a new geometry and/or analyze the existing model using finite element method. FEA converts the complex geometry into sub divisions and optimizes using mathematical equations. Subdivided geometrical sections are called elements which are achieved by meshing the preferred geometry for FEA analysis.All 3D femur models created into CATIAwere exported into ANSYS 12.0 using STP(.stp) format to perform finite element analysis. STP conversion was found more accurate in ANSYS during the present research. Complex geometry of a hip implant assembly appeared to provide higher accuracy with STP format. ANSYS could easily import stp files into the software database without compromising the accuracy and complexity of 3-D solid geometries. Another way used to import models into ANSYS was IGES (.igs) file format; however, it was not used for analysis due to failure of importing all solid geometries. Now it is certainly readymade for further analysis on the imported model.

3.4.3 Meshing

The meshing section of the program is where the individual bodies are defined.

These bodies are defined as Cobalt-chromium alloy (Co-Cr-Mo) alloy and titanium alloy. Cobalt-chromium-molybdenum (Co-Cr-Mo) alloy is defined with the following design parameters: 230 GPa Young’s modulus, 530MPa tensile strength, 890 MPa ultimate tensile strength, density of 8300 kg/m3 and a Poisson’s ratio of 0.3.Titanium alloy is defined with the following parameters: 114 GPa Young’s modulus, 828 MPa tensile strength, 960 MPa ultimate tensile strength, density of 4420 kg/m3 and a Poisson’s ratio of 0.3. By selecting all of the areas

of the geometry, the meshing function can be applied. Looking at the default mesh one can see that the mesh of this geometry is very coarse. Conducting the same procedure, selecting all the bodies and adding a refinement function of relevance size 100, the mesh is refined in all the bodies of the model, as seen in (Fig 3.7, 3.8, 3.9, 3.10). This meshing is uniform and aligns in transition points of bodies that are glued or merged together. Some of the areas that are meshed seem to be more concentrated with elements than others, this occurs primarily due to a transition from on geometric shape to another. For all models utilizes the 10-node tetrahedrons with patch conforming algorithm type mesh which contains to nodes per tetrahedron. This mesh is used for its ability to conform to the geometry being meshed and it gives the most nodal points per area for this geometry. It allows each element to contain 10 nodes. The overall geometry contains a multitude of nodes and elements that are summarized in table 3.2 for the complete number of nodes and elements for each type of model. To ensure its integrity, the mesh should be as fine as possible therefore depicting a realistic mathematical representation of the artificial femur implant geometry. However, a compromise must be made between computational performance and realism of the model.

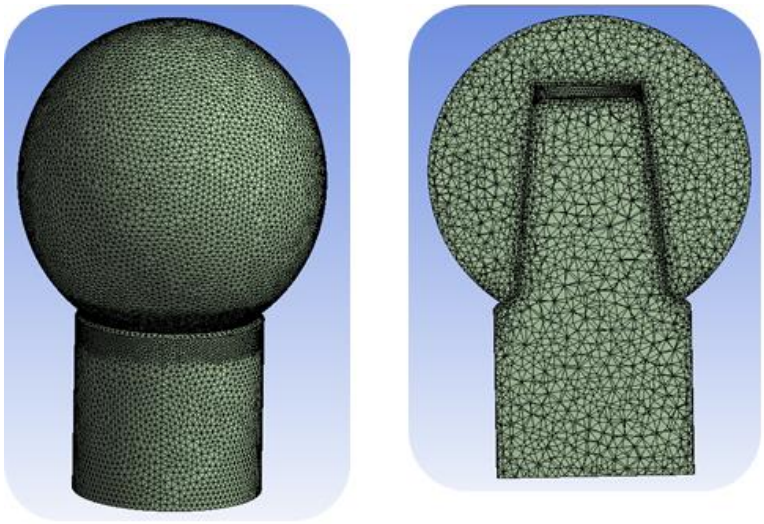

Fig: 3.7 Meshing of Femur Head

Table 3.3: Meshing Summary

Models	Relevance	Number of Node	Number of Elements
1	100	523990	339610
2	100	520514	337301
3	100	500647	322417
4	100	468849	299717
5	100	521071	337733
6	100	408925	262571
7	100		
8	100	417674	268910
9	100	424826	274079
10	100	419248	270027
11	100	501630	325749
12	100	447007	290173
13	100	517627	337045
14	100	507125	329796
15	100	511408	333075

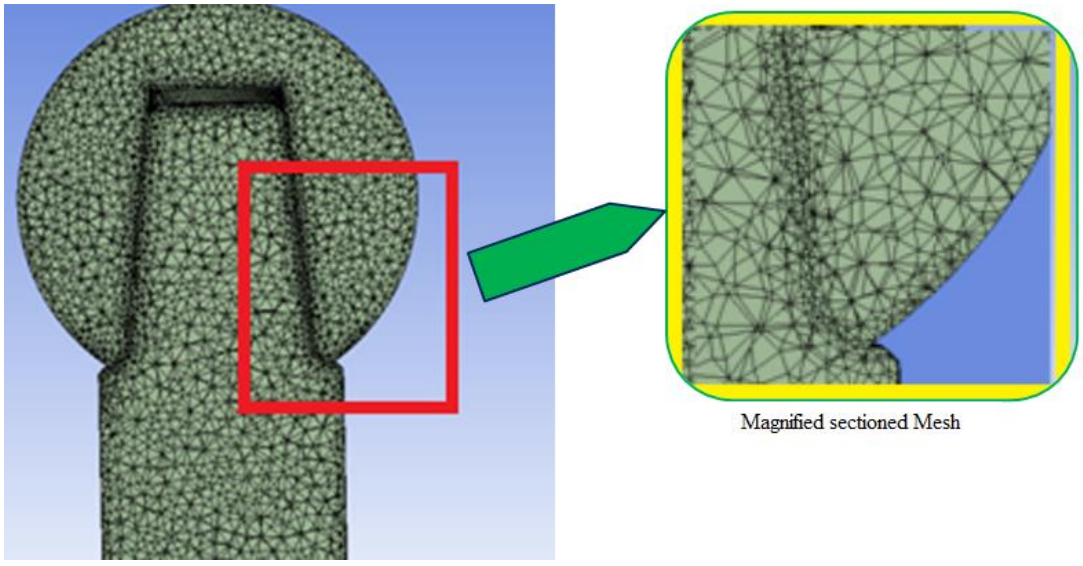

Fig: 3.8 Meshing at Borehole Contact

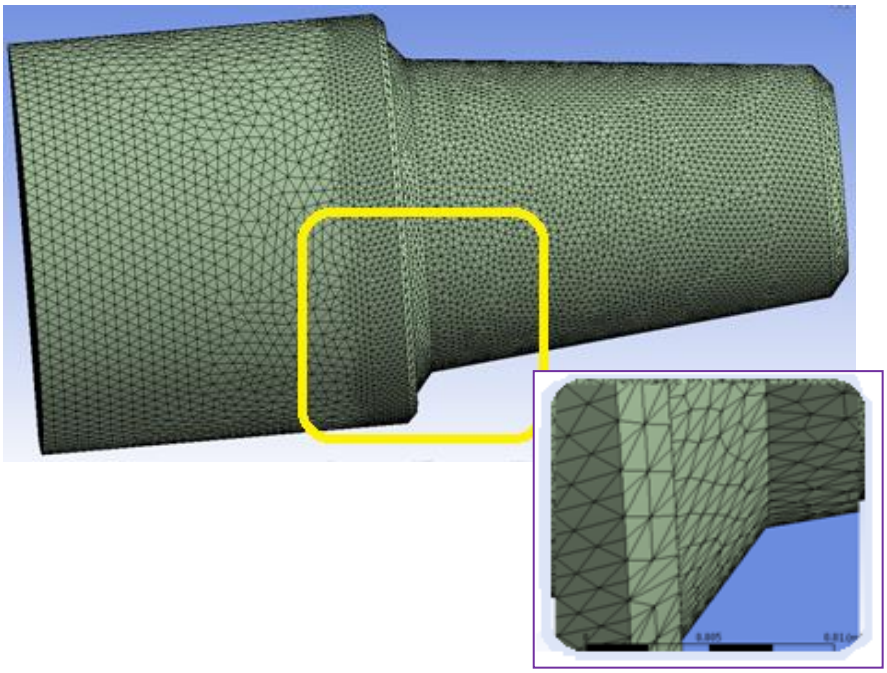

Fig: 3.9 Meshing at Stem Neck

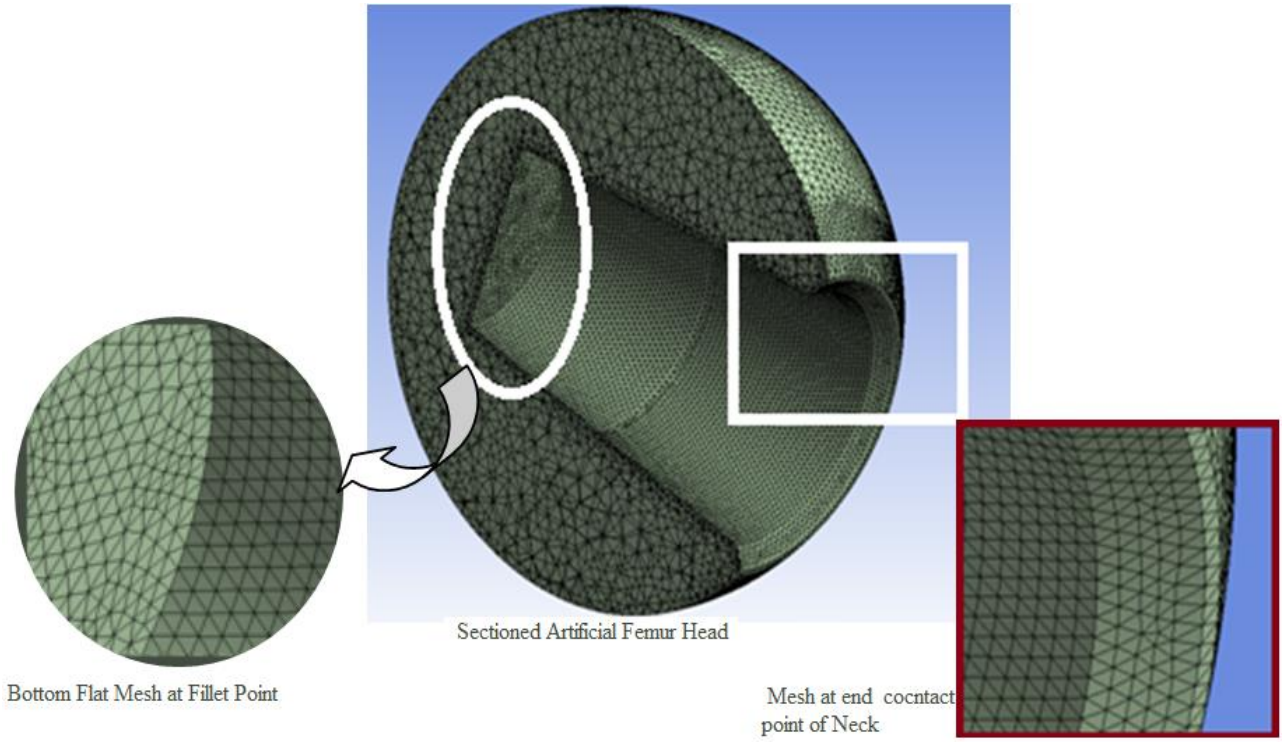

Fig: 3.10 Meshing at Femur Head Borehole

3.4.4 Contacts

For the static step using ANSYS V 12.0 Standard, a surface-to-surface contact that is no separation algorithm was used. A pure target and contact bodies relationship are used, with the femoral head as a target and the neck liner as the contact body. To enforce contact between the femoral head and the neck tapper, hard press- fit behavior with a small angle method waschosen. The press fit pressure enforced a permanent contact between the two bodies. For the static analysis step, a node-to-node contact algorithm was used with in all contact area using, which completely prohibits material interpenetration.

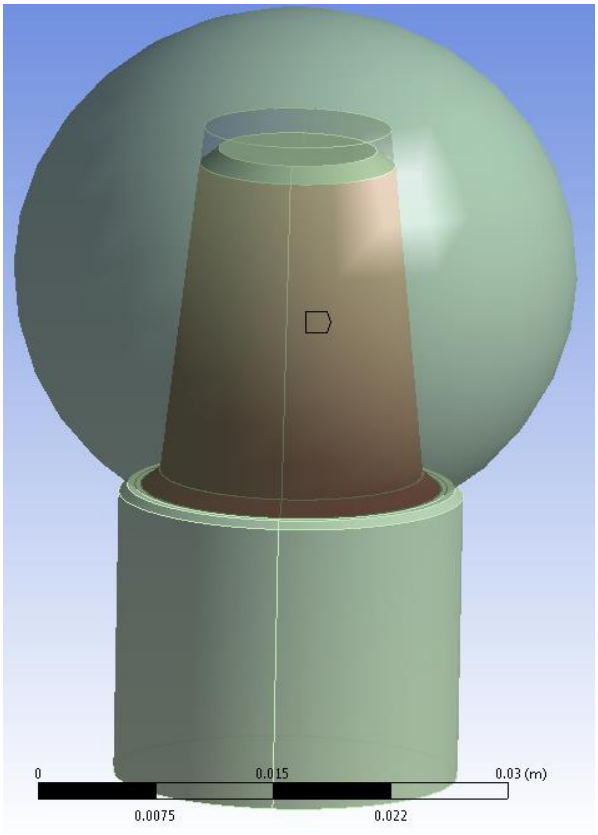

Fig: 3.11 Contact Regions

3.4.5 Loads and Constraints

The results show how the entire geometry reacts to the applied loads andconstraints. Loads can be displacements, forces, pressures, velocities, thermal,gravity etc. Load steps define the load application at certain time intervals. Thedefinedsubsteps record the results at given time durations in static or dynamicanalysis. Static structural loads were applied (Fig 3.12) in order to simulate the femur head, and structural constraints to restrict the neck. Static analysis in the present study needs to simulate loadsonly in vertical -direction and analyze the results for contact stresses and contactpenetration between femoral head and neck. The force of 11000 N was applied in vertical-direction at the nodes of an element located at contacts points.The load considered for optimization was derived from the realistic loads for testing hip implants for the maximum highest loads of 1000N body weight [136]. From this experimental result the contact peak load is defined by 11kN taking the worst case of stumbling.

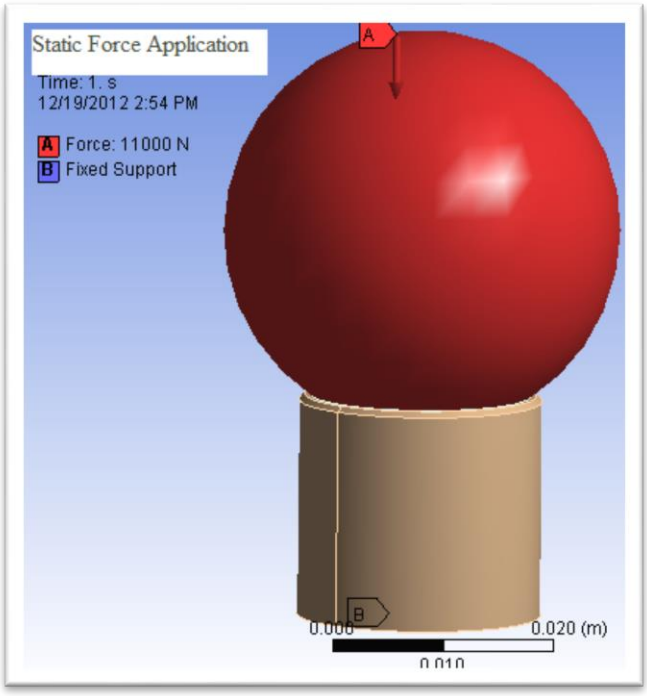

Fig: 3.12 Static Force Applications on Femur Head

Table 3.4: Show the measurement of the load on the hip joint in percentage of the body weight versus with the daily activities that humans have to pass in their life span [136].

Activity	Load on the hip joint (% of body weight)	Experimental Force (N)
Single-legged stance	300% -350%	3600
Walking	360% -400%	3900
Stumbling (peak value)	800%	11,000
Walking upstairs	300%	4200
Walking downstairs	500%	4200
Standing up(supine)	300%	2900
Sitting down	250%	2400

The load applied at the nodes was automatically transferred from nodes and elements. Nodes at the neck area were coupled using no separation contact with tapered press fit to move at one direction and achieve the similar pattern of motion with a neck inserted into a femur head. The nodes of the outer surface of the neck were fixed with structural fixed support constraint; which resisted the head motion within certain range without allowingfemoral component to swing in the space.

Customized solution controls were used for a static analysis. After load wasapplied, the analysis type was selected based on the desired simulationcharacteristics. Static analysis was performed with large static displacements ofnodes. Static analysis used in this study was time rate independent; which simplyconsidered time duration as a loadstep counter and recognized the loadsteps andloadsubsteps. The loadstep is a set of loads applied in the given time duration andloadsubsteps defines the time steps within a complete loadstep at which the solutions were calculated for final display of results. The time at the end ofload step was kept at 1seconds with

no automatic time stepping. This set up oftime applied constant load for oneseconds with no substeps to be recorded in between one seconds. Increase in the load substeps increases the time needed torun complete analysis and calculate results. Hence, current study was performed with loadsubsteps; however the results after the specified one second duration were successfully recorded. This finite analysis result displayed in the next chapter and discussed in fifth chapter.

CHAPTER FOUR

RESULT

This chapter describes results obtained from static force analysis during the present study. After completion of the static analysis in ANSYS, results were reviewed by result report. Four significant types of results were recorded from static analysis of all 15 models. In this chapter, results are presented for each of the four categories namely: von Mises, Shear, Principal and Normal stresses. The results illustrate the rapid structural responses in the femur and the femoral neck and, the contact mechanics of the bearing couples during the sudden femoral head loaded event as analyzed computationally.The most important step of finite element analysis procedure is the physiologically realistic interpretation of the results by the analysis. Since finite element analysis procedures are invariably accompanied by an extensive output of data, it is extremely important that we interpret the results correctly.

In this section all the modeling results of stresses Von misses, Principal, Shear and Normal stresses were presented from finite element analysis results with the condition of Short Neck (SN), Medium Neck (MN) and Long Neck (LN). The three contact length parameters will be conjugated with fillet radius.

4.1 Long Neck Stress Results

In the figure blow ANSYS results is displayed for the LN of 0.5 mm fillet radius. The rest of stresses are summarized in (table 4.1) and clearly shown in appendices.

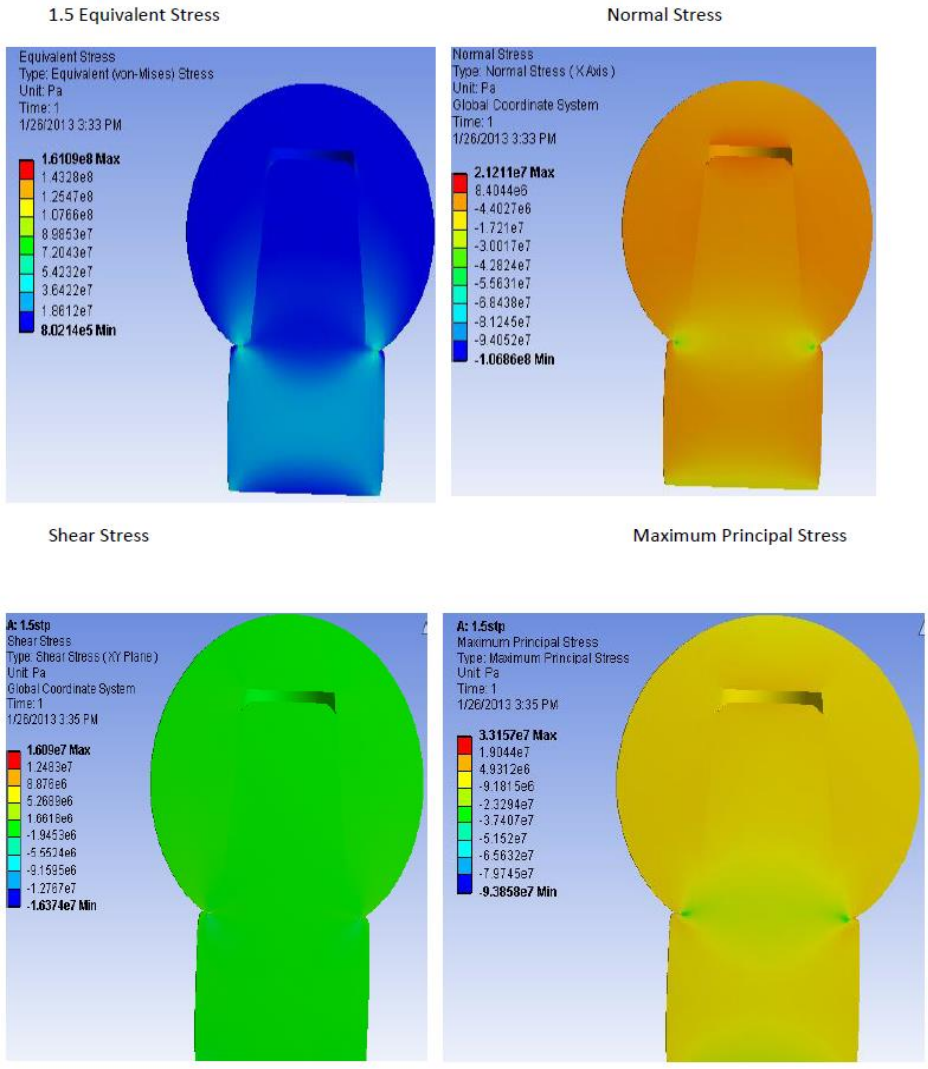

Fig 4.1: ANSYS stress results of LN at 0.5mm fillet radius

Table 4.1: Stresses Summary for Long Necked Contact Geometries

Fillet Radius(mm) / Stress (pa)	0.5	0.6	0.7	.0.8	0.9
Max. Von-Mises	1.61E+08	1.59E+08	1.58E+08	1.64E+08	1.59E+08
Min. Von- Mises	1.59E+08	7.98E+05	8.61E+05	8.76E+05	7.98E+05
Max. Principal	3.32E+07	3.56E+07	3.55E+07	3.85E+07	3.55E+07
Min. Principal	-9.39E+07	-9.7E+07	-9.66E+07	-9.60E+07	-9.70E+07
Max. Shear	1.61E+07	1.68E+07	1.68E+07	1.86E+07	1.61E+07
Min. Shear	-1.64E+07	-1.68E+07	-1.73E+07	-1.76E+07	-1.68E+07
Max. Normal	2.12E+07	2.14E+07	2.04E+07	2.88E+07	2.16E+07
Min. Normal	-1.07E+08	-1.03E+08	-1.03E+08	-1.04E+08	-1.03E+08

4.2Medium Neck Stress Results

In the figure blow ANSYS results is displayed for the MN of 0.5 mm fillet radius. The rest of stresses are summarized in (table 4.2) and clearly shown in appendices.

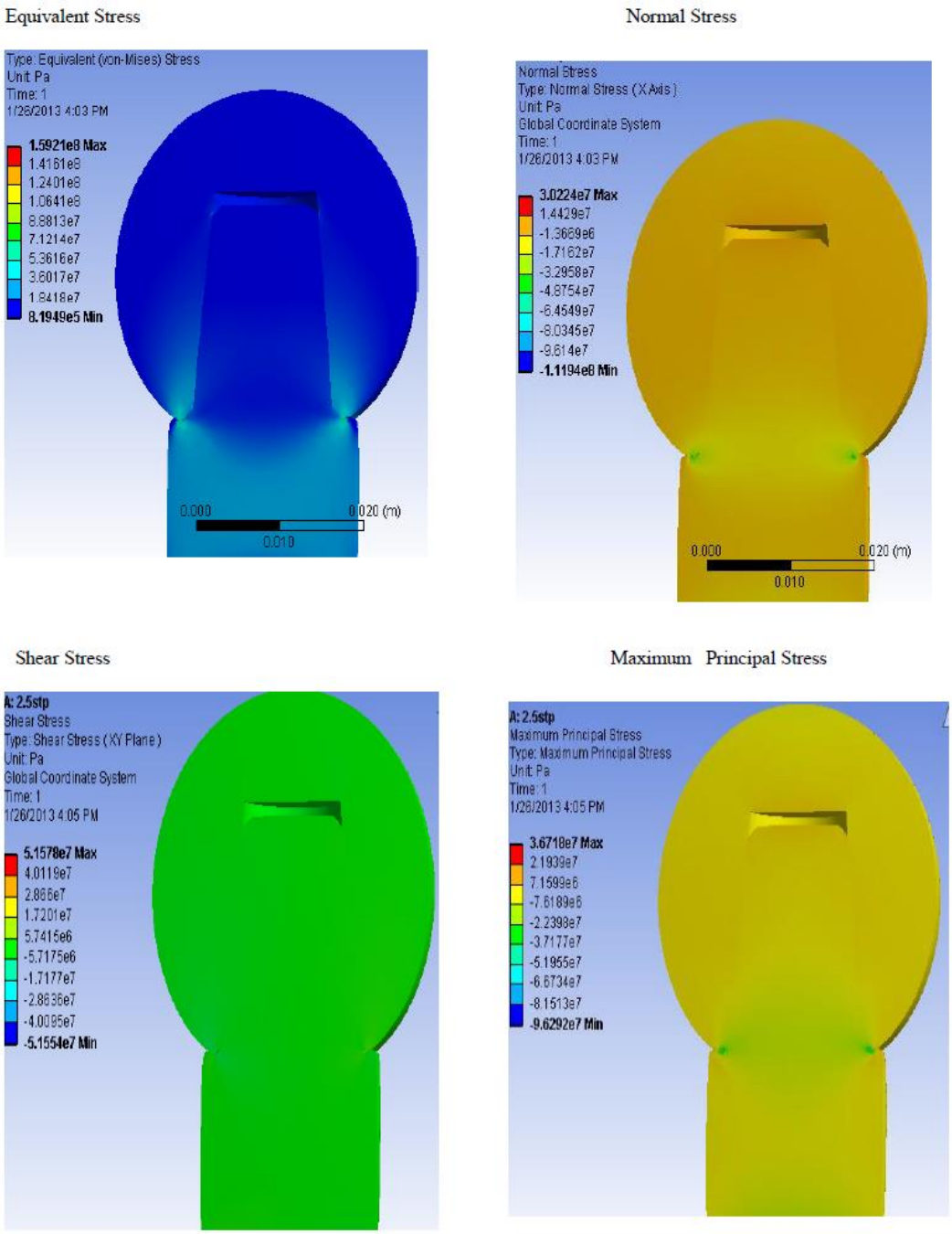

Fig 4.2 ANAYS stress results for MN at 0.5 mm fillet radius

Table 4.2: Stresses Summary for Medium Necked Contact Geometries

Fillet Radius(mm) / Stress (pa)	0.5	0.6	0.7	.0.8	0.9
Max.Von-Mises	1.59E+08	1.49E+08	1.49E+08	1.56E+07	1.51E+08
Min.Von- Mises	8.19E+05	1.37E+06	1.13E+06	1.14E+05	1.72E+06
Max. Principal	3.67E+07	3.34E+07	3.47E+07	3.47E+06	3.47E+07
Min. Principal	-9.63E+07	-1.86E+08	-9.54E+07	-8.98E+06	-9.44E+07
Max. Shear	5.16E+07	1.56E+07	4.86E+07	4.91E+06	1.64E+07
Min. Shear	-5.16E+07	-1.59E+07	-5.40E+07	-5.02E+06	-1.54E+07
Max. Normal	3.02E+07	3.09E+07	3.11E+07	2.98E+06	3.04E+07
Min. Normal	-1.12E+08	-1.06E+08	-1.10E+08	-1.09E+07	-1.06E+08

4.3 Short Neck Stress Results

In the figure blow ANSYS results is displayed for the MN of 0.5 mm fillet radius.

The rest of stresses results are summarized in (table 4.3) and clearly shown in appendices.

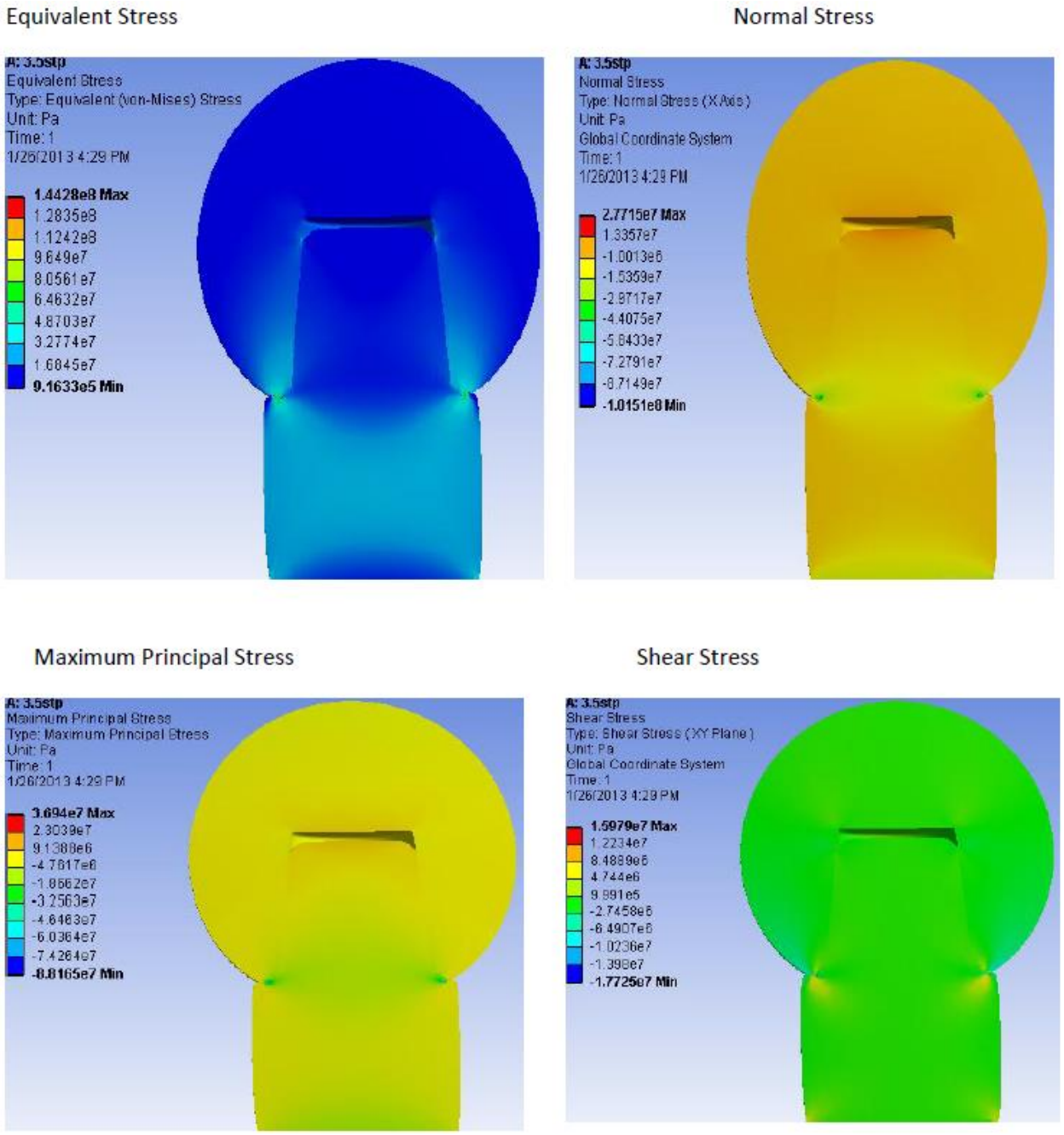

Fig 4.3: ANSYS stress results for SN at 0.5mm fillet radius.

Table 4.3: Stresses Summary for Short Necked Contact Geometries

Fillet Radius(mm) / Stress (pa)	0.5	0.6	0.7	.0.8	0.9
Max.Von-Mises	1.44E+08	1.42E+08	1.44E+08	1.44E+08	1.45E+08
Min.Von- Mises	9.16E+05	9.20E+05	1.02E+06	8.72E+05	9.55E+05
Max. Principal	3.69E+07	3.94E+07	3.86E+07	9.29E+07	4.07E+07
Min. Principal	-8.82E+07	-9.11E+07	-8.90E+07	-7.05E+07	-9.49E+07
Max. Shear	1.60E+07	1.67E+07	1.71E+07	4.95E+07	1.80E+07
Min. Shear	-1.77E+07	-1.65E+07	-1.48E+07	-5.11E+07	-1.71E+07
Max. Normal	2.77E+07	3.17E+07	3.13E+07	7.83E+07	3.03E+07
Min. Normal	-1.02E+08	-1.03E+08	-1.02E+08	-1.28E+08	-1.06E+08

CHAPTER FIVE

DISSCUSSION

The design parameters for all the fifteen solid femur head models were determined based on the review of literature. Design parameters were studied in this research to develop a hip implant model with an ideal combination of head diameter, neck diameter and neck length in order to achieve a stable artificial hip joint to prevent from post- surgery failure. Analytical results were used to develop stress prediction of models. All models were developed to predict contact stress penetration. This study provides new models to minimize the concentration of stress on contact areas. The results are discussed below for various categories.

5.1Effect of Fillet Radius at Corner of Borehole Shape

Fig 5.1 shows the stress value for maximum principal stress and shear stress in the femoral heads is minimized at 0.5 mm fillet radius. But von-mise and normal stress are minimized at

0.7mm.For LN geometries increasing fillet radius has influential effect on stress distribution around contact region, clearly shows that all stresses are maximized at 0.8mm. However, the rest fillet radius increment can reduce result of stress.

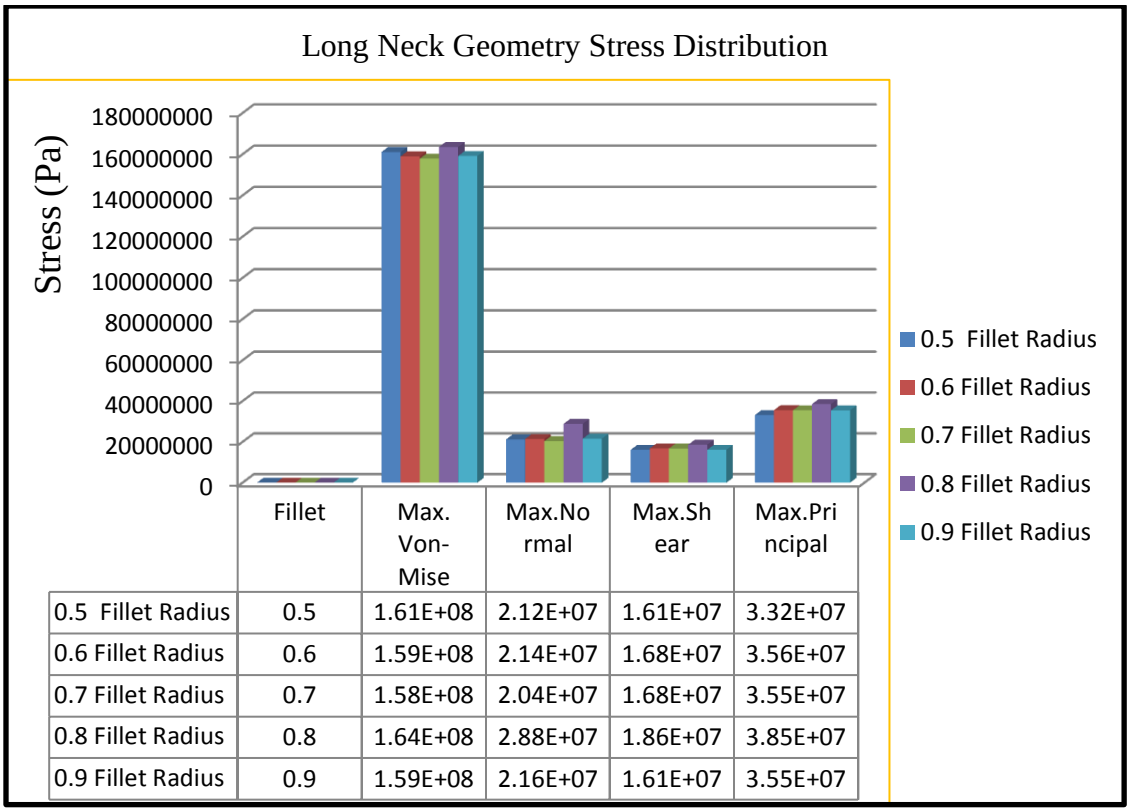

	Fillet	Max. Von-Mise	Max.Normal	Max.Shear	Max.Principal
0.5 Fillet Radius	0.5	1.61E+08	2.12E+07	1.61E+07	3.32E+07
0.6 Fillet Radius	0.6	1.59E+08	2.14E+07	1.68E+07	3.56E+07
0.7 Fillet Radius	0.7	1.58E+08	2.04E+07	1.68E+07	3.55E+07
0.8 Fillet Radius	0.8	1.64E+08	2.88E+07	1.86E+07	3.85E+07
0.9 Fillet Radius	0.9	1.59E+08	2.16E+07	1.61E+07	3.55E+07

Fig5.1: The chart show the Long Neck Contact Length Stress Distribution with all Fillet Radius

The MN geometries stress distribution is defined by the fig 5.2. On the 0.5 mm fillet radius all stresses except normal has maximum value. Consequently, this radius is not recommended. Having seen the radius at 0.6mm the values of the stresses are reduced by 6%comparing to previous fillet radius. At 0.7 mm the von-mise does not have any change the rest stresses values show some increment. The radius profile at 0.8mm fillet value has reduced the critical local stress concentration. This profile has a significant effect in all stress distribution and we might

deduce safest zone obtained comparing with the other introduced geometries. More over the stress is minimized approximately by 20%.

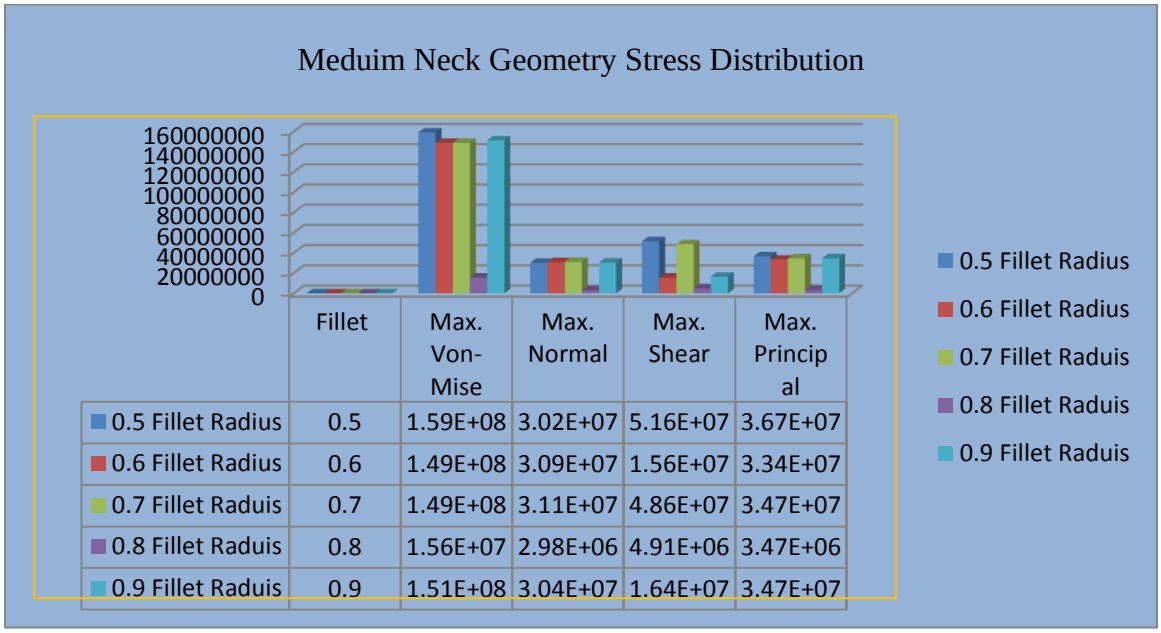

	Fillet	Max. Von-Mise	Max. Normal	Max. Shear	Max. Principal
0.5 Fillet Radius	0.5	1.59E+08	3.02E+07	5.16E+07	3.67E+07
0.6 Fillet Radius	0.6	1.49E+08	3.09E+07	1.56E+07	3.34E+07
0.7 Fillet Raduis	0.7	1.49E+08	3.11E+07	4.86E+07	3.47E+07
0.8 Fillet Raduis	0.8	1.56E+07	2.98E+06	4.91E+06	3.47E+06
0.9 Fillet Raduis	0.9	1.51E+08	3.04E+07	1.64E+07	3.47E+07

Fig 5.2: The chart shows the Medium Neck Contact Length Stress Distribution with all Fillet Radius

The artificial femoral head short necked geometries with 0.5mm fillet radius do not have such notch stresses in the region comparing with others. This can be attributed to the smallest fillet and smooth transition between the flat bottom and the tapered borehole. Hence, the maximum shear, normal and principal stresses are reduced to lower values. Consequently, increasing fillet radius it results an increasing the stresses around taped hole region. Specially, the maximum von-mises, shear and principal stresses is higher at fillet of 0.8and 0.9mm. On the other hand the normal stress is exhibited maximum at 0.6 and 0.7mm fillet. However, by determining an appropriate contact length and fillet radius, stresses at the taper-bore interface can be reduced, which will be discussed in the following sections of the paper. From the above analysis, it can be

seen that the new borehole shapes can potentially improve the mechanical reliability of the femoral heads in THR. As both the new designs are geometrically simple, they can be readily formed and fabricated by the machining processes available.

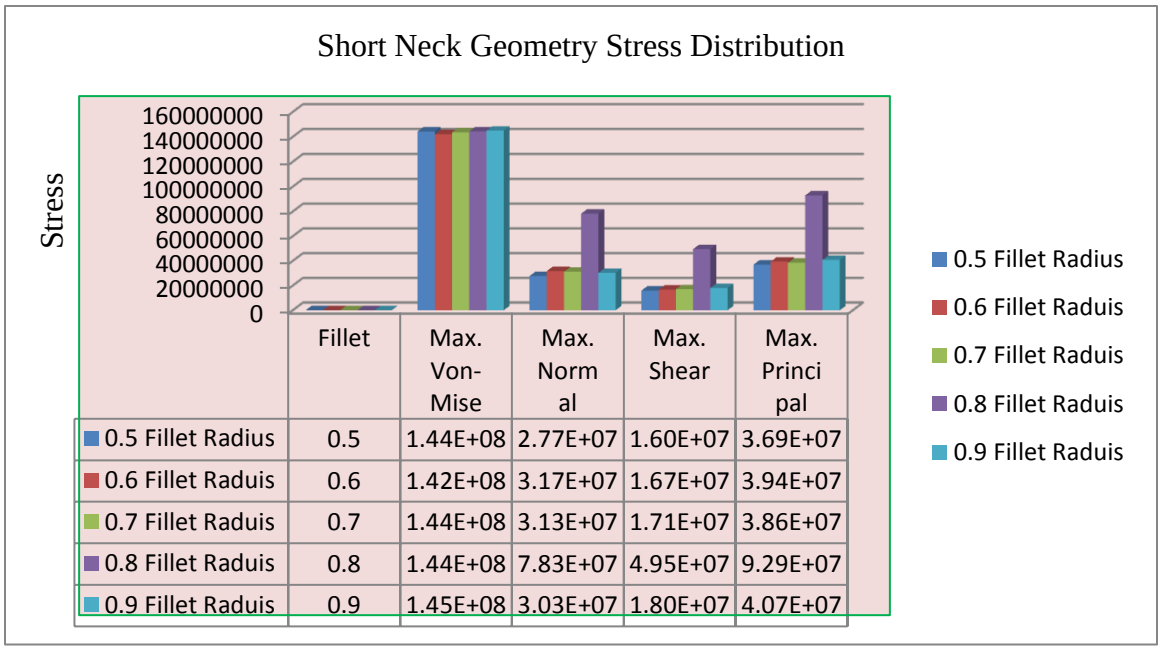

	Fillet	Max. Von-Mise	Max. Normal	Max. Shear	Max. Principal
0.5 Fillet Radius	0.5	1.44E+08	2.77E+07	1.60E+07	3.69E+07
0.6 Fillet Raduis	0.6	1.42E+08	3.17E+07	1.67E+07	3.94E+07
0.7 Fillet Raduis	0.7	1.44E+08	3.13E+07	1.71E+07	3.86E+07
0.8 Fillet Raduis	0.8	1.44E+08	7.83E+07	4.95E+07	9.29E+07
0.9 Fillet Raduis	0.9	1.45E+08	3.03E+07	1.80E+07	4.07E+07

Fig 5.3: The chart shows the Short Neck Contact Length Stress Distribution with all Fillet Radius

5.2Effect of Stem Neck and Taper-Borehole Contact Length

The taper-bore contact length, as defined in the chart below, is important, which affects the stress distribution and mechanical reliability of femoral head. In the current analysis, three taper-bore contact lengths are considered for the case of the femoral heads with the : (1) 23.5mm contact length (LN), (2) 21.5mm contact length (MN) and (3) 16.5mm contact length from the top of the taper-bore, appendices show all stress profiles along the inner wall of the taper-borehole and table 4.1,4.2 and 4.3 indicated with the decrease of the contact length from LN to MN, the stress decreases. This is due the increment thickness of ball head from the hole to outer surface to withstand the applied load. On the other hand the stress increases from MN to SN. This is due to

the less contact area at the interface to withstand the applied load. A reduction of contact length from LN to MN causes a decrease in the maximum von-mises, principal, shear and normal stresses by about 90%, 89.5%, 69.5% and 85.5% respectively. And a reduction of contact length from MN to SN causes an increment in the maximum von-mises, principal, shear and normal stresses by about 89%, 69%, 90.5%, and 89% respectively.This comparison indicating that, the contact length should be as medium as possible in the design of a borehole to minimize the stresses and hence to maximize the mechanical reliability of the artificial femoral head.

Fig 5.4: Shows the Stress Distribution of All Models

Finally, numerical optimization by means of the FEM was performed on a type LN, MN, and SN Co-Cr-Mo femoral head with a cone taper size 12/14. Although the maximum stresses occurs in the contact zone to the stem neck, the local maximum inside the borehole has to be considered, as local material flaws could reduce the strength of a ball head. The resulting design was applied on all three ball types SN, MN, and LN, whose geometry mainly differs with respect

to the borehole depth. Validation was performed for all ball head. The results of the finite element calculations showed considerable improvements, i.e. a reduction in the maximum Von-mise, Shear, Normal and principal stress in the fillet by 90, 69.5, 85.4 and 89.5 percent respectively on medium neck contact length at 0.8mm fillet radius. The stress distribution and therefore the failure mechanism in the examined system of the Cobalt-Chromium alloy ball head, the titanium alloy replacement stem neck, and loading device strongly depend on the amount of the external load and on the bearing geometry type. In addition, the load level strongly influences the effectiveness of the shape optimization. The optimized shape is still ideal for a load level of 11 kN considering stumbling case; higher loads of more than this, however, lead to a stress relocation where, on the one hand, the shape is not optimal any longer and, on the other hand, the global maximum of principal stress moves from the fillet to the contact zone with the stem. Best results were obtained in a configuration according to ANSYS result, as this load case also had been considered for optimization with taking into account the contact between the stem neck and the ball head. The load case with point loading did not show any improvement, as the high stress concentration around the filleted zone always induced the Co-Cr-Mo ball to burst. But in this paper would not happen because optimally minimized all failure stress from the vicinity area of filleted part. On the other hand due to higher load the stress was forced to relocate and the maximum stresses moved back to the conical surface of the borehole till dead bottom of opposite end from filleted part. The stress relocation might not lead to failure since material applied has good properties in the ease of stiffness to resist deformation and wear having around fifteen safety factors allowance.

CHAPTER SIX

CONCLUSIONS AND FUTURE WORK

6.1 Conclusions

This paper has carried out a finite element stress analysis of femoral head in hip joint prostheses by considering the design of borehole shape geometry. The design geometric parameters were stem taper-bore contact length and the stem neck interface fillet radius at bottom of head ball. It was found that the new borehole shapes introduced in this study contains fifteen design alternatives; among them one can reduce the maximum stresses significantly and can enhance the mechanical reliability of the femoral heads. Moreover because of its simple geometries, this borehole shapes can be readily manufactured with superior surface finish. It was also found that the stem taper-bore contact length should be maximized till safe zone. This safest zone minimize the stresses in a contact of the neck and head at a single fillet radius, and that point is a greater achievement between the stem neck and the femoral head in the assembly of a hip joint

prosthesis. Because of it can be able to reduce the magnitude of the maximum failure stresses in the Co-Cr-Mo femoral head and thus improve its mechanical reliability.

6.2 Limitation

The current study has some limitations. First, only analytical method was used in the study. It would be more statistically powerfuland interesting to apply the method of experimental test. Secondly, the number of loads used for representing thehip contact force was limited to one load. In order to be able to capture the effects of the loads on our daily movement, one has to use several loads. Moreover,increasing the number of forces representing the hip contactforcewould enable it to better capture the stress distributionof the other parts of the femoral head. If the number ofloads is increased, the number of parameters that needto be identified will increase. Thirdly, generic geometric shapes introduced were used in the currentstudy is few in number. For a more accurate representation of stresses, it would be fine to introduce more optional shapes.

Despite these limitations and simplifications, the current paper shows the feasibility and applicability of the proposed geometries to predict safe zone that the stress distribution was minimized to enhance the mechanical reliability for longer life time of femur head prosthesis using finite element algorithm.

6.3 Future work

The work presented in this paper can be extended in manydirections. In this subsection, we discuss two of thosedirections, namely estimating of stress parameters and applying the proposed material to femoral prosthetic for the introduced geometries. The stress estimated comes from

analytical further experimental test is crucial for greater validity. The loading parameters influence the stress distribution in a direct way; meaning that the contributions ofdifferent loads to the resulting stress distribution cannot beseparated from each other. In order to capture the best result using behavior of the different loading parameters, future work will be needed to derive more accurate contact stress prediction models in the introduced geometries. Parameters such as femoral head stem orientation, clearance, surface roughness and subject body weight may be included to predict linear wear rate for higher accuracy. Future research will include investigation biotribological effects of wear rate using dynamic simulation of gait pattern to estimate the lifespan of the hip implant.

REFERENCES

1. Eng. Radu RACA'AN,(2011) Contributions Regarding the use of Modern Techniques for Measuring and Modeling Complex Surfaces in the Wear Evaluation of Total Hip Replacements, Appointed through order nr. 372/02.08 issued.
2. JIANG Hai-bo, LIU Hong-tao, HAN Shu-yang, LIU Fen, Biomechanics Characteristics of New Type Artificial Hip Joint, Advances in Natural Science Vol. 3, No. 2, 2010, pp. 258-262, www.cscanada.net
3. J. Lord, T. Joyce, Analysis of failed metal-on-metal hip prostheses, pp: 1
4. Dianne-Anand , Wear Analysis of Acetabular Components in a Total Hip Replacement, pp:1
5. D Dowson, New joints for the Millennium: Wear control in total replacement hip joints, Journal of Engineering in Medicine 215: 335
6. R.W. Buchoz, J.D. Heckman, C.M. Cort-Brown, K.J. Koval, P. Tornetta III, and M.A. Wirth, "Rockwood and Green's Fractures in Adults Volume 2," 6th ed, Lippincott Williams & Wilkins, 2001.
7. [http://www.thehipdoc.com/history.htm]
8. [http://www.utahhipandknee.com/history.htm]
9. Charnley, J: (1964) The bonding of prosthesis to bone by cement. J. Bone JntSura. 46B. 518-529.
10. Charnley, J. (1965) A biomedical analysis of the use of cement to anchor the femoral head prosthesis. J. BoneJnt Surg. 47B, 354-363.
11. Charnley, J. and Smith, D. C. (1968) The physical and chemical properties of self-curing acrylic cement for use in orthopaedic surgery. Centre of Hip Surgery, Wrightington Hospital, Int. Pubn. No. 16

12. SumitPramanik, Avinash Kumar Agarwal, and K. N. Rai, (2005) Chronology of Total Hip Joint Replacement and Materials Development, Trends Biomater. Artif. Organs, Vol 19(1), pp. 15-26
13. http://www. my.clevelandclinic.org/services/hip_revision/or_overview.aspx
14. http://www.orthopedics.about.com/od/hipkneereplacement/a/revisionhip.ht
15. http://www. evertsmith.com/treatment/hip-revision/
16. http://www.zimbio.com/Hip+Implants/articles/V3sZAMKoFve/Hip+Replacement+Failure+Leads+More+Painful
17. Abdul H.,Mohd N.,Mohd S., and TardanGiha, (2009) Finite Element Analysis of Cemented Hip Arthroplasty: Influence of Stem Tapers.
18. Makarand G. Joshi, Suresh G. Advani, Freeman Miller, Michael H. Santare, (2000). Analysis of a Femoral Pip prosthesis Designed to Reduce Stress Shielding. Journal of Biomechanics 33, 1655-1662
19. Huiskes, R., (1990) The various stress patterns of press-fit, Ingrown and Cemented Femoral Stems. Clinical Orthopedics 261, 27-38.
20. Huiskes, R., Weinans, H., Van Rietbergen, B., 1992. The Relationship between Stress Shielding and Bone Resorption around Total Hip Stems and the Effects of Flexible Materials. Clinical Orthopedics 272, 124-134.
21. Garino, J. P. (2005) Ceramic component fracture: trends and recommendations with modern components based on improved reporting methods. In bio ceramics and alternative bearings in joint arthroplasty, Proceedings of the Tenth International BIOLOX Symposium (Eds J. A. D'Antonio and M. Dietrich), pp. 157–168 (Springer-Verlag, Berlin).
22. Higuchi, F., Shiba, N., Inoue, A., and Wakebe, I. (1995) Fracture of an alumina ceramic head in total hip arthroplasty. J. Arthroplasty, 10(6), 851–854.
23. Krikler, S. and Schatzker, J. Ceramic head failure. J. Arthroplasty, 1995, 10(6), 860–862.
24. Willmann, G. (1998) Survival rate and reliability of ceramic femoral heads for total hip arthroplasty. MaterialwissenschaftWerkstofftechnik, 29(10), 595–604.
25. Willmann, G. (2003) Fiction and Facts Concerning the Reliability of Ceramics in THR. In Ceramics in orthopaedics, Proceedings of the Eighth International

BIOLOX Symposium (Eds H. Zippel and M. Dietrich), pp. 193- 196(Steinkopff-Verlag, Berlin).

26. Weisse, B., Zahner, M., Weber, W., and Rieger, W. (2003) Improvement of the reliability of ceramic hip joint implants. J. Biomechanics, 36(11), 1633–1639.
27. Begand, S., Oberbach, T., and Glien, W. ATZ (2005) A new material with a high potential in joint replacement. Bio ceramics, 17, 983–986.
28. Forensic Anthropology, The Human Skeleton
29. RajiNareliya et al (2011) Biomechanical analysis of Human femur Bone: International Journal of Engineering Science and Technology (IJEST), Vol. 3 No. 4, ISSN: 0975-5462
30. Anderson Maciel (2002), Biomechanics of Hip Joint Capsule, Internal Report For Project COME10: 3D Visualization of Joints From MRI Data.
31. JIANG Hai-bo, LIU Hong-tao, HAN Shu-yang, LIU Fen, Biomechanics Characteristics of New Type Artificial Hip Joint, Advances in Natural Science Vol. 3, No. 2, 2010, pp. 258-262, www.cscanada.net
32. [5] A O Andrisano, E Dragoni and A Strozzi (1990) : Axisymmetric Mechanical Analysis of Ceramic Heads for Total Hip Replacement , Journal of Engineering in Medicine 204: 157 The online version of this article can be found at:http://pih.sagepub.com/content/204/3/157
33. C. Affolter et al.: Journal of Engineering in Medicine Proc. IMechE Vol. 223 (2009), pp.237, doi: 10.1243/09544119JEIM429
34. J. Middleton et al.: Journal of Materials Science and Materials in Medicine Vol. 5 (1994), p.503, doi: 10.1007/BF00058992
35. M. Sharif and L.C. Zhang (2010): Minimizing Stress Concentrations in the Femoral Heads of Hip Joint Prostheses: Effect of Borehole Shapes Engineering Materials Vol. 443 pp. 736-741
36. Shuyang Han, ShirongGe, Effect of Fomoral Head Shape on Mechanical Behaviours of Artificial Hip Joint, 978-1-4244-6498-2/10/ ©2010 IEEE
37. F. Menschik, "The hip joint as a conchoid shape," Journal of Biomechanics, vol. 30, pp. 971-973, September 1997.

38. Hammond and Charnley, "The sphericity of the femoral head," Journal of Medical and Biological Engineering, vol. 5, pp. 445-453, April 1967.
39. SumitPramanik, Avinash Kumar Agarwal, and K. N. Rai, Chronology of Total Hip Joint Replacement and Materials Development, Trends Biomater. Artif. Organs, Vol 19(1), pp 15-26 (2005)
40. Smith-Peterson MN. Arthroplasty of the hip. A new method. J Bone Joint Surg Am. 1939; 21: 269-288.
41. Venable CS, Stuck WG. Electrolysis controlling factor in use of metals in treating fractures. JAMA 1938;111: 1349-1352.
42. Moore AT, Bohlman HR. Metal hip joint: a case report. J Bone Joint Surg Am. 1943;25: 688-691.
43. Bohlman HR. Replacement reconstruction of the hip. Am J Surg. 1952: 84(3): 268-278.
44. Ferguson AB Jr, Laing, PG, Hodge ES. The ionization of metal implants in living tissues. J Bone Joint Surg Am. 1960; 42: 77-90.
45. McKeeG.Mckee- Farrar total prosthetic replacement of the hip. In: Jayson M,ed. Total Hip Replacement. London: Sector publishing; 1971: 47-67.
46. McKee GK, Watson- Farrar Replacement of arthritic hips by the McKee- Farrar prosthesis. J Bone Joint Surg Br.1968; 48:245-259
47. Thompson FR. An essay on the development of arthroplasty of the hip. ClinOrthopRelat Res. 1966; 44: 73-82.
48. Townley CO, Walker S. Intramedullary cup-stem arthroplasty of the hip J Bone Joint Surg Am. 1961; 43:602.
49. Ring PA. Complete replacement arthroplasty of the hip by the ring prosthesis. J Bone Joint Surg Br.1968; 50: 720-731.
50. Charnley J. Arthroplasty of the hip. A new operation. Lancet. 1961;1: 1129-1132.
51. McBride ED. Metallic femoral head prosthesis for the hip joint. J IntColl Surg. 1951; 15(4) 498-503
52. Müller ME. The benefits of metal-on-metal total hip replacements. ClinOrthopRelat Res. 1995; 311: 54-59

53. Urist MR. The principles of hip-socket arthroplasty. J Bone Joint Surg Am. 1957; 39(4):786-810.
54. Jones DA, Lucas HK, O'Driscoll M, Price CH, Wibberley B. Cobalt toxicity after McKee hip arthroplasty. J Bone Joint Surg Br. 1975; 57:289-296.
55. Haboush EJ. A new operation for arthroplasty of the hip based on biomechanics, photo elasticity, fast-setting dental acrylic, and other considerations. Bull Hosp Joint Dis. 1953;14: 242-277.
56. Pritchett J. Curved-stem hip resurfacing: minimum 20-year followup. ClinOrthopRelat Res. 2008;466:1177-1185.
57. Pritchett J. Conservative total articular replacement arthroplasty: minimum 20-year follow-up. In: McMinn DJW, ed. Modern Hip Resurfacing. London: Springer; 2009:408-414.
58. Della Valle CJ, Nunley RM, Raterman SJ, Barrack RL. Initial American experience with hip resurfacing following FDA approval. ClinOrthopRelat Res 2009:467:72-78.
59. Hing C, Back D, Baily M, Young D, Dalziel R, Shimmin A. The results of primary Birmingham hip resurfacings at a mean of five years: an independent prospective review of the first 230 hips. J Bone Joint Surg Br. 2007;89: 1431-1438.
60. Pandit H, Glyn-Jones S, McLardy-Smith P, Gundle R, Whitwell D, Gibbons CL, Ostlere S, Athanasou N, Gill HS, Murray DW. Pseduotumours associated with metal-on-metal resurfacings. J Bone Joint Surg Br. 2008;90: 847-851.
61. Begand, S., Oberbach, T., and Glien, W. ATZ – A new material with a high potential in joint replacement. Bio ceramics, 2005, 17, 983–986.
62. Astion DJ, Saluan P, Stulberg BN, and Rimnac CM. The porous-coated anatomic total hip prosthesis - Failure of the metal-backed acetabular component. J Bone Joint Surg 1996; 78A: 755-766.
63. Braune, W. and Fischer, O., Der Gang des Menschen. Abhandlong, Math.-Phys. Classe d. Konigl. Sachs. GesellschaftderWissenschaft, 1898-1904, pp.21-28
64. Fick, R., Handbuch der Anatomie und Mechanik der Gelenke under Berucksichtigung der bewegendenMuskeln, G. Fischer, Jena, 1904-I 911

65. Bernstein, N.A. Biodynamics of Locomotion, Vsesoiuz. Instit. Eksper. Med. (VIEM), Moscow, U.S.S.R., 1935
66. Elftman, H., Forces and Energy Change in the Leg during Walking, Amer. J. Physiol. 1939, 125,339
67. Elftman, H. The Function of Muscles in Locomotion, Amer.J. Physiol. 1939,125,357
68. Elftman, H., The Action of Muscles in the Body, Biol. Symp. 1941, 3, 191
69. Inman, V.T., Functional Aspects of the Abductor Muscles of the Hip, J. Bone Jt. Surg. 1947,29,607
70. Blount, W., Don't Throw Away the Cane, J. Bone Jr. Surg. 1956,38A,695
71. Strange, F.G.St.C., The Hip, Heinemann, London, 1963
72. Williams, J.F., A Force Analysis of the Hip Joint, Biomed. Eng. 1968,3 , 365
73. Bresler, B. and Frankel, J.P.,The Forces and Moments in theLeg During Walking, Trans ASME 1950,72,27.
74. Rydell. N.W., Forces in the Hip-Joint. Part (II): lntravital Measurement, Symposium on Biomechanics and RelatedTopics(Ed. R.M. Kenedi) Pergamon Press, New York, 1964, p. 351
75. Rydell, N.W., Forces Acting on the Femoral Head Prosthesis, ActaOrthop. Stand. Suppl. 1966, 88
76. Sorbie, C. and Zalter, Ft., Bio-Engineering Studies of the Forces Transmitted by Joints (I): The Phasic Relationships of the Hip Muscles in Walking, Symposium on Biomechanics and RelatedBio-Engineering Topics (Ed. R.M. Kenedi) Pergamon Press, New York, 1964, p.359
77. Ghista, D.N., Toridis, T.G. and Srinivasan, T.M., Human Gait Analysis: Determination of Instantaneous Joint Reactive Forces, Muscle Forces and the Stress Distribution in Bone Segments-l I, BiomedizinischeTechnik1976,21,3
78. Paul, J.P., Bio-Engineering Studies of the Forces Transmitted by Joints (I I): Engineering Analysis, Symposium ofBiomechanics and Related Bio-Engineering Topics (Ed. R .M. KenedijPergamon Press, New York, 1964, p.369

79. Paul, J.P., Forces at the Human Hip Joint, Ph. D. Thesis, University of Glasgow,Scotland, 1967.
80. Paul, J.P., Forces Transmitted by Joints in the Human Body, Proc. Inst. Mech. Eng. 1967,181,8
81. Paul, J.P., Load Actions on the Human Femur in Walking and Some Resultant Stresses, Exp. Mech. 1971,ll. 121
82. Morrison, J.B., The Forces Transmitted by the Human Knee Joint During Activity, Ph.D. Thesis, University of Strathclyde,Glasgow, Scotland, 1967.
83. Chao, E.Y., Opgrande, J.D.andAxmear, F.E., Three dimensional Force Analysis of Finger Joints in Selected Isometric Hand Functions, J. Biomech. 1976,9,387
84. Seireg, A. and Arvikar, R.J., A Mathematical Model for Evaluation of Forces in Lower Extremeties of the Musculoskeletal System,J. Biomech. 1973,6,313
85. Penrod, D.D., Davy, D.T.and Singh, D.P.,An Optimization Approach to Tendon Force Ana1ysis.J. Biomech. 1974,7,123
86. Crowinshield, R.D., Johnston, R.C., Andrews, J.G. and Brand, R.A., A Biomechanical Investigation of the Human Hip, J. Biomech. 1978, 11,75
87. Debrunner, H.U., StudienzurBiomechanik des Huftgelenkes I: Einneues Model1 fur die Berechnung der Huftbelastung, Z. Orthop. 1975, 113,377
88. Wolff, J., Das Gesetz der Transformation der Knochen, Quarto, Berlin, 1892
89. Toridis, T.G., Stress Analysis of the Femur, J. Biomech. 1969,2,163
90. Rybicki, E.F., Simonen, F.A. and Weis, E.B. Jr., On theMathematical Analysis of Stress in the Human Femur, J. Biomech. 1972,5,203
91. Piotrowski, G. and Wilcox, G.A. Jr., The Stress Program: A Computer Program for the Analysis of Stresses in Long Bones, J. Biomech. 1971,4.497
92. Nowinski, J.L. and Davis, C.F., The Flexure and Torsion of Bones Viewed as Anisotropic Poroelastic Bones, Int. J.Engng. Sci. L. 1972,10,1063
93. Grunewald, J.,TheBeam spurtingthe LongtubebonesZ. Orthop. Chir. 1920, 39,27
94. Marique, P., Etudes sur le Femur. Anatomy, axes and angles, deformations, resistance, Stoops, Bruxelles, 1945
95. Backman, S., The Proximal End of the Femur,AcraRadio/ Supp. 1957,146

96. Brekelmans, W.A.M., Poort, r!.W. and Sloof, T.J.J.H. A New Method to Analyse the MechdnicalBehaviour of Skeletal Parts, ActaOrthop. Stand. 1972,43,301
97. Valliappan. S., Svensson, N.L. and Wood, R.D., Three Dimensional Stress Analysis of the Human Femur, Comp. Biol. Med. 1977,7.253
98. Svensson, N.L., Valliappan, S. and Wood, R.D., StressAnalysis of Human Femur with Implanted CharnleyProsthesis, J. Biomech. 1977, 10, 581
99. Hampton, S.J., Andriacchi, T.P. and Galante, J.O., Three Dimensional Stress Analysis of the Femoral Stem of a Total Hip Prosthesis, J. Biomech. 1980,13,443
100. Martens, M., Aernoudt, E., de Meester, P., Ducheyne, P., Mulier, J.C., de Langh, R. and Kestelijn, M., Factors in Mechanical Failure of the Femoral Component in Total Hip Prosthesis. Report of Six Fatigue Fractures of the Femoral Stem and Results of Experimental Loading Tests, ActaOrthop. Stand. 1974,45,693
101. McNeice, G.M., Eng, P. and Amstutz, H.C., Finite Element Studies in Hip Reconstruction, J. Biomech. 1965,4,394
102. Andriacchi, T.P., Galante, J.O., Belytschko, T.B. and Hampten. S.J., A Stress Analysis of the Femoral Stem in Total Hip Prosthesis, J. Bone Jt. Surg. 1976, 58A, 618
103. Bartel, D.L. and Desormeaux, S.G., On Design Objectives and Testing Techniques for Femoral Stems, 23rd AnnualOrthopaedic Research Society, Las Vegas, 1977
104. Saha, S., Anisotropic Analysis of Bone-Some Two- Dimensional Problems, J. Biomech. 1973,6,641
105. Kuntscher, G., The Presentation of KrattflussesimKnochen, Centralblart of Surgery 1934,61, 2130
106. Kuntscher, G., The Importance of the Representation of Kraftflussesim for Bone Surgery, Arch. F. K/in.Chir. 1935, 182.489

107. Kuntscher, G., About the Detection of Spikes on Human Bone ThreadRus, Morph. Jahrb. 1935, 75, 427

108. Evans, F.G. and Lissner, HR., Stresscoat Deformation Studies of the Femur under Static Vertical Loading,Ana/. Rec. 1948,199,159

109. Evans, F.G., Lissner, HR. and Pedersen, H.E., Deformation Studies in the Femur under Dynamic Vertical Loading,Anal. Rec. 1948,101,225

110. Evans, F.G., Hayes, J.F. and Powers, J.E., Stresscoat Deformations Studies of the Human Femur Under Transverse Loading, Anal. Rec. 1953,116,171

111. Rabischong, P. and Avril, J., Role Biomechanics the Postures Composites of Muscles, Rev. Chir. Drthop. 1965,51,437

112. Leduc, A., Contribution ExperimentalStudy Biomechanics of femur, Thesis, Univ. LibreBruxelles, 1966.

113. Blaimont, P. and Wagner, J., Preliminaries of Biomechanics of Prostheses, Austin Moore, ActaChir.Belg. 1965, 54, 829

114. Gurdjian, E.S. and Lissner, HR., Mechanism of Head Injury as Studied by the Cathode Ray Oscilloscope. Preliminary Report, J. Neurosurg. 1944. 1,393

115. Evans, F.G., Methods of Studying the Biomachanical Significance of Bone Form,Amer. J, Phys. Anthrop. 1953, 11,413

116. Evans, F.G., Stress and Strain in Bones, Charles C. Thomas, Spring field, Ill., 1957

117. Frankel, V.H., The Femoral Neck, Charles C. Thomas, Spring field, Ill., 1960

118. Evans, F.G., Bibliography on the Physical Properties of the Skeletal System, Artif. Limbs 1967, 11,48

119. Milch, H., Photo elastic Studies of Bone Forma,J.BoneJt. Surg. 1940,22,621

120. Habousch, E.J., Photo elastic Stress and Strain Analysis in Cervical Fractures of the Femur, Boll. Hosp. Joint Dis.1952, 13, 252

121. Pauwels, F.,The Importance Of The Principles Of Construction Of Musculoskeletal System For The Stress On The Pipe Bone, Acta Anal.1951,12 , 207

122. Fessler, H., Load Distribution in a Model of the Hip Joint, J. Bone Jt. Surg. 1957,398,145

123. Williams, J.F. and Svensson, N.L., An Experimental Stress Analysis of the Neck of the Femur, Med. Biol. Engng. 1971, 9,479

124. Chand, R., Haug, E. and Rim, K., Stresses in the Human KneeJoint, J. Biom. Biomech. 1976, 9,417

125. Maquet, P., Biomechanics and Osteoarthritis of the Knee, SOCIT, 11 th Congress, Mexico, 1969

126. ASTMF1537 & ISO 5832-12

127. http://ihcp.jrc.ec.europa.eu/

128. http://www.jrc.ec.europa.eu/

129. P. Sury and M. Semlitsch, "Corrosion behavior of cast and forged cobalt-based alloys for double-alloy joint endoprostheses," J Biomed Mater Res A, Vol. 12, pp. 723–741, 1978.

130. Proceedings of International Conference On Innovations, Recent Trends And Challenges In Mechatronics, Mechanical Engineering And New High-Tech Products Development – MECAHITECH'11, vol. 3, year: 2011

131. E. Wintermantel and S. Ha, BiokompatibleWerkstoffe und Bauweisen: ImplantatefürMedizin und Umwelt. Springer, 1998.

132. ASTMF136 & ISO 5832-3

133. The Electolizing Corporation of Ohio, "Titanium Anodizing Provides the Advantages of Hardening and Coloring": 2008, [online] Available:http://www.Elecrohio.com/finishing/tianodizing/tianodizing.htm (Accessed August 2008)

134. Y. Kwon and H. Bang, "The Finite Element Method Using Matlab," Boca Raton: CRC Press, 2000.

135. S. Moaveni, "Finite Element Analysis Theory and Application with ANSYS," 3rd ed., New Jersey: Pearson-Prentice Hall, 2008.

136. G. Bergmann, F. Graichen, A. Rohlmann, A. Bender, B. Heinlein, G.N. Duda, M.O. Heller and M.M. Morlock , "Realistic loads for testing hip implants": Bio-Medical Materials and Engineering 20 (2010), 65–75; DOI 10.3233/BME-2010-0616

APPENDIX

1. ANSYS Stress Results for Long Neck Contact at 0.5mm Fillet Radius

1.5 Equivalent Stress

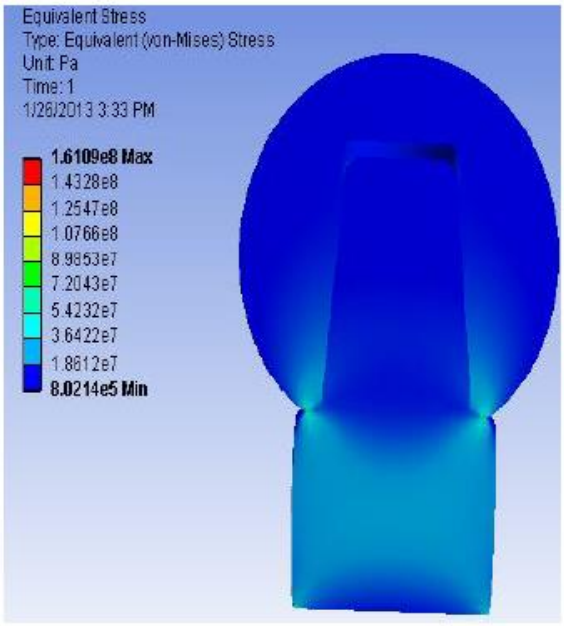

Normal Stress

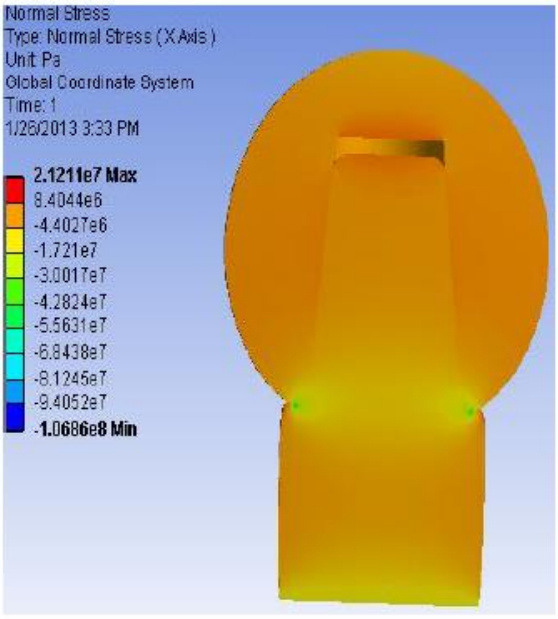

Shear Stress

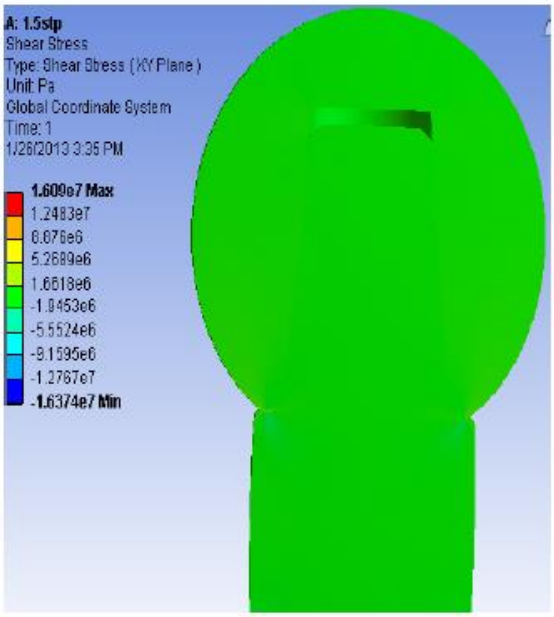

Maximum Principal Stress

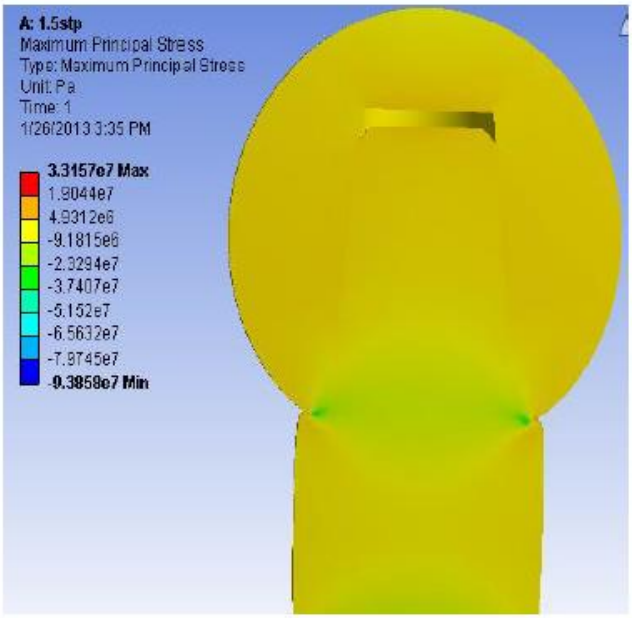

2. ANSYS Stress Results for Long Neck Contact at 0.6mm Fillet Radius

Equivalent Stress

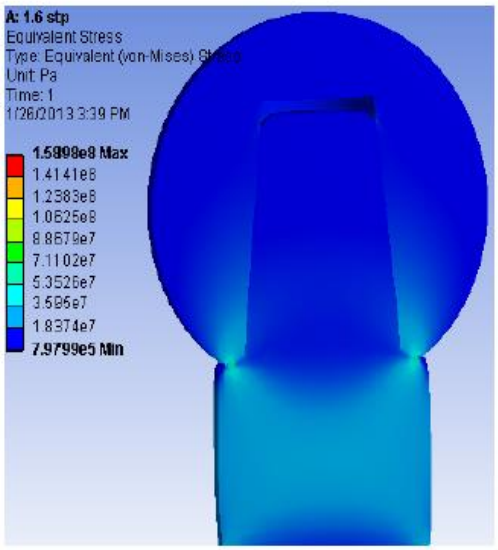

Normal Stress

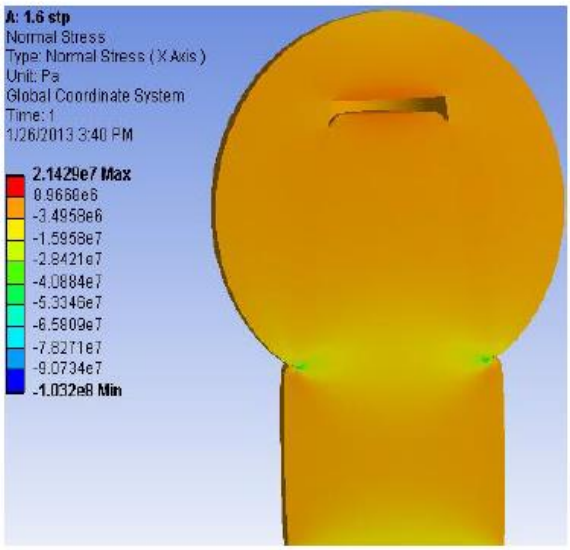

Shear Stress

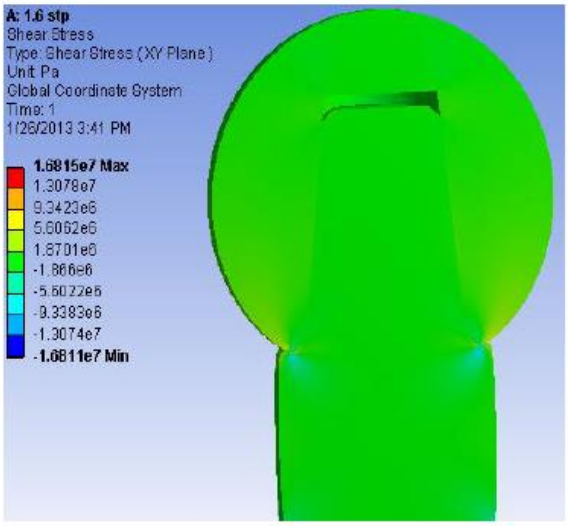

Maximum Principal Stress

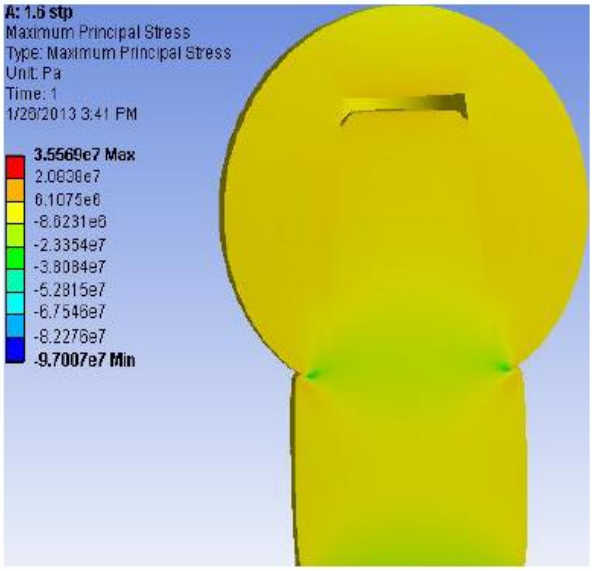

3. ANSYS Stress Results for Long Neck Contact at 0.7mm Fillet Radius

Equivalent Stress

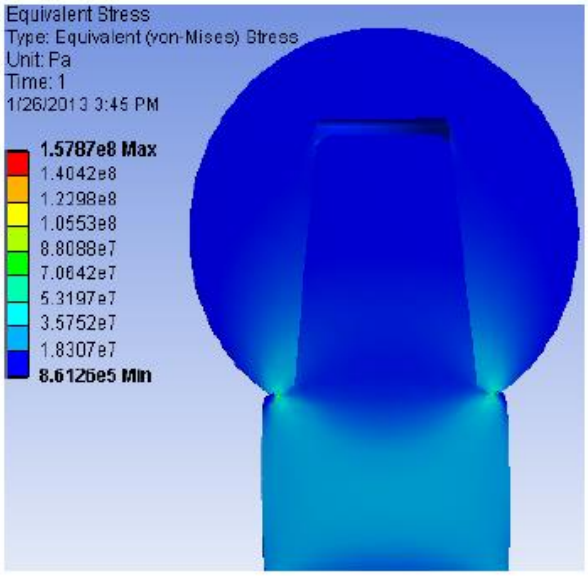

Normal Stress

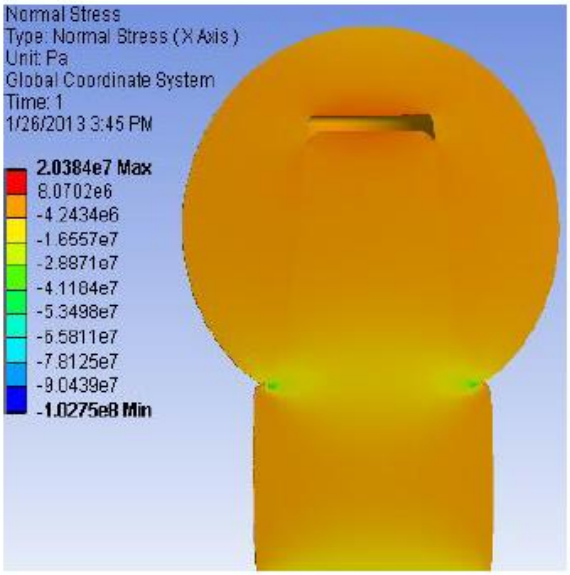

Shear Stress

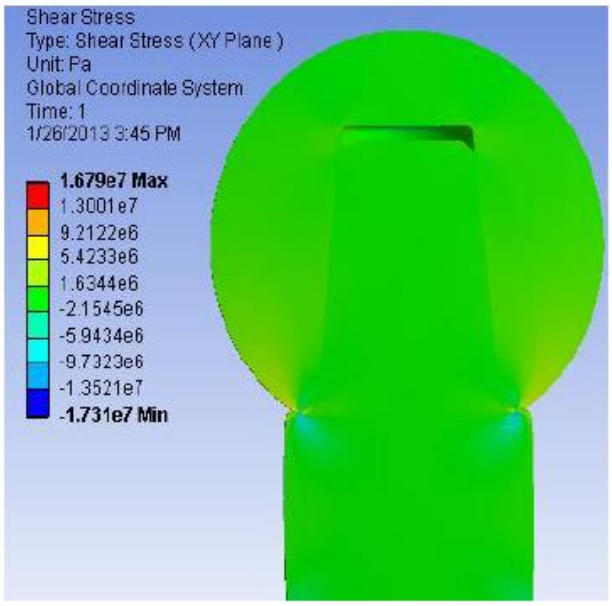

Maximum Principal Stress

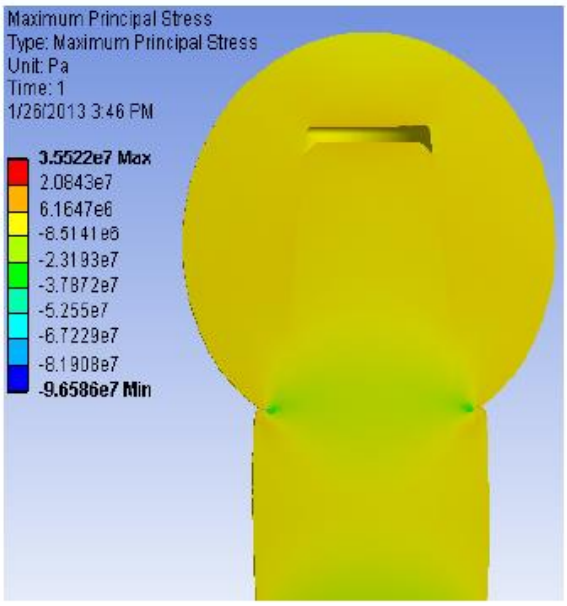

4. ANSYS Stress Results for Long Neck Contact at 0.8 mm Fillet Radius

Equivalent Stress

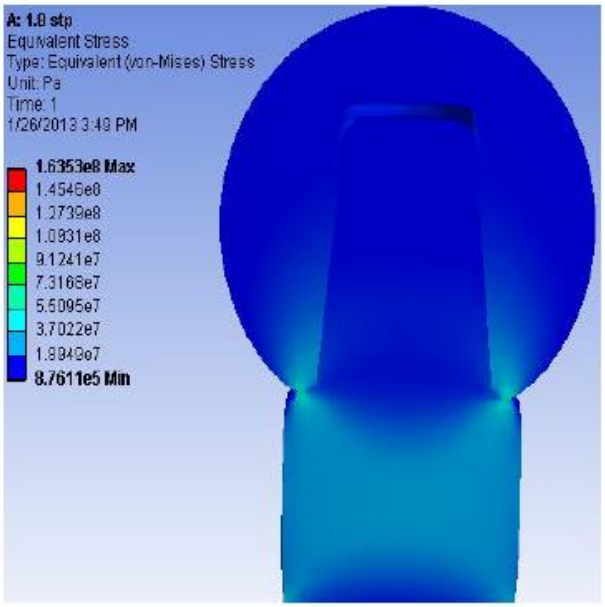

Normal Stress

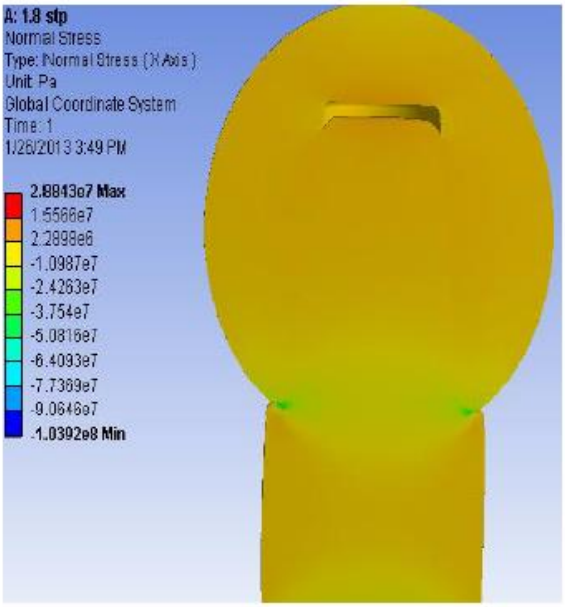

Shear Stress

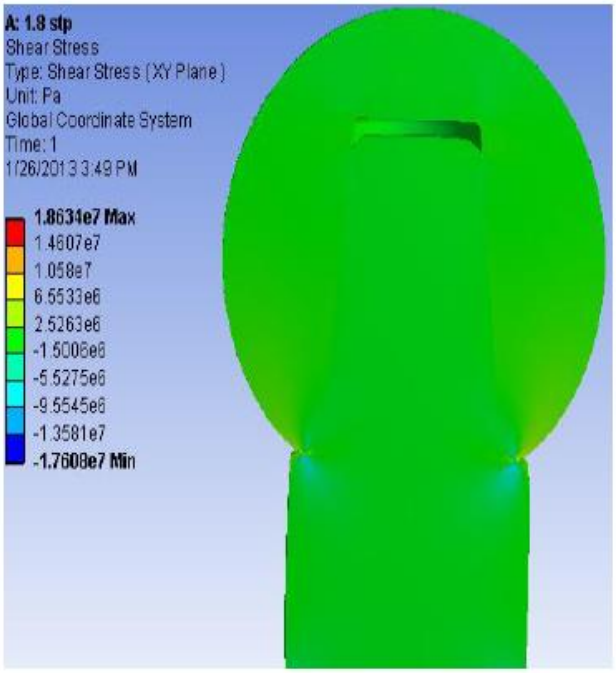

Maximum Principal Stress

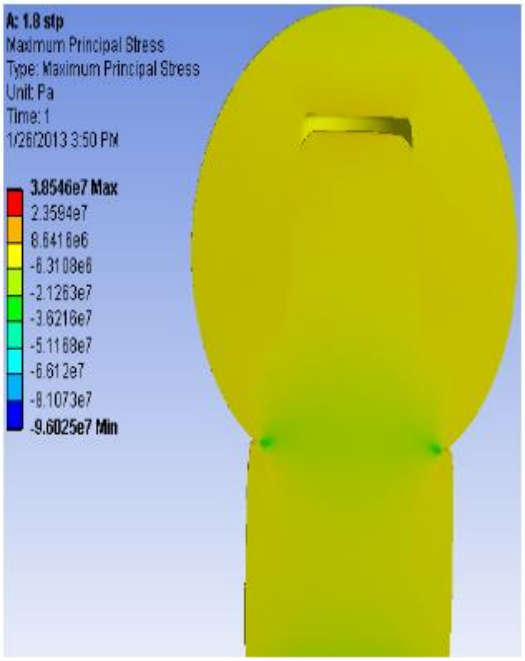

5. ANSYS Stress Results for Long Neck Contact at 0.9 mm Fillet Radius

Equivalent Stress

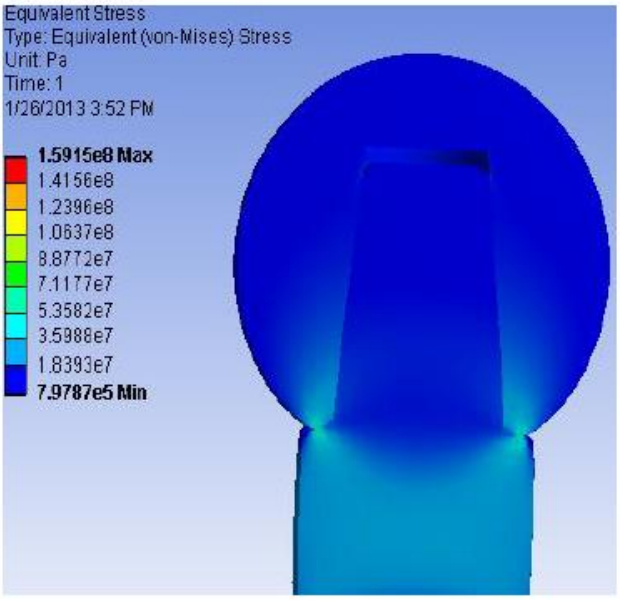

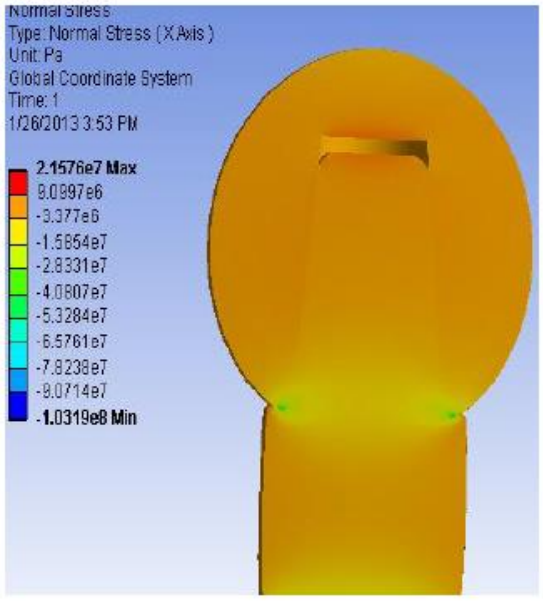

Shear Stress

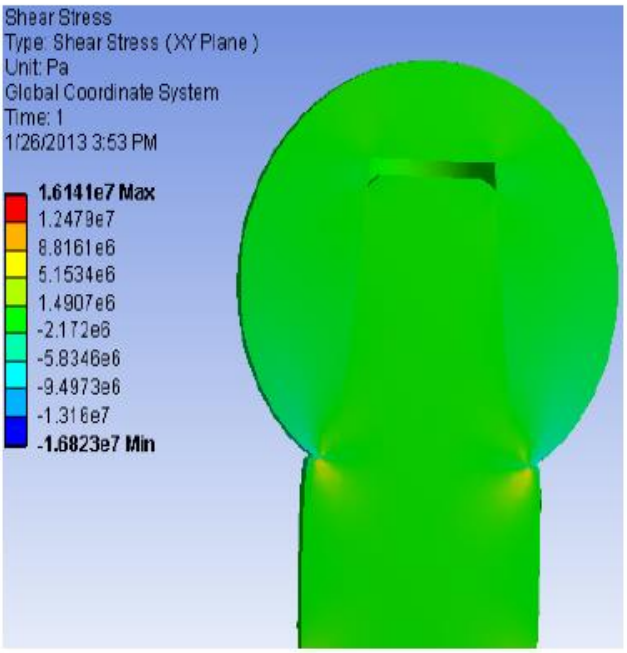

Maximum Principal Stress

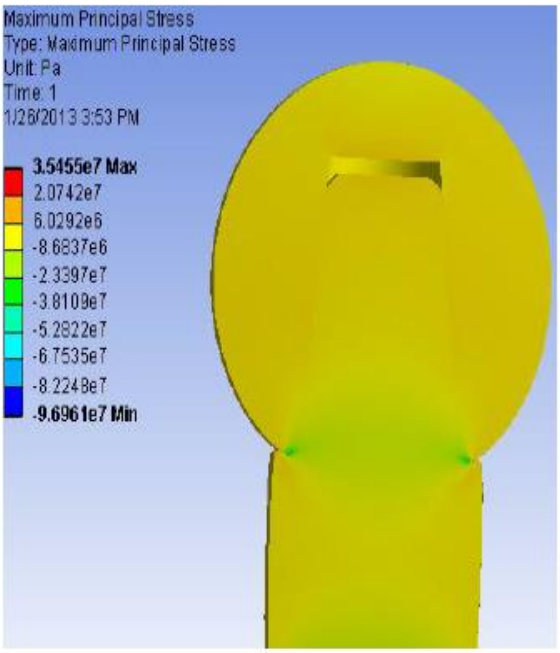

6. ANSYS Stress Results for Medium Neck Contact at 0.5 mm Fillet Radius

Equivalent Stress

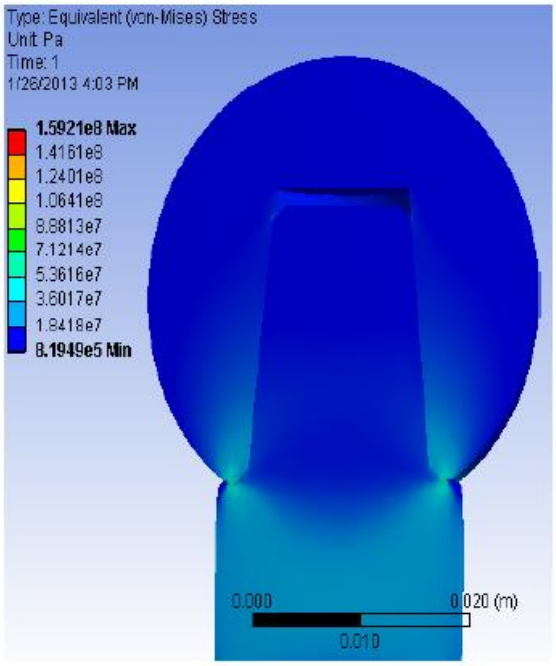

Normal Stress

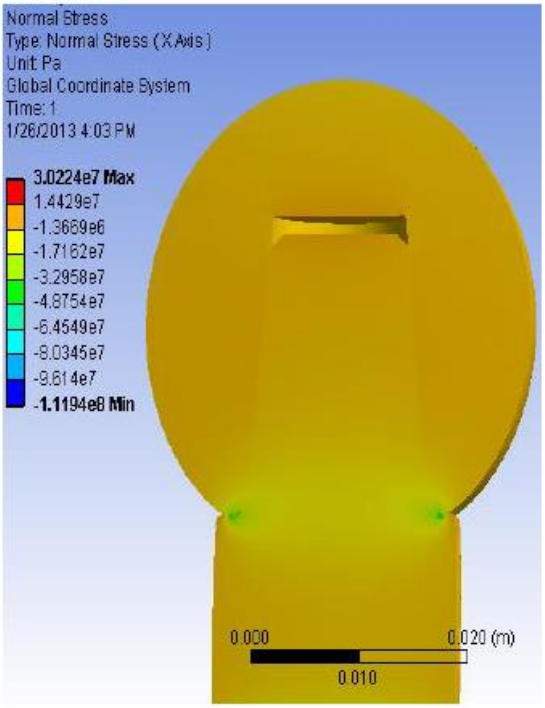

Shear Stress

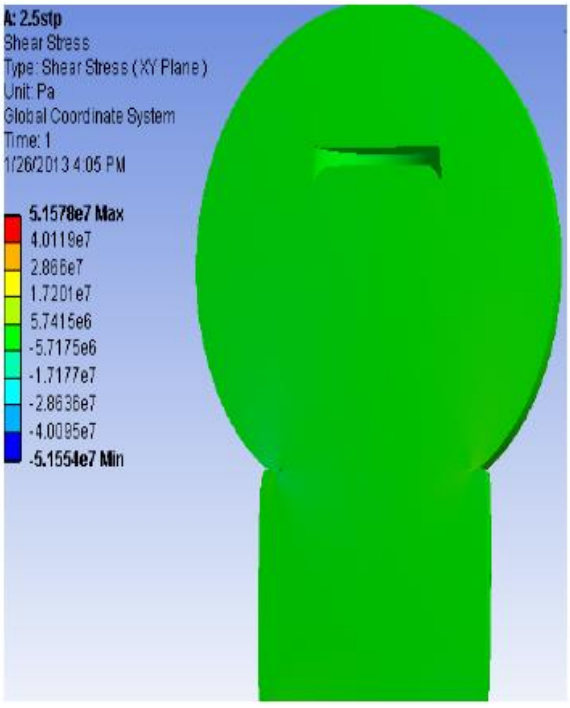

Maximum Principal Stress

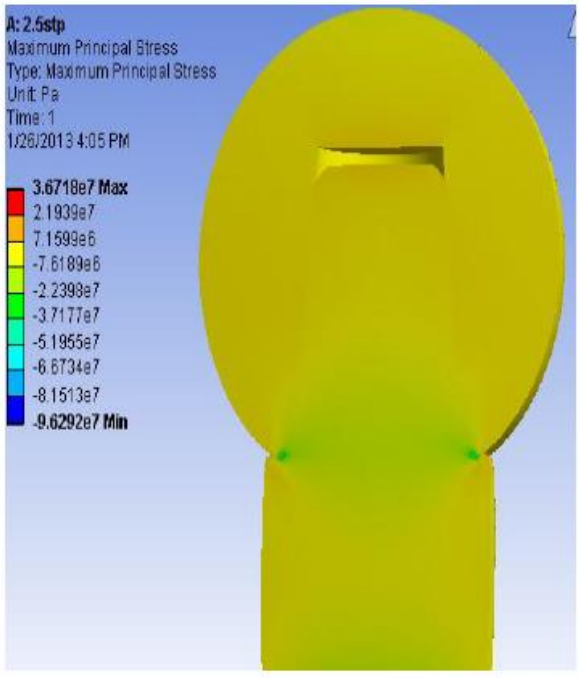

7. ANSYS Stress Results for Medium Neck Contact at 0.6 mm Fillet Radius

Equivalent Stress

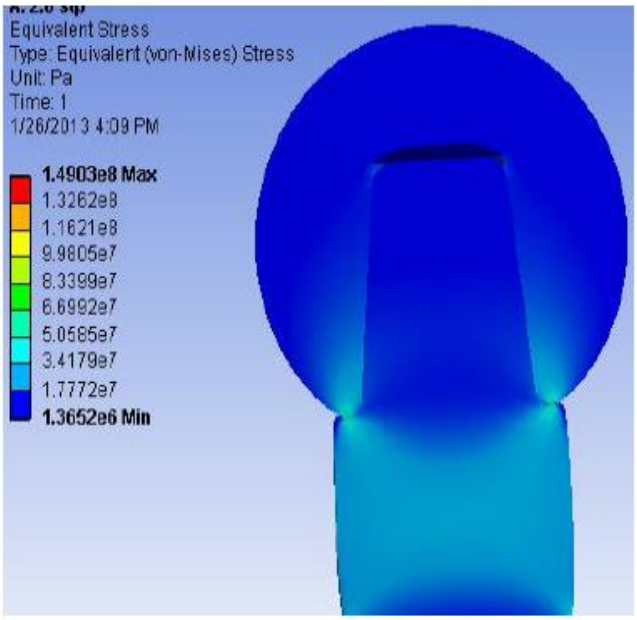

Normal Stress

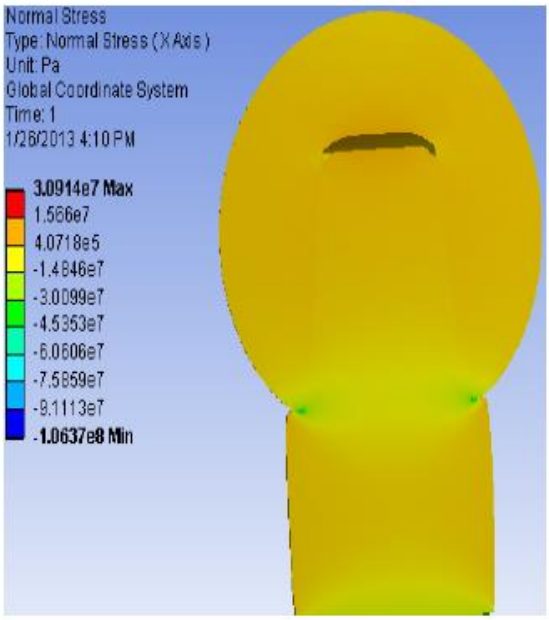

Maximum Principal Stress

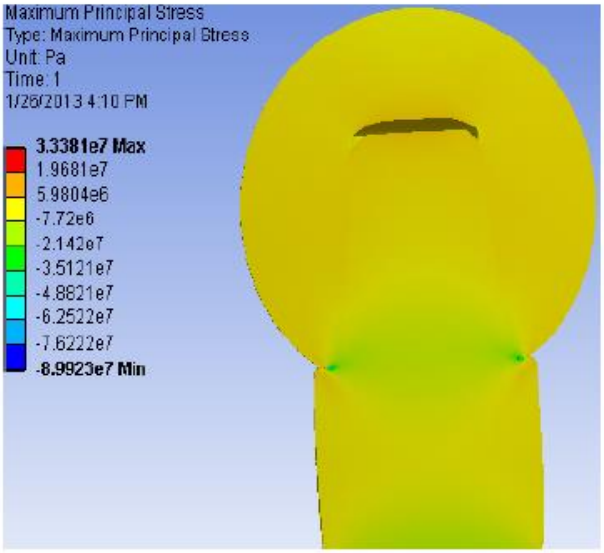

Shear Stress

8. ANSYS Stress Results for Medium Neck Contact at 0.7 mm Fillet Radius

Equivalent Stress

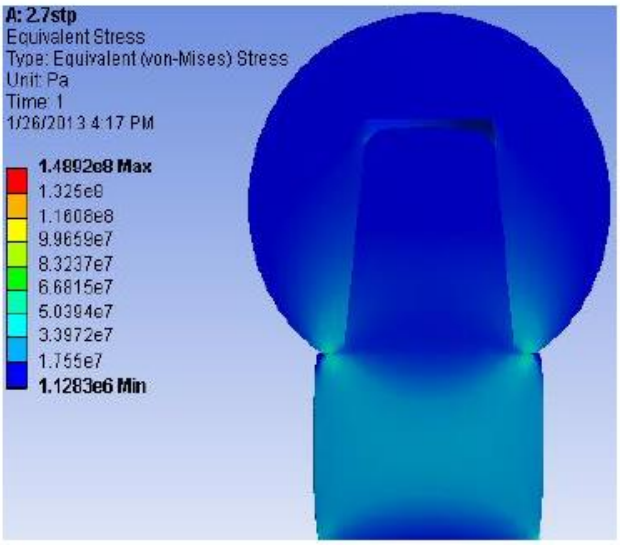

Normal Stress

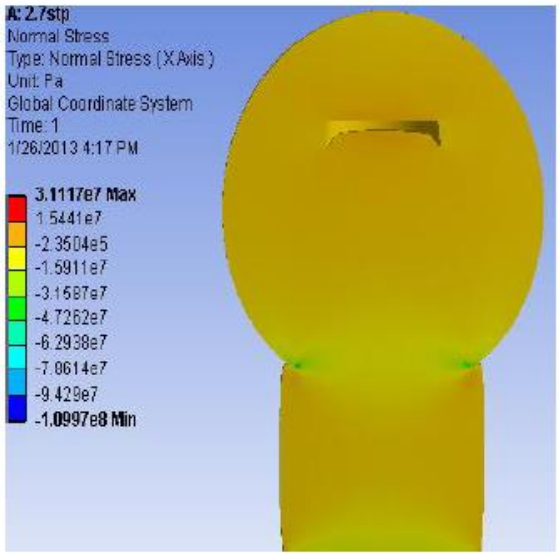

Maximum Principal Stress

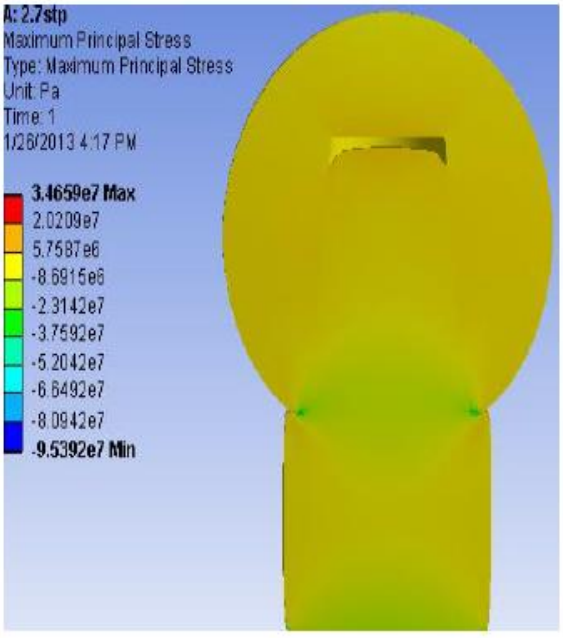

Shear Stress

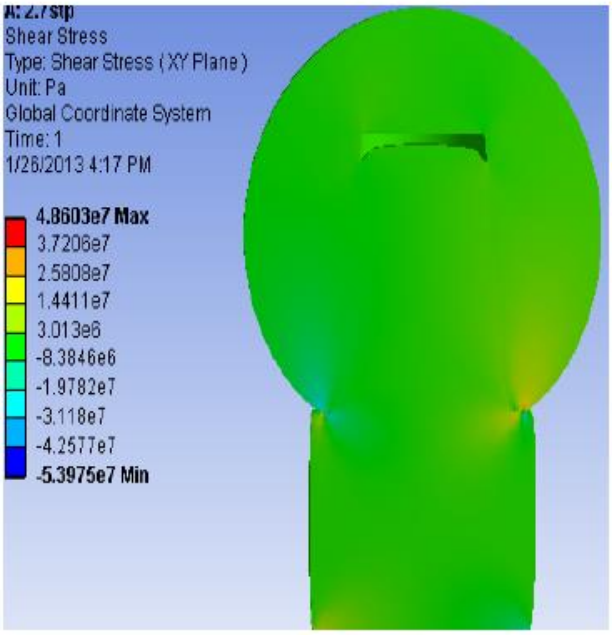

9. ANSYS Stress Results for Medium Neck Contact at 0.8 mm Fillet Radius

Equivalent Stress

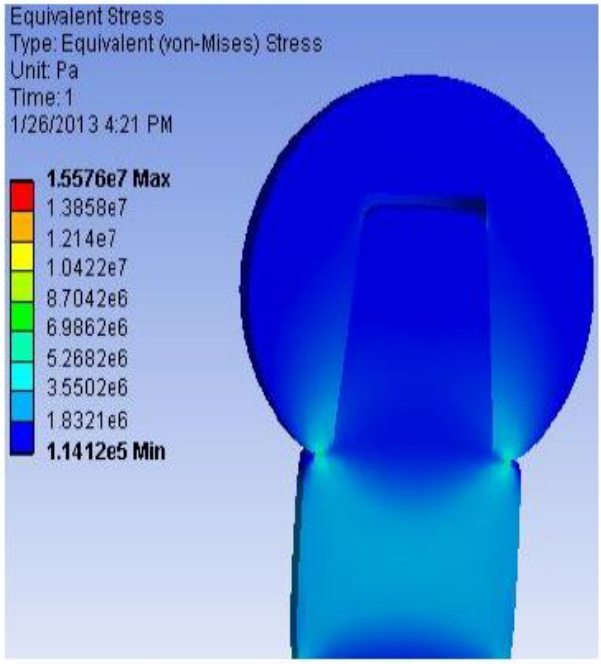

Normal Stress

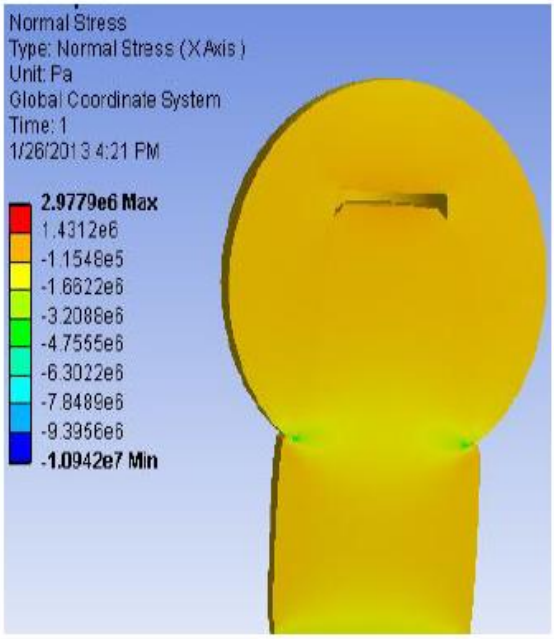

Maximum Principal Stress

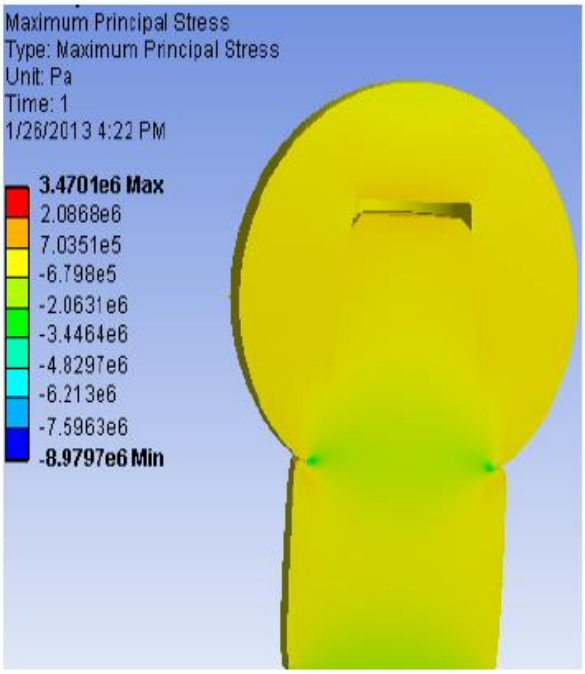

Shear Stress

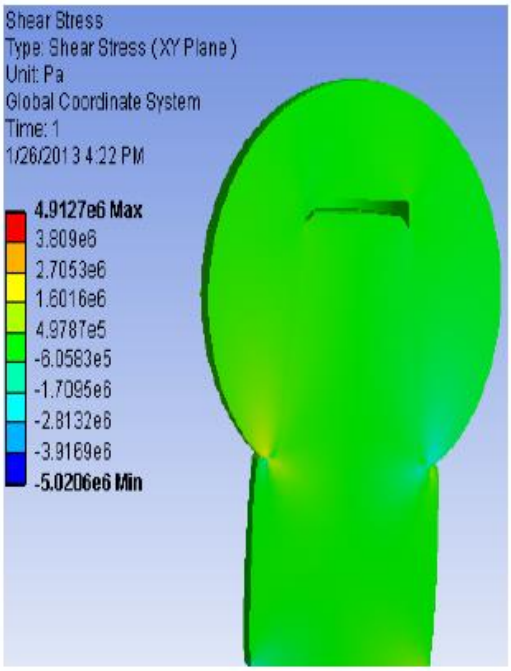

10. ANSYS Stress Results for Medium Neck contact length at 0.9mm Fillet Radius

Equivalent Stress

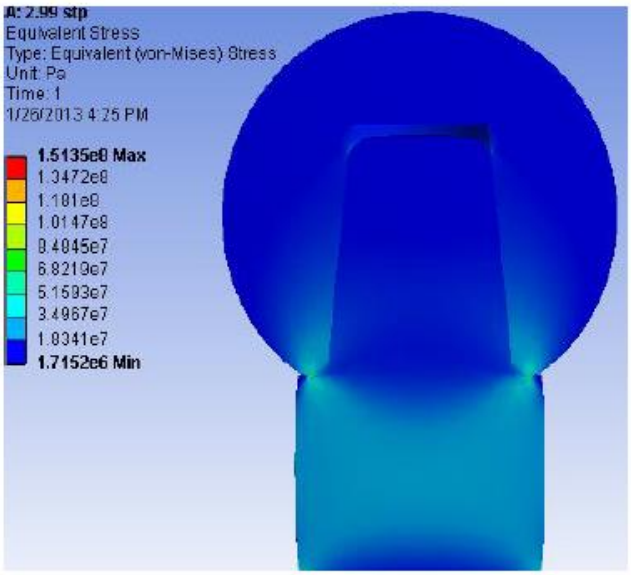

Normal Stress

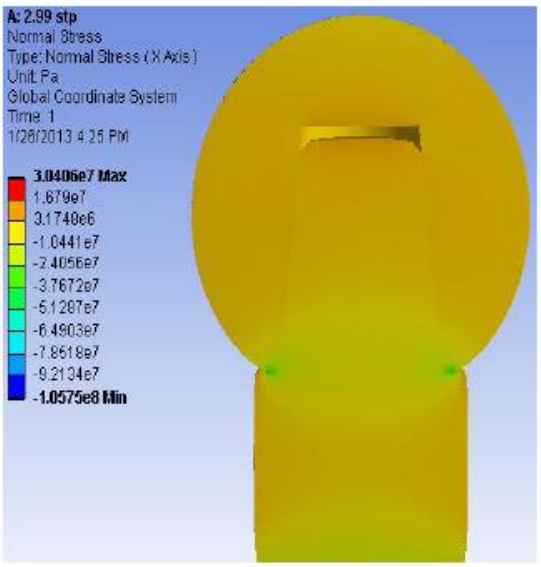

Maximum Principal Stress

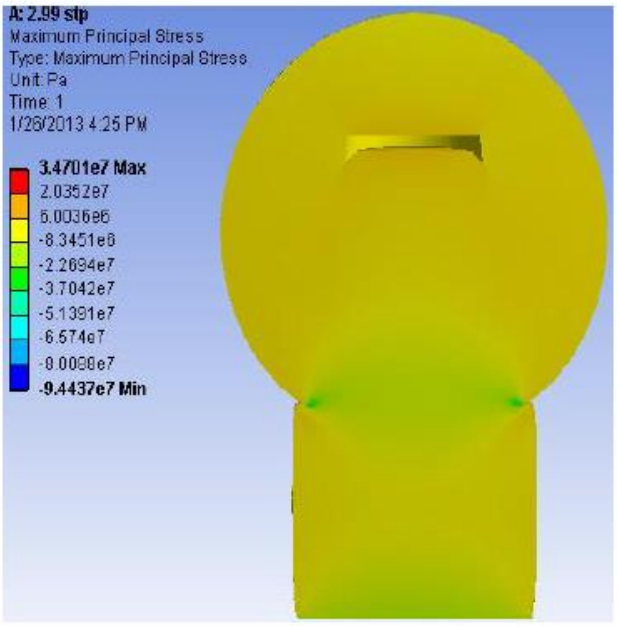

Shear Stress

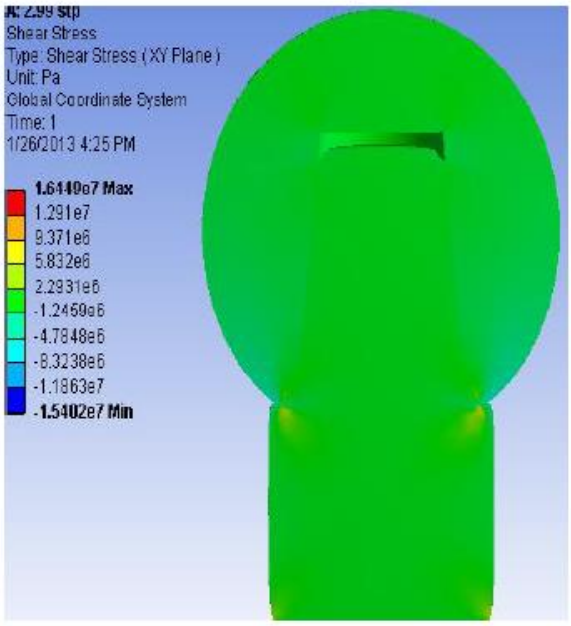

11. ANSYS Stress Results for Medium Neck Contact at 0.5 mm Fillet Radius

Equivalent Stress

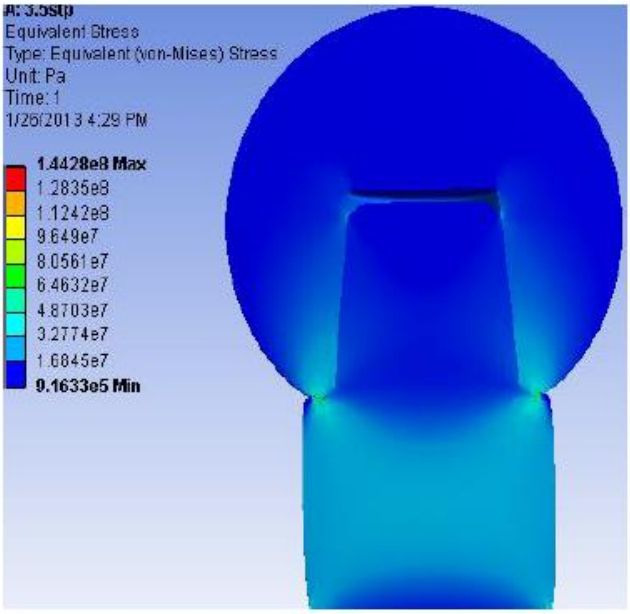

Normal Stress

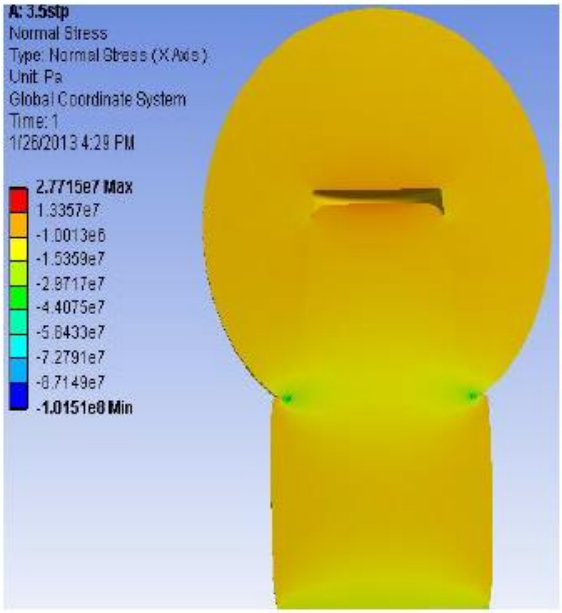

Maximum Principal Stress

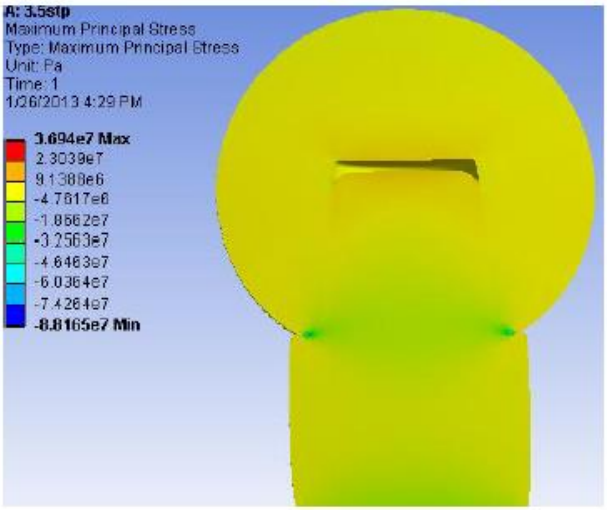

Shear Stress

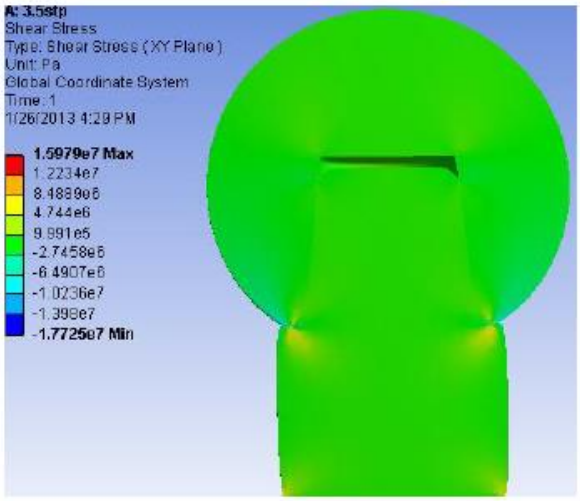

12. ANSYS Stress Results for Medium Neck Contact at 0.6 mm Fillet Radius

Equivalent Stress

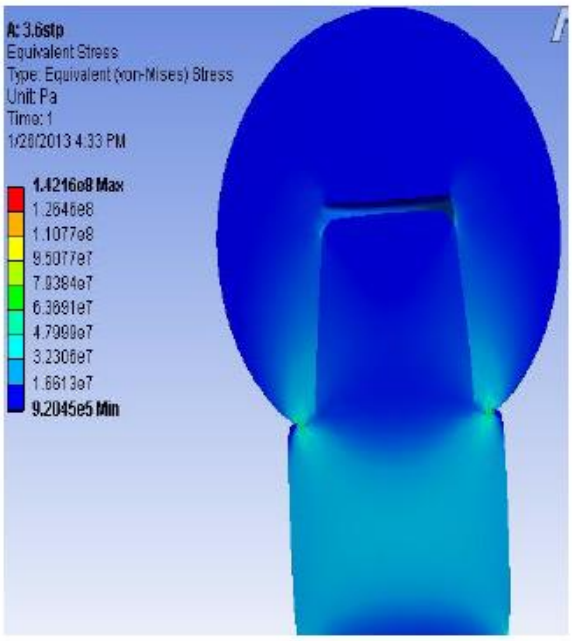

Normal Stress

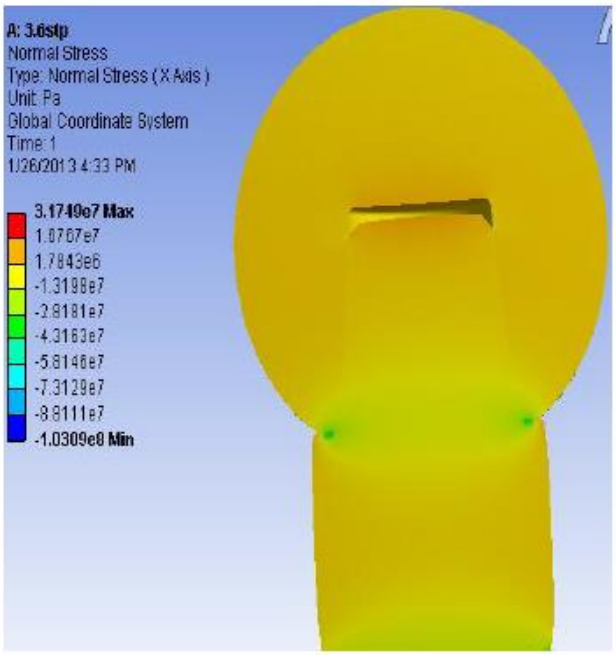

Maximum Principal Stress

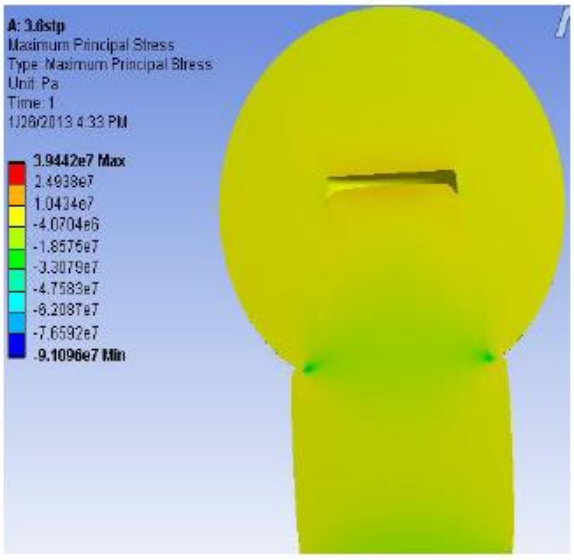

Shear Stress

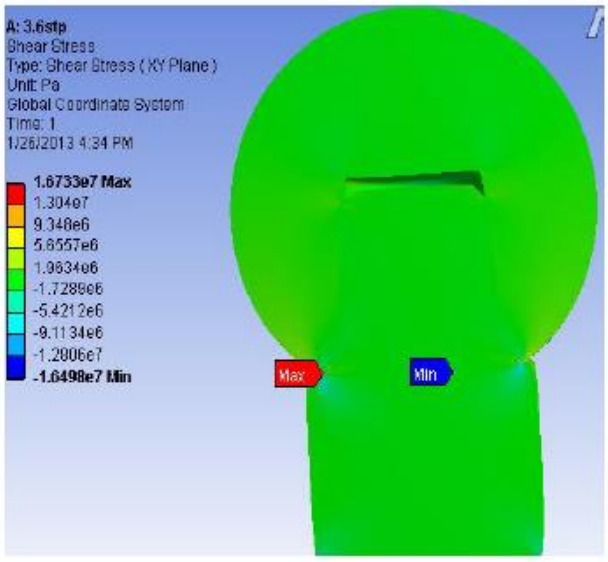

13. ANSYS Stress Results for Medium Neck Contact at 0.7 mm Fillet Radius

Equivalent Stress

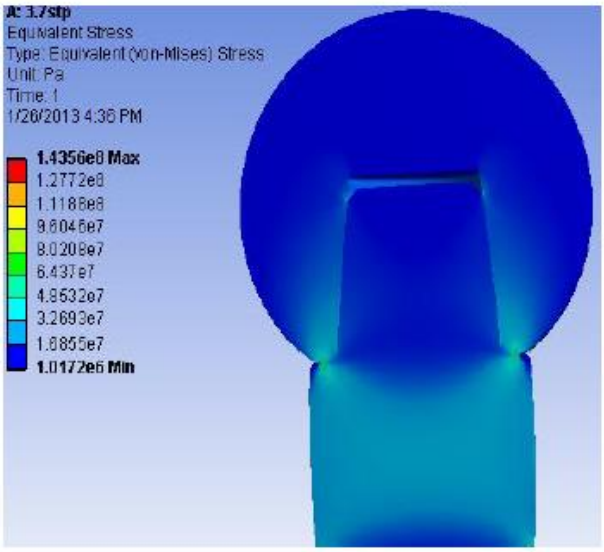

Normal Stress

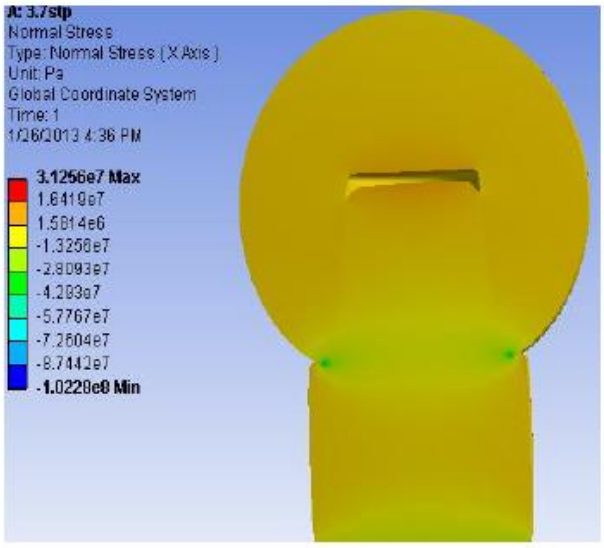

Maximum Principal Stress

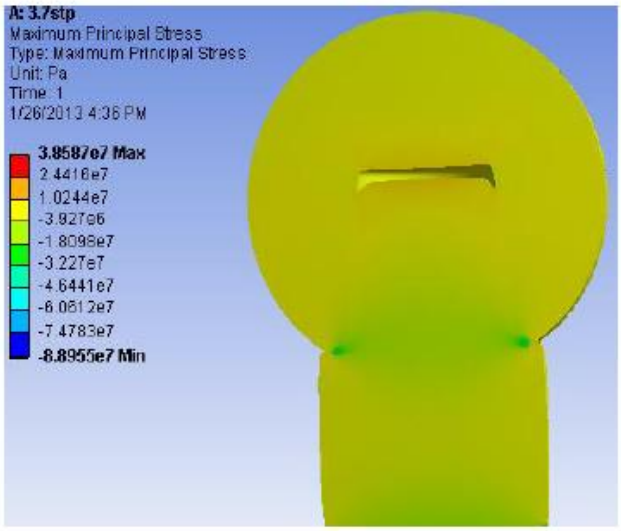

Shear Stress

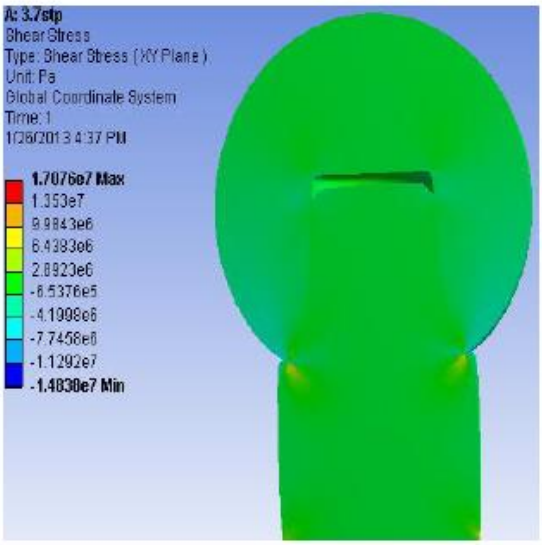

14. ANSYS Stress Results for Medium Neck Contact at 0.8 mm Fillet Radius

Equivalent Stress

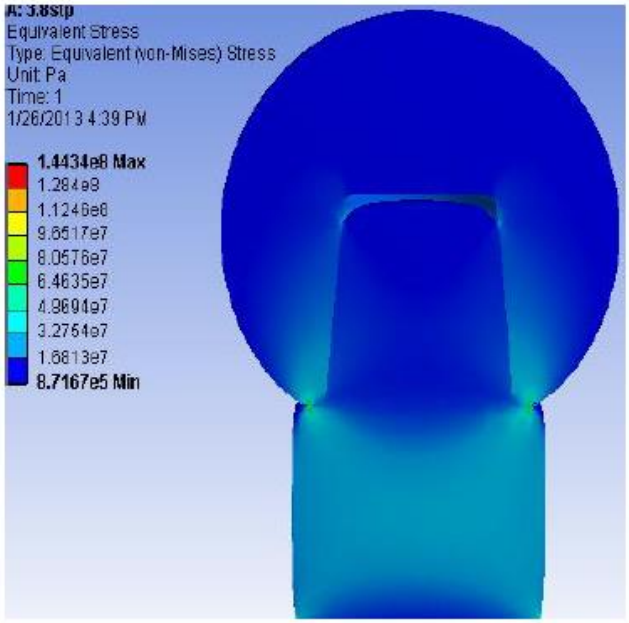

Normal Stress

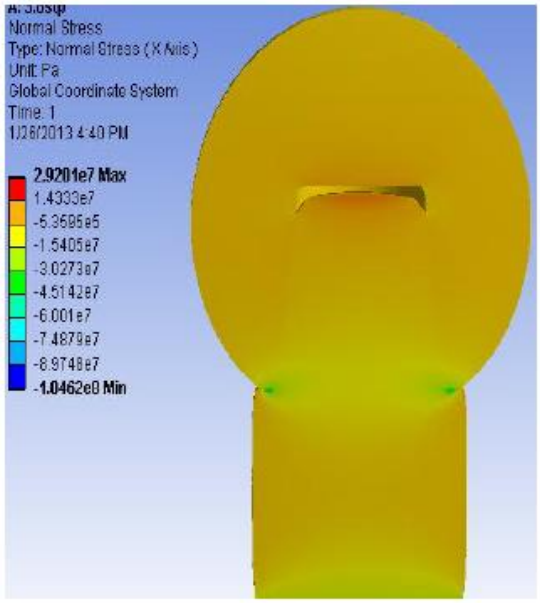

Maximum Principal Stress

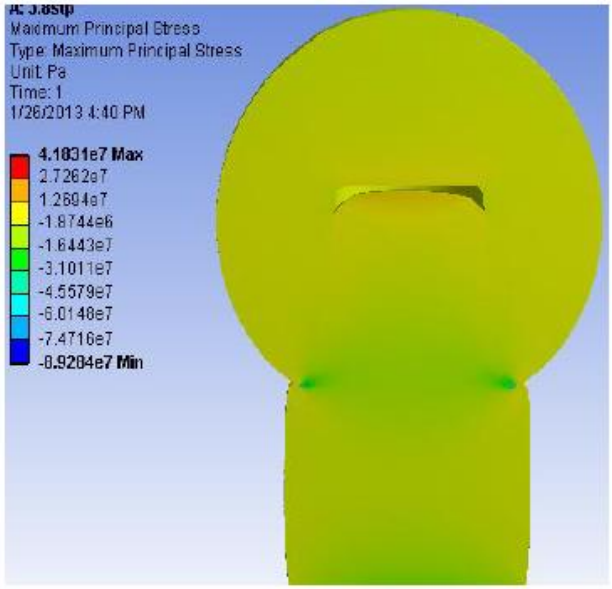

Shear Stress

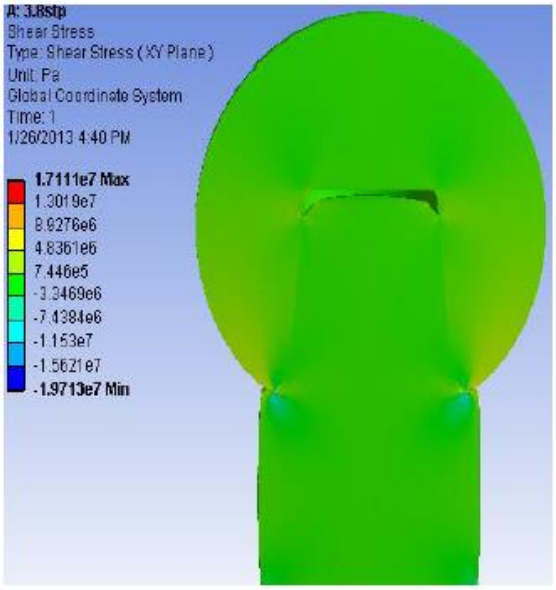

15. ANSYS Stress Results for Medium Neck Contact at 0.9 mm Fillet Radius

Equivalent Stress

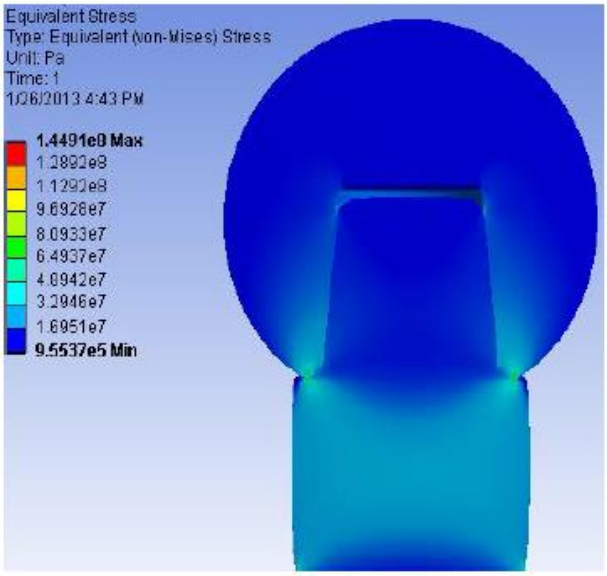

Normal Stress

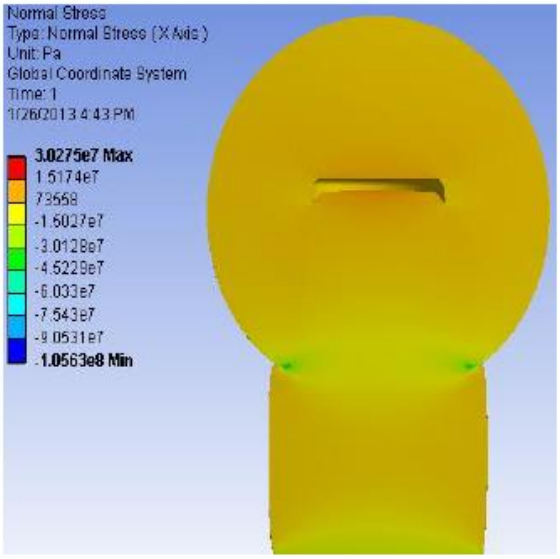

Maximum Principal Stress

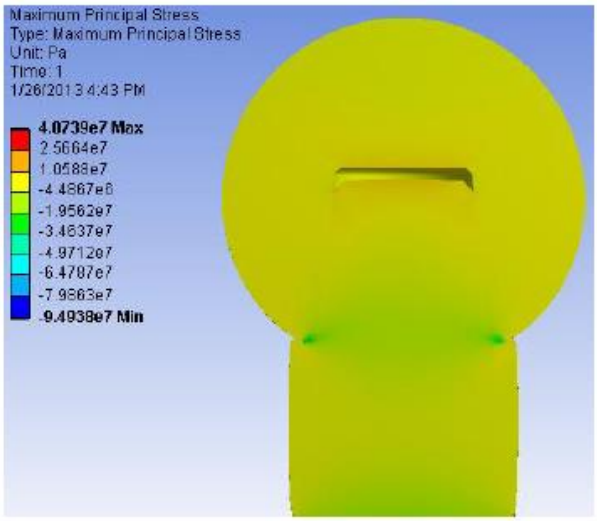

Shear Stress

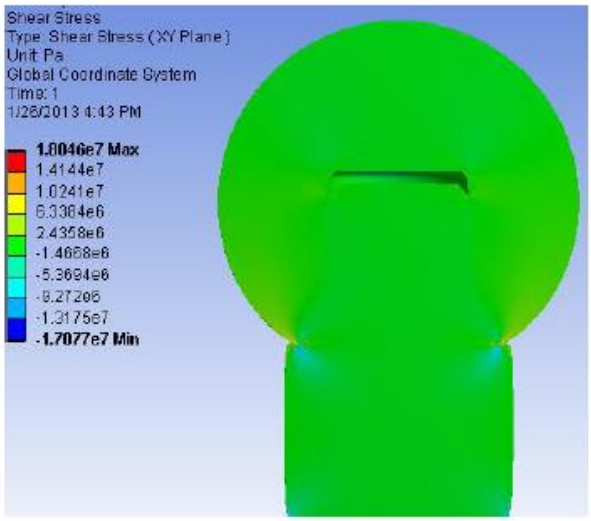

GLOSSARY

Acetabulum: the cup-shaped cavity formed by the illiac, pubic and ischiac bones of the pelvis in which the femoral head of the hip joint fits.

Arthroplasty: an orthopaedic surgical procedure that replaces or remodels a defective natural joint.

Aseptic loosening: the mobilization of a prosthesis caused by bone resorption in absence of any infection process (sepsis).

Avascular necrosis: the consequence of temporary or permanent cessation of blood flow to the bones. The absence of blood causes the bone tissue to die, resulting in fracture or collapse of the entire bone

Cortical bone: the compact bone of the shaft of a bone that surrounds the medullary canal. For its compact structure it differs from the spongy bone (cancellous bone) which is, on the contrary, less dense, softer, and organized in trabeculae (small tissue elements in the form of a small beam, strut or rod). Cortical bone facilitates bone's main functions: to support the whole body, protect organs, provide levers for movement, and store and release chemical elements, mainly calcium.

Dislocation: displacement of a bone from its normal position, especially at a joint.

Distal: anatomically located far from a point of reference, such as an origin, a point of attachment, or the midline of the body. Opposed to Proximal

Edge loading: a particular loading condition that occurs when the femoral head interacts only with the rim of the acetabular cup.

Femoral head: the rounded proximal articulating extremity of the femur constituting part of the hip joint.

Femoral neck: the column of bone connecting the head of the femur and the shaft

Femur: a bone of the leg situated between the pelvis and knee in humans. It is the largest and strongest bone in the body. It articulates with the pelvis through the femoral head, which constitutes, together with the acetabulum, the hip joint.

Fibrous capsule: also referred as foreign body granuloma, a layer of connective tissue formed as part of the biological response to an implanted foreign material. It consists primarily of collagen fibres, but may also contain a variety of inflammatory cell types and new capillaries, depending on the degree of the response.

Hip resurfacing: a particular type of hip prosthesis that is anchored to the natural femoral neck

Mechanical fatigue: a material subject to a cyclic loading, whose maximum value is below material's yield stress, can show fatigue effects due to progressive crack propagation, up to a point when the component is so weakened that it suddenly breaks.

Natural joint: the location at which two or more bones make contact. Joints are constructed to allow movement and provide mechanical support. Some of them are hip, knee, shoulder, wrist, ankle and elbow.

Osteoarthritis: a form of arthritis, occurring mainly in elder persons, that is characterized by chronic degeneration of the cartilage of the joints. Also called degenerative joint disease.

Osteo integration: the direct structural and functional connection between living bone and the surface of a load-bearing implant.

Periposthetic tissue: the tissue surrounding the prosthesis.

Press-fitting: a match between the size and shape of two parts, such that force is required for assembly as one part is slightly larger than the other.

Primary THA: the first surgical intervention during which the natural hip joint is replaced by an artificial

Prosthesis: The following surgeries, aimed either at the partial or total replacement of the artificial joint, are called revisions.

Prosthesis survival: the percentage of prostheses that are still in place after a certain number of years. The percentage decreases when prosthesis has to be replaced by revision surgery.

Proximal: nearer to a point of reference such as an origin, a point of attachment, or the midline of the body. Opposed to Distal

Stiffness: a property of a mechanical component. It determines the extent to which a component resists to deformation in response to an applied force. Typically the stiffness describes how easily a piece can be bent.

Total Hip Arthroplasty:replacement of both articulating surfaces of a degenerated hip joint. On the acetabular side an artificial acetabular cup is inserted and on the femoral side, the femoral head is replaced completely by a spherical component, which can be anchored in the femur with a stem (conventional THA), or the femoral head is trimmed and covered with a metal cap that provides the new articulating surface (see hip resurfacing THA).

Tribology: the science and engineering of interacting surfaces in relative motion. It includes the study and application of the principles of friction, lubrication and wear. Tribology is a branch of mechanical engineering.

Trochanter: a broad, flat ledge on the femur, at the upper end of its lateral surface (greater trochanter), or a short conical ledge on the posterior border of the base of its neck (lesser trochanter).

Young's elastic modulus: also referred as modulus of elasticity, the ratio of the stress applied to a body to the strain those results in the mechanical body in response to it. In particular Young's modulus is the ratio of the longitudinal strain to the longitudinal stress.